Peramunage, Dharmasena

PHOTOELECTROCHEMICAL AND ELECTROREFLECTANCE STUDY OF ORGANIC SEMICONDUCTORS

City University of New York PH.D. 1986

PLEASE NOTE:

In all cases this material has been filmed in the best possible way from the available copy. Problems encountered with this document have been identified here with a check mark __✓__.

1. Glossy photographs or pages _____
2. Colored illustrations, paper or print _____
3. Photographs with dark background _____
4. Illustrations are poor copy _____
5. Pages with black marks, not original copy _____
6. Print shows through as there is text on both sides of page _____
7. Indistinct, broken or small print on several pages ✓
8. Print exceeds margin requirements _____
9. Tightly bound copy with print lost in spine _____
10. Computer printout pages with indistinct print _____
11. Page(s) _____ lacking when material received, and not available from school or author.
12. Page(s) _____ seem to be missing in numbering only as text follows.
13. Two pages numbered _____. Text follows.
14. Curling and wrinkled pages _____
15. Dissertation contains pages with print at a slant, filmed as received ✓
16. Other _____

_____

_____

University
Microfilms
International

PHOTOELECTROCHEMICAL AND ELECTROREFLECTANCE STUDY OF ORGANIC SEMICONDUCTORS.

by

Dharmasena Peramunage

A dissertation submitted to the Graduate Faculty in Chemistry in partial fulfillment of the requirements for the degree of Doctor of Philosophy, The City University of New York.

1986

This manuscript has been read and accepted for the Graduate Faculty in Chemistry in satisfaction of the Dissertation requirement for the degree of Doctor of Philosophy.

1/2/86
Date

M. Tomkiewicz
Prof Micha Tomkiewicz.
Chairman of the Examining Committee.

1/2/86
Date

A. N.
Executive Officer.

Seymour Aronson
Prof. S. Aronson. Brooklyn College

Ronald D. Birke
Prof. R. Birke. City College

H. Zieger
Prof. H. Zieger. Brooklyn College

Supervisory committee

The City University of New York.

ABSTRACT

Photoelectrochemical and Electroreflectance study on

Organic Semiconductors.

by

Dharmasena Peramunage

Advisor: Professor Micha Tomkiewicz

Techniques, that are traditionally used to study Semiconductor/Electrolyte interface of Inorganic Semiconductors, such as Electrolyte Electroreflectance (EER), Photocurrent Spectroscopy and Impedance spectral Analysis, were used to study the Organic Semiconductor/ Electrolyte Interface. Eventhough one expects complications arising from the special topology of the space charge layer within the fibre and the possibility of the film, undergoing chemical changes in aqueous electrolyte, we could still extract useful data specific for this interface.

EER of lightly doped Polyacetylene has two peaks. One at 1.45ev and other at 1.55 ev. These peaks were assigned tentatively, to an excitonic transition and direct band to band transition. EER of Neutral Poly-3methylthiophene (P3MT) has one peak at 2.05 ev, which could be fitted to a third derivative lineshape expected from lowfield EER. Lineshape corresponds to a bandgap value of 2.1

ev, and it confirms the quasi one dimentionality of the polymer. EER of moderately doped P3MT showed an additional structure, which could be correlated to a polaron level 0.15ev below the conduction band. EER of both trans -$(CH)_x$ and P3MT showed evidence for firmi level pinning.

Relaxation spectra of moderately doped P3MT shows a flat band of about 0.7 v vs.SCE. Trans -$(CH)_x$ and neutral P3MT gave Impedance spectra which could not be analysed in terms of frequency independent passive elements.

The action spectra observed for trans -$(CH)_x$ and P3MT were analysed, in terms of the Gartner model. Both polymers were shown to be direct gap semiconductrors. The deposition of Pt improved the photoresponse with the maximum somewhere around $2x10^{-7} mol/cm^2$.

ACKNOWLEDGEMENTS

I would like to express my gratitude to my advisor Prof.Micha Tomkiewicz, who suggested the work described here, and providing necessary guidance, with patience and encouragement during it's course. Special thanks are however due to Professors in my committee, with special reference to Prof. Seymour Aronson for stimulating conversations, and other assistance during the course of my graduate education at the City University of New York.

I express my deep appreciation and gratitude to Dr.David C.Ginley, who gave me this opportunity to work on this project, in collaboration with Sandia National Laboratories, Alberquerque, new Maxico, maintaining a constant supply of painstakingly synthesised polymer samples, and most important of all financing this project.

Thanks are also due to Messrs, Ottmar Safferling, Marty Berman, Sol Colton, Patsy M.Bevilacqua, William C.Knoop Carl E,Paparella, Vincent R.Pinkes, who always stood behind me with their support and expert services throughout my work and, in general to all those who created a convivial atmosphere, making my stay in New York enjoyable.

It was a pleasure to work with my colleagues Drs. Withana Siripala, Padmanaban Parayantal and Mr.Yuan Renkuwn. Finally I would like to offer my sincere thanks to my wonderful wife

Wimala for her dedication and encouragement during the course of this work.

Dharmasena Peramunage.

Feb. 1986

to my parents & parents in law

with love and appreciation

CONTENTS

LIST OF FIGURES.

LIST OF TABLES.

Chapter 1

INTRODUCTION

Until the second world war, solid state and material scientists paid very scanty attention towards the study of organic solids as potential electronic materials. But eventually, mechanical and electrical properties of organic solids were exploited in the quest for developing a substitute for natural rubber and better insulators. The most attractive class of organic materials seemed to be polymers. They particularly captured the world attention because of their amazing versatility. In the hand of organic synthetic chemists, polymers could be tailored to an amazing degree to obtain superior chemical and mechanical properties, to comply with requirements demanded by millions of applications [1]. Design and synthesis of polymers became as much of an art as it was a science.

The investigation of electronic and photoconductive properties was a natural extension of this situation. Particularly great prospects have been opened up in the synthesis and study of organic solids possessing extended conjugation of Π electrons or, the ability to form charge transfer complexes. Such compounds acquired the name "Organic Semiconductors" [2]. Parallel to the synthetic efforts, the study of the electronic properties of organic solids opened up an interesting frontier for solid state physicists too. Concepts developed exclusively for the understanding of inorganic semiconductors, either changed or found inadequate [3] for the interpre-

tation of the experimental results. Concept of soliton transport in Polyacetylene [4,5] and nature and origin of proposed localized electronic states in anthracene [6], can be given as examples. On the practical side, organic semiconductors have established themselves in a wide spectrum of commercial applications [7]. Potential use of organic semiconductors in unconventional applications, such as diode formation [8] and Photoelectrochemical cells [9,10,11] are being actively investigated.

1.1 Polymers with linear conjugation in the main chain

Polyacetylene can be considered as a unique example for this class of polymers. Many subsitituted acetylene polymers have been reported. Polypropyne, polybutyn-1, polypentyn-1 and polyphenylacetylene [12] are few examples. Being a model for a quasi one dimensional material, polyacetylene aroused a great deal of interest within the scientific community in the past decade. Acetylene can be polymerized to Polyacetylene in the presence of various catalysts, such as metal carbonyls [13] or Ziegler-Natta type [14] systems. But unfortunately, the products obtained with these catalysts were either in powder form or spongy masses that were virtually insoluble in any solvent. This factor alone could have been a major objection to the exploitation of this material. But a long awaited break through was achieved in 1974, which resulted in the preparation of Polyacetylene as a free standing silvery films possessing p- type semiconductive behaviour [15]. This achievement stimulated a world wide

activity on this material, to investigate its fundamental properties and potential applications as well.

Polyacetylene is ideally a planar compound composed of a succession of CH units joined by alternating single and double bonds. Bonding orbitals in polyacetylene are the sp_2 hybrid of Carbon 2s and 2p orbitals and bonding is similar to that of Ethylene, which results in the formation of a carbon chain bound together by sigma bonds and Π electron cloud delocalized over it. In chemical terms, this is a conjugated chain and may be presented as a sequence of alternating single and double bonds. When the polymer chain is of appreciable length, there may be a wide choice of conformational structures. The most probable isomers are shown in Fig.1

Cis and Trans content of Polyacetylene is strongly dependent on the polymerisation temperature. At temperatures as low as -78°C the film is formed completely as the Cis isomer. Temperatures around 150°C or higher give exclusively the trans material. Intermediate temperatures give varying amounts of isomer contents. For example, the film is approximately 60% Cis and 40% Trans, if the preparation is carried out at room temperature [17,18,19]. Differential thermogram of Cis Polyacetylene exhibits an exothermic peak around 140°C, which has been assigned to Cis-Trans isomerisation. In other words the Cis isomer may be conveniently converted to the thermodynamically more stable Trans isomer by heating [19]. Infrared spectra provide an easy way to estimate the relative quantities of Cis and Trans isomers, in a Polyacetylene sample. Relative intensities

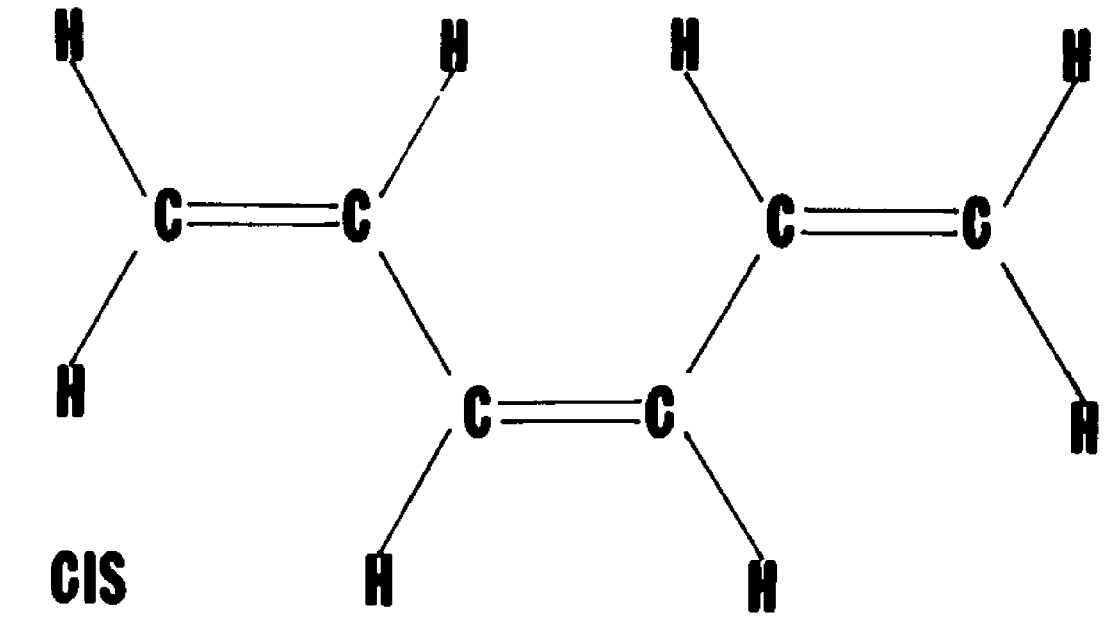

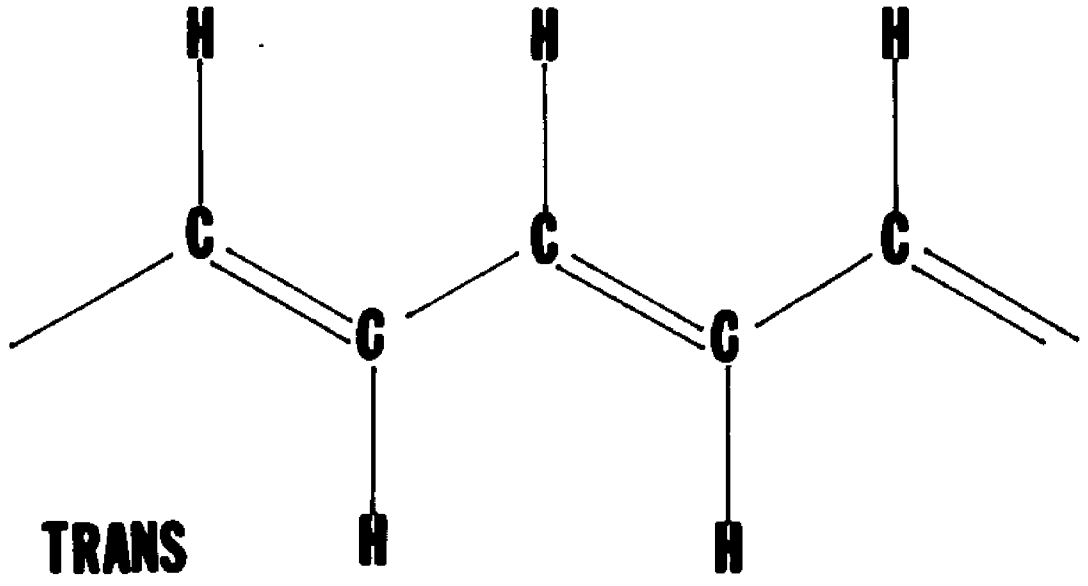

Fig.1 Molecular Structure of Cis and Trans Isomers of Polyacetylene $-(CH)_x$.

of trans out of plane hydrogen deformation band at 1015 cm^{-1} and Cis out of plane C-H deformation band at 740 cm^{-1} can be used for this purpose [17]. Under the electron microscope a Polyacetylene film is seen as a randomly oriented mass of fibers with diameter of about 200 A° and indefinite length [18]. The bulk density obtained from weight and physical volume ranges from 0.3 to 0.6 g/cm^3. Considering the floating density of 1.15 g/cm^3, it is clear that only one fourth to one half of the bulk volume of the film is really occupied by the fibre [19]. Morphology and density of Polyacetylene depends on experimental parameters such as the catalyst concentration, the acetylene pressure and the temperature of the synthesis. Depending on the conditions used the morphology of the final product may vary from free standing films to a reddish gel [20,21,22]. Radio quenching techniques have been used to determine the average molecular weight of Polyacetylene [23]. This study has shown that, Polyacetylene made by the standard procedure contains an average of 850 -CH units. In terms of elementary Quantum mechanics, using simple one dimensional particle in a box, one would immediately anticipate a high carrier mobility and carrier concentration in a conjugated structure of this magnitude. But in practice, this situation is far from being a reality. The room temperature conductivity of films of polyacetylene depends on the Cis/Trans contents of the film ranging from $10^{-5}ohm^{-1}cm^{-1}$ for the trans isomer to $10^{-9}ohm^{-1}cm^{-1}$ for the cis material [24], which is quite contrary to our expectations. In any quasi one dimensional material such as Polyacetylene, bond alternation

defect tends to set in [25]. As a result of this, alternatively long and short bonds occur and delocalization becomes self limited. In quantum mechanical sense, this situation is recognized as Peierl's distortion [4,26]. Raman study on trans Polyacetylene suggests the existence of length distribution for undisturbed conjugation [27]. Cross linking, chain bending also affect the conductivity of the material.

1.2 Polymers containing aromatic nuclei in the chain of conjugation

This class of polymers is popularly known as Polyaromatics. With regards to the conjugation, these polymers resemble Cis Polyacetylene. In this case, the continuity of the chain of conjugation is established by the aromatic rings included directly in the main chain. A few examples of this kind of materials are, P-Polyphenylene [28], Polypyrrole [29], and Polythiophene and its derivatives [30]. These polymers are now conveniently prepared by electrochemical methods. Chemical preparation is also feasible [31]. These materials especially, polythiophenes have exceptional thermal stability, 200-250°C in air and 700-800° C in an inert atmosphere or vacuum [32].

Polythiophene has a structure, which is somewhat analogous to that of Cis $-(CH)_x$ containing sp^2p_z carbons in the main chain, but stabilized by an intrachain sulphur bridge, which covalently bonds to two carbon atoms to form a five membered ring. Electrochemical synthesis of Polypyrrole or polythiophenes results in the

formation of a polymer oxidized to a certain degree. In the case of Poly-3methyl thiophene, electrochemically deposited from a solution containing $N(Bu)_4^+CF_3SO_3^-$ supporting electrolyte, oxidation levels of about 25-30% can be achieved. In other words electrochemically grafted polymer, consist of a positively charge polymer matrix, intercalated with anions from the supporting electrolyte, to preserve the electrical neutrality. Structure of Poly-3 methylthiophene is shown in the fig.2, along with that for neutral polymer, which is obtained from the as grown material by electrochemical reduction or chemically, by reacting with dilute ammonia.

The morphological structure of electrochemically prepared Poly-3methylthiophene (P3MT) has been investigated by using scanning and transmission microscopes (SEM and (TEM) [33]. SEM has revealed that, undoped thiophene polymers have "noodle" like structure, as already observed in the case of Polyacetylene [18]. The diameter of these fibers was of the order of 250 A°, but unlike Polyacetylene P3MT structure is fairly compact. Doping process has shown to be associated with an increase in diameter of these fibrills, as much as 800A° and, when the doping density became about 50%, the fibriller structure could not be detected by TEM [33]. When the polymers are grafted as thin films, the polymer surface has shown to be homogeneous, regardless of the anion of the supporting electrolyte used during the grafting process. Homogeneous films of this type made themselves very useful in applications, such as electrochromic materials [34]. Thick films are more likely to produce inhomogeneous

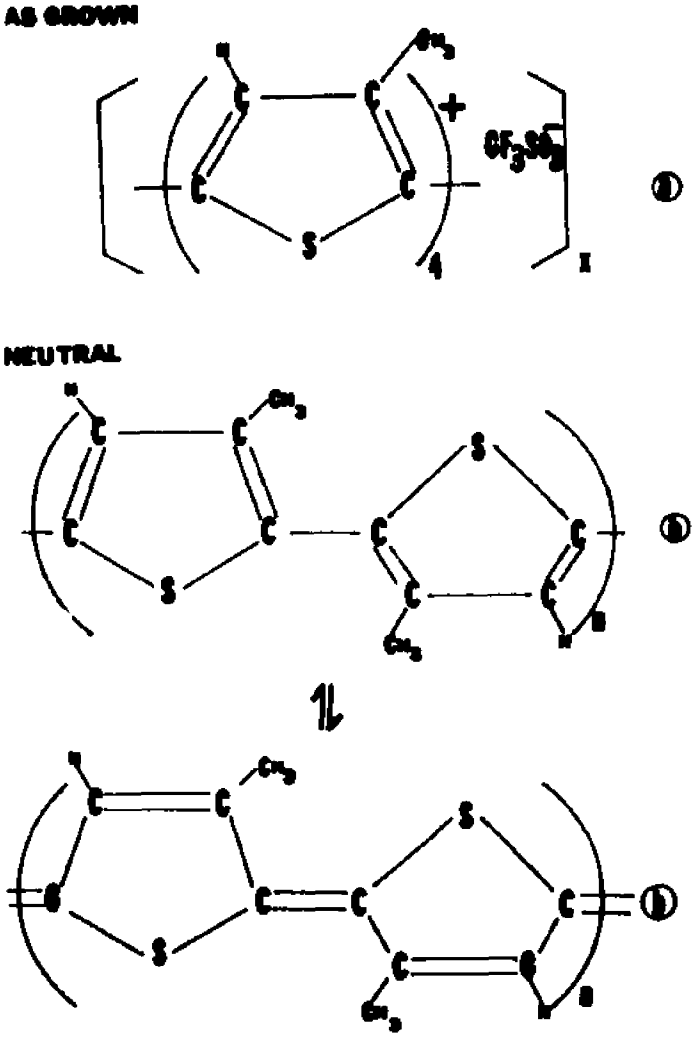

Fig.2 (a) Molecular Structure of "as grown" Poly-3Methylthiophene with an oxidation level of 25%.
(b) Molecular Structure of Neutral Poly-3Methylthiophene. Both resonance structures are shown.

surfaces. Also the identity of the intercalating anion is also important in determining the morphology of the grafted polymers. Properties of the anion such as the size, geometry, polarizability, and symmetry of the charge play a deciding role in determining the final morphology. In the case of Poly-3methylthiophene $CF_3SO_3^-$ is known to give a polymer with the highest homogeniety [33].

1.3 Electronic structure of polymers.

As seen before polyenes consist of a carbon back bone formed by C-C sigma bonds and Π bonds, originated from $2p_x$ orbitals in which the charge density is perpendicular to the plane of the molecule. In terms of an energy band description this situation corresponds to a low lying, completely filled, band formed by sigma electrons and half filled band originated from Π electrons. These Π electrons could be metallic provided there is negligibly small distortions of the carbon chain.

Electronic structure of polymers has been the focus of attention even in early years. In a theoretical study based on Huckel theory of molecular orbitals J.E.Lennard-Jones [35] concluded that, in the limit of infinite chain length C-C bonds in polyenes attain a limiting length of 1.38A°. This study was later supported by Coulson [36]. But agreement between their conclusions and experimental observations seemed not very promising [37]. Application of MO theory or free electron model to a polyene in which electrons are considered as delocalized over the entire carbon chain shows that the

energy difference between LUMO and HOMO decreases with respect to the increasing chain length. This rule worked well with lower polyenes. But experimentaly for the higher polyenes the energy for the transition to the lowest excited state reaches a limiting value of about 2 ev [37]. Bond alternation in polyenes has been accounted for this limiting value [38].

Higgins and Salim [25] carried out an in depth theoretical analysis and concluded that the most stable configuration for an infinite polymer is one of unequal bond length. Although many people advanced evidences such as optical spectra [39], direct evidence for the presence of unequal bond lengths came from X-ray measurements. This study showed that the double bond is about 0.03A° shorter. The alternating short and long bonds can be considered as a Peierl's distortion [40,41], producing a gap at the fermi energy. In Trans polyacetylene, two structures having the double bonds in the two possible positions, are possible (say A & B). The band structure for any of these degenerate structures is shown in the Fig.3, where the bond width [42], $4T_0$=10 ev and the dimerisation energy gap [43] $E_g=2\Delta=4t_1$=1.4 ev.

As stated above, there are two degenerate arrangements of Polyacetylene, A & B. One can now imagine a situation where A and B coexist in a chain with a transition region or a domain wall in between, connecting two phases with opposite bond alternation. In early calculations [44], it was shown that the domain wall contains a single unpaired spin. Further, the width of the wall

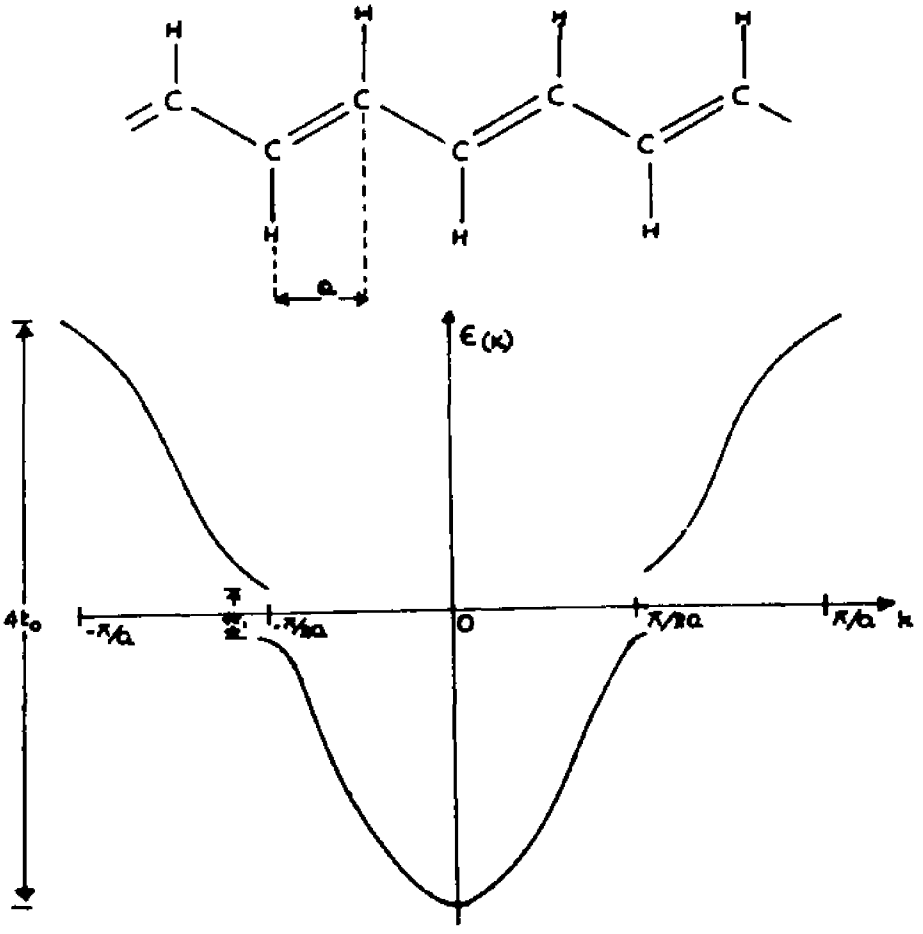

Fig.3 E-band structure of Trans Polyacetylene (after ref.4)

was assumed to be of one bond length, leading to a large activation energy for motion. But electron resonance studies [24,45] of $-(CH)_x$ suggest the presence of highly mobile, unpaired electron species even down to 10°K. In real situations we expect this transition region or domain wall extending over a number of lattice sites [5,46]. This strongly mobile domain wall is referred to as a kink soliton. It has been shown that the soliton is associated with a mid gap localized state [4,5] and this electronic state is a solution of the schrodinger equation in the presence of the structural domain wall and can therefor accomodate 0,1 or 2 electrons. Theoretical analysis has shown a charged soliton represents the smallest possible energy configuration for an excess charge on a trans $-(CH)_x$ chain. Energy for creation of a soliton is given by [4,5,47]

$$E_S = (2/\pi)\Delta \qquad [1]$$

Soliton mid gap states have been invoked to interpret an extensive body of experimental results. Electrochemical Voltage Spectroscopy ,EVS [48], combined with in situ optical studies [49] demonstrated that the charge is stored in the mid gap states. Further, EVS data give directly the threshold for charge injection and removal [50]. Analysis of these data gives a value for the soliton formation energy E_s, in good agreement with the eq.[1] given above. Vardeny et al [51] and Blanchet et al [52] have observed the pho-

toinduced absorption originating from the midgap electronic transition and the associated infrared active modes introduced by the local lattice distortions. Esmad et al [53] observed that the photoconductivity in trans $-(CH)_x$ turns on below the single particle gap and increase exponentially above threshold as hν approach 2Δ. Based on their results they concluded that the Photogenerated carriers are charged solitons generated either directly (threshold $4\Delta/\pi$) or indirectly, through the coupling of the lattice to Photogenerated e-h pairs ($h\nu>2\Delta$). Infrared spectroscopy studies [54] of lightly doped Trans $-(CH)_x$ have demonstrated spectroscopic features originating from mid gap soliton states which arise upon doping. Further, these doping induced absorptions are independent of the identity of the dopant and are therefor identified as intrinsic features of the doped Trans $-(CH)_x$ chain. Topological soliton has been invoked to analyse the magnetic resonance [45,55,57], and magnetic susceptibility [58,59] data for undoped Polyacetylenes.

These results and others involving lineshape analysis [60] indicate that both the photoinduced spectroscopic features and those induced by doping are associated with the same charge state. As in any other case there are critics, who argue against the concept of solitonic midgap levels [61]. But considering all the experimental evidences that go along with the soliton concept, odds are certainly against them.

The degenerate ground state of Trans $-(CH)_x$ is something unique. Indeed there exist many polymers analogous to $-(CH)_x$

with a nearly degenerate ground state. Examples are poly(paraphenylene) polypyrrole, polythiophene and its derivatives. For polythiophene there are two chemical structures corresponding to local minima in the Ground state, as shown in fig.2. but they do not have the same energy. This situation lifts the ground state degeneracy leading to the "confinement" of the soliton pairs into bipolorons, which is the lowest energy charge transfer configuration in such a chain [50]. Detailed theoretical analysis has been carried out for Cis $-(CH)_x$ [51] and, for Poly(Paraphenylene) [52]. It was found that, two localized electronic states appear symmetrically in the energy gap. As in the case of soliton state, these mid gap bipolorons (or confined solitons) can be readily ionized by charge transfer doping to give charged confined soliton antisoliton pairs or bipolorons with charge 2e. In a study on electrochemical voltage spectroscopy of Polythiophene, in conjunction with variation of optical absorption with different doping levels, Chung et al demonstrated the presence of bipoloron energy levels located within the gap [62]. They compared their results with the well known FBC model on polorons [63].

1.4 Doping of organic semiconductors

The charge transfer interactions between organic semiconductors and electron donors or acceptors has been studied extensively [64]. All charge transfer complexes show a marked increase in conductivity compared with either components. Interest in organic semiconducting polymers has been stimulated by the successful dem-

onstration of charge transfer doping of Polyacetylene with associated control of electronic properties over a wide range. As a result of chemical and electrochemical doping, the electrical conductivity of Polyacetylene can be varied over twelve orders of magnitude, starting from insulator ($\sigma<10^{-10}ohm^{-1}cm^{-1}$), to semiconductor, to metal ($\sigma>10^{3}ohm^{-1}cm^{-1}$), [65]. By the use of donors and acceptors n type or p type materials can be produced respectively [66-70]. Vapour of electronic acceptors $Br_2, I_2, AsF_5, H_2SO_4, HClO_4$ have been used to dope Polyacetylyne, which resulted in a p-type material [65]. The possibility of using species like $(NO)^+$ and $(NO_2)^+$ as p dopants in a solution phase [71] has also been demonstrated.

$-(CH)_x$ films may be doped electrochemically to the semiconductor or metallic regime [72]. This has been the most important and popular development in the doping process, since it opened up a simple general and readily controlable means of doping, with a variety of species, that cannot be introduced by conventional means. In this case p doping is done anodically via the electrochemical Oxidation reaction [70]:

$$-(CH)_x + xyLiClO_4 \longrightarrow [-(CH)^{+y}(ClO_4)_y]_x + xyLi \qquad [2]$$

N- type doping of $-(CH)_x$ involving electron donating i.e., "N- type" dopants can be accomplished by using a THF solution of Sodium napthalate [71].

$$-(CH)_x + 0.21x Na^+ Npth^- \longrightarrow [Na_{0.21}-(CH)]_x + 0.21x Npth \qquad [3]$$

or electrochemically, e.g: Electrolysis of a solution of LiI in THF using a $-(CH)_x$ film as the cathode. Considering the doping of pristine $-(CH)_x$, y values up to .005 are considered as lightly doped, range of y values $.005<y<0.02$ is known as the pretransitional region and at y values beyond this limit, transition from semiconductor to metal takes place [72]. Magnetic susceptibility measurements of lightly doped Trans $-(CH)_x$ have cast some light into the mechanism of doping. Below the pretransitional region, the number of Curie spins does not show any appreciable change with doping. This has been interpreted in terms of the creation of a pair of charged solitons thereby keeping the total number of spins at a constant value.

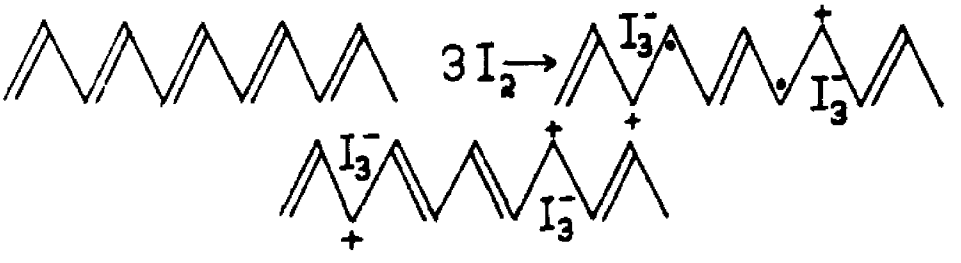

[4]

Within the pretransitional region i.e., when $y>10^{-3}$ the number of curie spins dropped sharply [58,59]. Out of several possible interpretations , the possibility of anihilation of the neutral

defects is the most probable one.

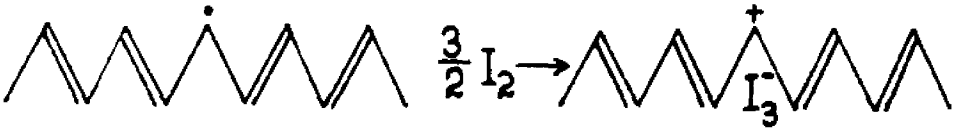

[5]

The conversion of a paramagnetic neutral soliton into diamagnetic charged soliton causes the total number of spins to decrease. In the case of polythiophene [62], or its methyl derivative, Poly 3-methylthiophene (P3MT) the story is somewhat different. Unlike Polyacetylene, which is prepared chemically, these materials are conveniently prepared electrochemically under anodic conditions. The anodic reaction involves simultaneous polymerisation and doping, and the resulting polymers show reversibility of the doping and undoping process. They can be reduced to a neutral polymer in a cathodic process [32].

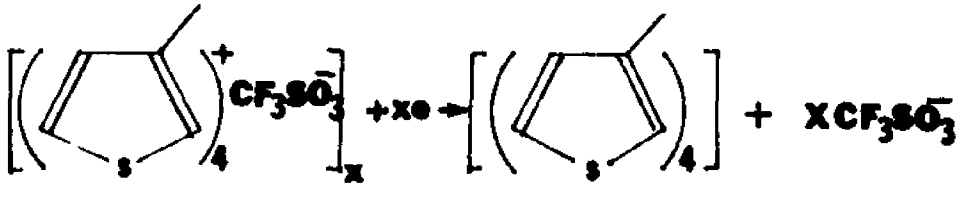

[6]

The reverse process corresponds to doping

1.5 Is bond theory adequate for Organic Semiconductors.

Traditional organic semiconductors, such as anthracene which are made of discrete molecules or, other saturated polymers such as Polyethylene are not bandgap semiconductors in the same sense as for example Si,Ge,or GaAs. The basis of this difference arises directly from the molecular nature of these organic materials. They interact very weakly through Van der Walls forces. The later results in small transfer integrals, which in turn results in a narrow band width. Very high reduced mass m^* is the direct result of a narrow band width. Consequently, transport models which are developed for inorganic metals and semiconductors may not be appropriate for organic semiconductors. In addition to this, strong electron phonon interactions and spacial variations in the local composition and structure create additional problems [3].

However, polymeric organic semiconductors with extended Π system are fundamentally different from conventional organic semiconductors. Strong interactions within the Π system makes the transfer integral t_o as high as 2 - 2.5 ev. This estimate implies a band width of the order of 8-10 ev, $w = 4t_o$ [42]. This higher band width make Polyacetylene and polymeric semiconductors with extended Π system more nearly analogous to traditional inorganic semiconductors. However transverse band width due to interchain coupling is very small and the system is regarded as quasi one dimensional [73]. The fact that the polymeric Π systems are analogous to inorganic semiconductors, has some favourable consequences. It

really justifies one's position to try various equations, that are originally derived to deal with the photoelectrochemical properties of inorganic semiconductors, even though these relationships originate from a model based on an abrupt junction between the semiconductor and the ambient. Since "abrupt junction" is hardly a reality for organic semiconductors, there must be complications arising from the static and dynamic disorder and from the porous or diffused nature of the interphase. But possibility of using equations already available to extract useful informations is extremely important to investigate otherwise, still an unknown territory.

1.6 Semiconductor/Electrolyte interface :Space charge effect

Space charge region is associated with all the Photoelectrochemical phenomena connected with semiconductor electrolyte junctions [74-77]. Because, all these processes primarily depend on the semiconductor's ability to separate charge carriers at the interface. Carrier separation takes place in the space charge region.

Assume a liquid junction is created by bringing a semiconductor into contact with an electrolyte containing a suitable redox couple. For semiconductors, electrochemical potential of electrons is given by μ_e^{sc}, which is equivalent to the Fermi level in the semiconductor. For the electrolyte, electrochemical potential of electrons μ_e^{sol} is determined by the redox potential of the redox couples present in the electrolyte and these redox potentials are also identified with the solution Fermi level. Since, the initial electrochemical poten-

tial of electrons in the two phases are different, charge is transferred from one phase to the other until the electrochemical potential of electrons in both phases becomes equal i.e.,

$$\mu_e^{sc} = \mu_e^{sol} \qquad [7]$$

The initial Fermi level difference between the semiconductor and the electrolyte is the parameter which determines the direction of actual charge transfer. In the case of a p-type semiconductor, if the Fermi level of the electrolyte is higher than that of the semiconductor, electrons will transfer from solution phase to the semiconductor phase. This process will continue until the system attains equilibrium and at the end, solution phase will carry an excess positive charge and the semiconductor, an equal but opposite excess charge. The excess charge in the semiconductor will be distributed in a region called space charge region. This region is similar to the electrical double layer in the electrolyte. The distribution of charge in the space charge region is associated with an electric field which is represented by bending of bands downwards. As a result of this band bending, an excess electrons (minority carrier in this case) will move towards the surface, while an excess holes (majority carriers in this case) will move towards the bulk. Photoelectrochemical activity of the electrode depends on this carrier separation process. The Potential distribution in the space charge region is shown in the

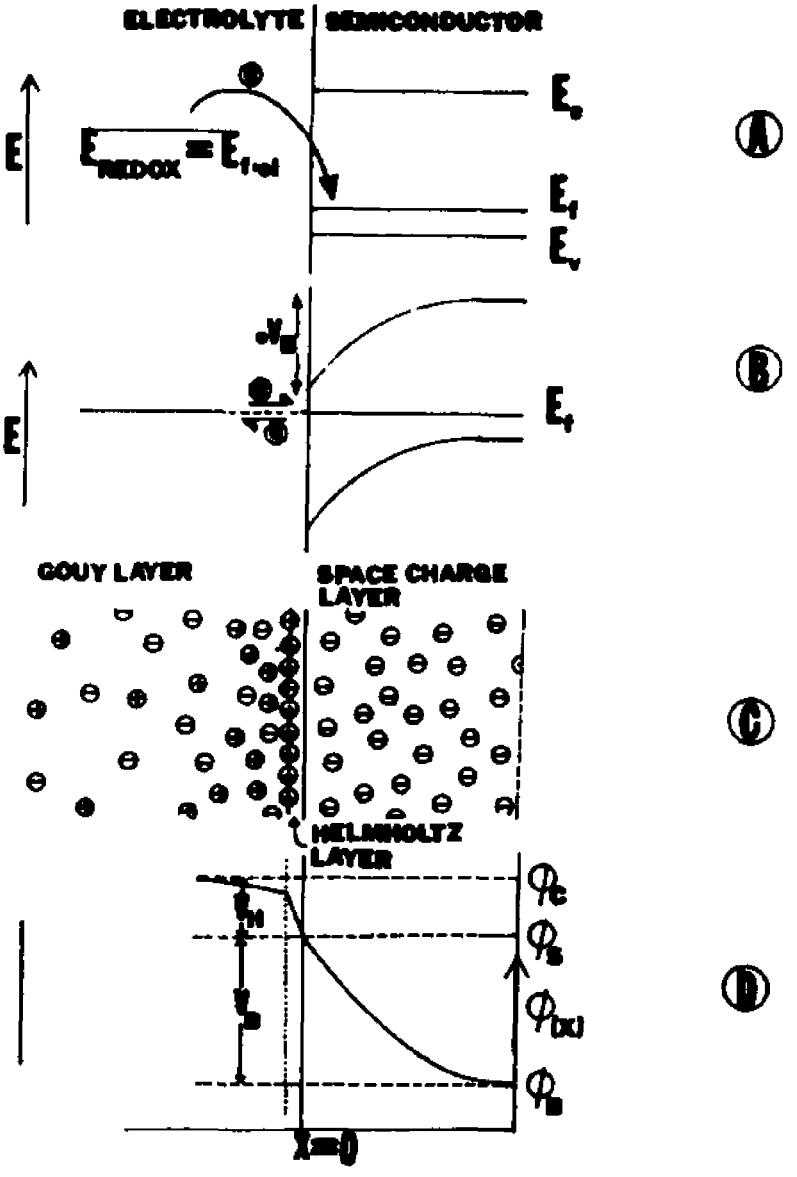

Fig.4 Schematic Representation of (a) p-type Semiconductor/ Electrolyte interface before equilibrium. (b) After equilibrium (c) Charge distribution at the Interface. (d) Electrostatic Potential distribution at the interface.

Fig. 4

The potential at which the electric field in the space charge region vanishes is referred to as the flat band potential, U_{fb}. Bands become flat and excess charge in the space charge region vanishes. It was shown [78] that the thickness of the space charge region is given by

$$d = [2\varepsilon_o \varepsilon V_B / eN_D]^{1/2} \qquad [8]$$

Here N_D is the concentration of acceptor impurities and V_B is the difference between the galvanic potential at the surface ϕ_S and that of the Bulk, ϕ_B i.e.,

$$V_B = \phi_s - \phi_B \qquad [9]$$

If one measures potentials against a reference electrode such as SCE the following relationship holds.

$$U = -V_B + V_H + V_{ref} \qquad [10]$$

Where U, is the potential measured against a reference electrode, V_B is the Galvanic potential drop in the Helmholtz region.

V_{ref} is the Galvanic potential difference between the reference electrode and bulk of the electrolyte. Since V_B is equal to zero at the flat band

$$U_{fb} = V_H - V_{ref} \qquad [11]$$

The last two equations are combined to get the following relation

$$-V_B = U - U_{fb} \qquad [12]$$

If one consider a p-type material, under depletion layer conditions (i.e., at very positive values of V_B and in the absence of surface states) Capacitance of the space charge layer is given by [79]

$$C_{SC} = \left(\frac{\epsilon\epsilon_0 N_A}{2}\right)^{\frac{1}{2}} \left(V_B - \frac{KT}{e}\right)^{-\frac{1}{2}} \qquad [13]$$

or by substituting for V_B followed by squaring

$$\frac{1}{C_{sc}^2} = \left(\frac{-2}{e\epsilon_0 \epsilon N_A A^2}\right)\left(U - U_{fb} + \frac{KT}{e}\right) \qquad [14]$$

This equation is called a Mott Schottky relationship. A plot of $1/c^2$ vs Potential U should be linear. The potential where the line intercepts the potential axis yields the value of U_{fb} and slope will give the doping level N_A. Purturbating effects such as those attributed to surface states can cause deviations from this predicted behaviour [82]. Polymers create additional problems. Polymers consist of fibrils of about 200A° of width. Since the thickness of the depletion layer is related to the doping density as given by the equation [8] there is a possibility that the physical width of the fiber could be smaller than the thickness of the depletion layer. Under this situation validity of Mott Schottky equation seems to be questionable.

1.7 Photoeffect at the Semiconductor/Electrolyte interface.

As with any other semiconductor, when the organic semiconductor electrolyte interface is illuminated with light of energy greater than the band gap, photons are absorbed and electron hole pairs are created. But as shown before [53], the Photoconductivity in Trans $-(CH)_x$ turns on before the single particle gap and this has been attributed to the Photogeneration of soliton antisoliton pairs.

The absorption coefficient of the materal as a function of photon energy is an intrinsic property of the material, and is

determined by the band structure of the material. It has been shown that near the band edge the optical absorption coefficient of a semiconductor α can be expressed as [81]

$$\alpha = A \frac{(h\nu - E_g)^{n/2}}{h\nu} \qquad [15]$$

Where hν = Photon energy, A is a constant, E_g is the band gap and n = 1 for direct gap semiconductors and n = 4 for indirect gap semiconductors. Provided the kinetics of the electrode reaction do not limit the photocurrent, one can express the Photocurrent J by

$$J = e\phi_o \left\{ 1 - \frac{\exp[\alpha W_o (U - U_{fb})^{\frac{1}{2}}]}{1 + \alpha L_p} \right\} \qquad [16]$$

Where e is the electronic charge, ϕ_o is the photon flux, α is the absorption coefficient U is the applied potential, U_{fb} is the flat band potential. L_p is the minority carrier diffusion length and W_o is the depletion layer thickness for one volt across the junction. Provided the argument of the exponent in equation [16] is small the equations [15] and [16] can be put together to give

$$\frac{Jh\nu}{e\phi} = \left\{ L_p + \omega_0 \left(U - U_{fb}\right)^{\frac{1}{2}} \right\} A \left(h\nu - E_g\right)^{-\frac{\eta}{2}} \quad [17]$$

1.8 Layout

The main objectives of this study are a) Photoelectrochemical characteristics of trans Polyacetylene and Poly 3methylthiophene, P3MT, in liquid junction cell configuration. b) EER study to investigate the optical properties of the interface.

Three experimental techniques, fundamentally used to study inorganic semiconductor/Electrolyte interface were employed in this study. Whenever possible, observations were analysed in terms of the basic concepts and mathematical relationships, basically developed to describe the properties of an abrupt interface.

In Chapter two, I will discuss the experimental details of the three techniques employed in this study. They are, Photocurrent Spectroscopy, Electrolyte Electroreflectance Spectroscopy and Relaxation Spectral Analysis. This Chapter will also include details on the sample preparation and electrode preparation etc.

Chapter three is entirely dedicated to the trans Polyacetylene /Electrolyte interface. Initially, IR measurements related to the electrochemical doping of trans Polyacetylene will be presented. The rest of the chapter includes the experimental results of Photo current measurements and EER measurements. Photocurrent measurements include investigations on the dependence of photoresponse on

the doping level and effect of soaking of trans Polyacetylene in an aqueous electrolyte on its photoresponse photocurrent/voltage, and action spectra. The EER measurements basically include, actual spectra and variation of peak height with the applied potential. Results on the Photocurrent measurements will be fitted to the Gartner model to demonstrate the "direct gap" nature of the band to band photoexcitation. EER data will be presented and an attempt will be made to fit them to a theoretical lineshape. This Chapter will also include some measurements related to achieving homogeniety in doping. Chapter.3 will conclude with a summary and the conclusions resulted from the observations made on this interface.

Chapter.4 will be dealing with the Poly 3-methylthiophene, P3MT/Electrolyte interface. Observations on "as grown", neutral and partially reduced P3MT will be presented. These observations are based on the application of all three techniques described in Chapter.2. Variation of the photoeffect with the doping density will be described. Again, applicability of Gartner model to analyse the Photocurrent measurements of "as grown" and neutral P3MT will be demostrated. EER measurements obtained for neutral and partially reduced P3MT will be analysed for their line shape. A sub band gap response observed in the EER of partially reduced P3MT will be analysed in terms of the poloron model. The strong dependence of EER signal for neutral P3MT on reverse bias (depletion) will be discussed in terms of fermi level pinning. A comparison between the doping densities estimated from the coulombic data and, from Mott

Schottky plots will be attempted Observations on the improvement of Photoelectrochemical response of P3MT by the deposition of Pt will be described. Finally, evidence for the possibility of P3MT undergoing chemical changes in aqueous electrolyte will be reported. Summary and conclusions will end this Chapter.

As the final feature of this dissertation, a comparison of the properties of Polyacetylene and P3MT based on the observations made in this study, will be presented.

Chapter 2

EXPERIMENTAL TECHNIQUES

Two major experimental techniques have been employed in this work. These are Electroreflectance Spectroscopy and Photochemical Spectroscopy. A third technique, Relaxation spectral analysis was used to a limited extend. Nevertheless all three techniques will be described. Basically, these three are different, with regard to the basic principles involved in the process that determine the system's response. EER involves electro optic characteristics of the system in question. In photocurrent spectroscopy, only the optical response of the system is sought and in relaxation spectra, electrical response of the cell consisting of the electrode in question, to a passage of an ac signal is investigated.

2.1 Electrolyte Electroreflectance Spectroscopy (EER)

The relative modulation $\Delta R/R$ impressed onto the reflected beam of intensity R by, a periodic change of an external parameter such as an electric field is the basic quantity measured in Electroreflectance [82,86]. If this external parameter is the electric field in the space charge region of Semiconductor/Electrolyte interface, the technique is called Electrolyte Electroreflectance (EER) [87]. EER is a powerful technique to study details of electronic band structure in inorganic Semiconductors [88].

As stated earlier, because of the strong interac-

tions along the chain, organic polymers with a backbone of conjugated bonds have features of wide band semiconductors. Sebastian and Wiser [89], demonstrated the usefulness of the ER method for such organic polymers.

The fundamental quantity that describes the optical response of the material is the complex dielectric function [90].

$$\varepsilon(\omega) = \varepsilon_1(\omega) + i\varepsilon_2(\omega) \qquad [18]$$

For near normal incidence, the reflectivity at the boundary surface separating the two media can be written using the Fresenel's equation as [90]

$$R = (n - n_a)/(n + n_a)^2 \qquad [19]$$

where $n^2 = \varepsilon$ and $n_a^2 = \varepsilon_a$, and n and n_a symbolize the refractive indices of the material and the ambient, which is in the case of EER, the electrolyte, respectively. Experimentally, R shows peaks in the spectrum that can be attributed to direct interband transitions at points on K space, critical points at which the combined density of states for optical transition has a singularity [90].

$$\Delta_k[E_c(k) - E_v(k)] = 0 \qquad [20]$$

In EER these critical points can be observed directly. It is assumed that the dielectric function shown above is uniformly changed by the modulation by an amount $\Delta\varepsilon_1$ and $\Delta\varepsilon_2$. As a result of this R is changed by ΔR and relative modulation $\Delta R/R$ is measured with respect to wavelength. At sufficiently low values of modulating electric field (low field regime) the ER signal for the fully depleted space charge layer is given by [86,91].

$$\Delta R/R = -\left(2eN_d V_{sc}/\varepsilon_s\right)L(\hbar\omega) \qquad [21]$$

where V_{sc} is the fundamental harmonic component of the applied voltage across the space charge layer and ε_s is the static permittivity. The quantity $L(\hbar\omega)$ is a spectral lineshape function determined by the electric field distribution and properties of the material

The spectral lineshape for each critical point in the low field regime is given by [84].

$$\Delta R/R = \mathrm{Re}\left[Ce^{i\theta}\left(E-E_g+i\Gamma\right)^{-n}\right] \qquad [22]$$

Where E_g, C, and θ are the energy gap, amplitude, and the phase factor respectively, Γ is the broadning parameter and n>2 is characteristic of the critical points for simple parabolic models. n = 3.5 is for one dimensional model, n=2 is for excitones.

EER is a powerful tool to elucidate both the optical

properties of semiconductors and the nature of charge accumulation modes at the interface which give rise to the potential distribution there. By studying the variation of the EER signal with the bias one could determine the flatband potential [92]. EER signal changes its sign at the flatband. Also the potential variation of the EER signal determines the states of the fermilevel in situ at the semiconductor/ electrolyte interface [93,94]. According to equation [21], for a fully depleted space charge region, the EER signal must be independent of the applied d.c bias. But if high density of surface states are present at the interface that are fast enough to equilibrate at the modulating frequency, then only a fraction of the modulation voltage will appear across the space charge layer. This results in the strong dependance of the EER signal on the DC bias [93,94].

Fig.5 shows the schematics of the experimental set up used for the EER measurements [83,92]. The light source is a 150 watt xenon arc lamp (Oriel), in conjunction with a high intensity monochromater (Heath model EU 700-56). The monochromatic beam of intensity I_o emerging from the monochromater is focused onto the sample by a qartz lens, and the sample is mounted on an appropriate electrode and is immersed in an electrolyte, which is contained in a glass cell with a qartz window. The cell is equipped with a reference electrode , which is usually SCE (fisher), and a Pt counter electrode. These three electrodes are connected to a potentiostatgGalvanostat (PAR model 173). A signal generator (HP 3311 A) connected to the potentiostat, supplies the modulating voltage between

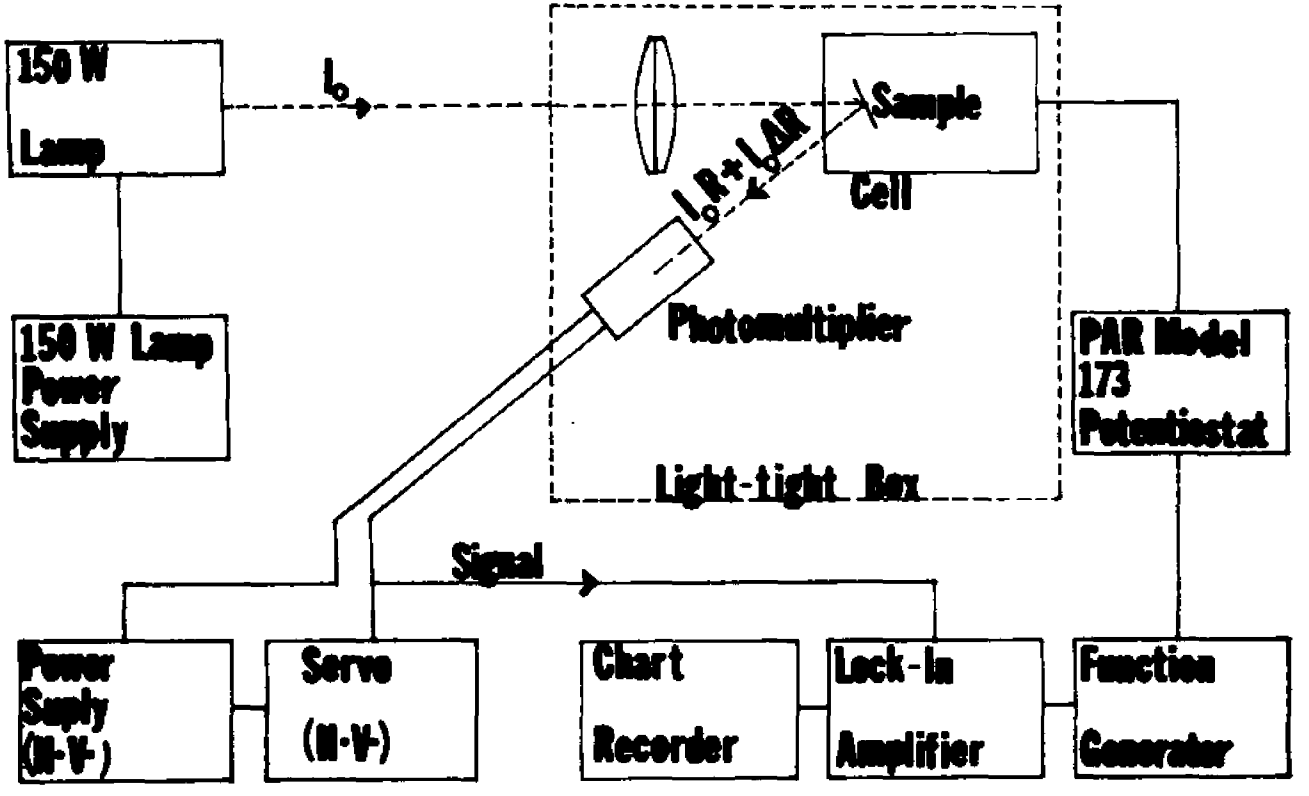

Fig.5 Schematic funtional block diagram of EER set up

the semiconductor and the counter electrode. D.C bias is derived from the potentiostat and is superimposed on the modulating voltage. The reflected light comming onto the photomultiplier has two components, a d.c component I_oR and a modulated value $I_o\Delta R$. The dc output of the photomultiplier is kept at a constant level by the use of a servo mechanism, which adjust the High voltage to the photomultiplier accordingly. The ac component $I_o\Delta R$ is detected by phase sensitive detection using a lockin amplifier (Ithaco-Dynatrac 391A Lockin analyser) with the reference signal from the signal generator. In this way the Locking amplifier gives an output which is equal to the relative reflectance $\Delta R/R$. This relative signal is fed into chart recorder.

2.2 Photocurrent Spectroscopy

The measurement of light induced photocurrent is the basis of this technique. Actual measurements can be taken either directly or using phase sensitive technique, depending on the magnitude of the photocurrent. Photoresponse of a semiconductor dipped in an electrolyte, depends on several factors such as optical properties of the semiconductor in question, Its flat band potential, position of electrochemical potentials in the semiconductor and in the electrolyte, kinetics of the charge transfer across the interface, surface states, recombination mechanisms and most importantly, The energy of the incident radiation employed. Experimental measurements in conjunction with theoretical derivation has led to the understanding of the

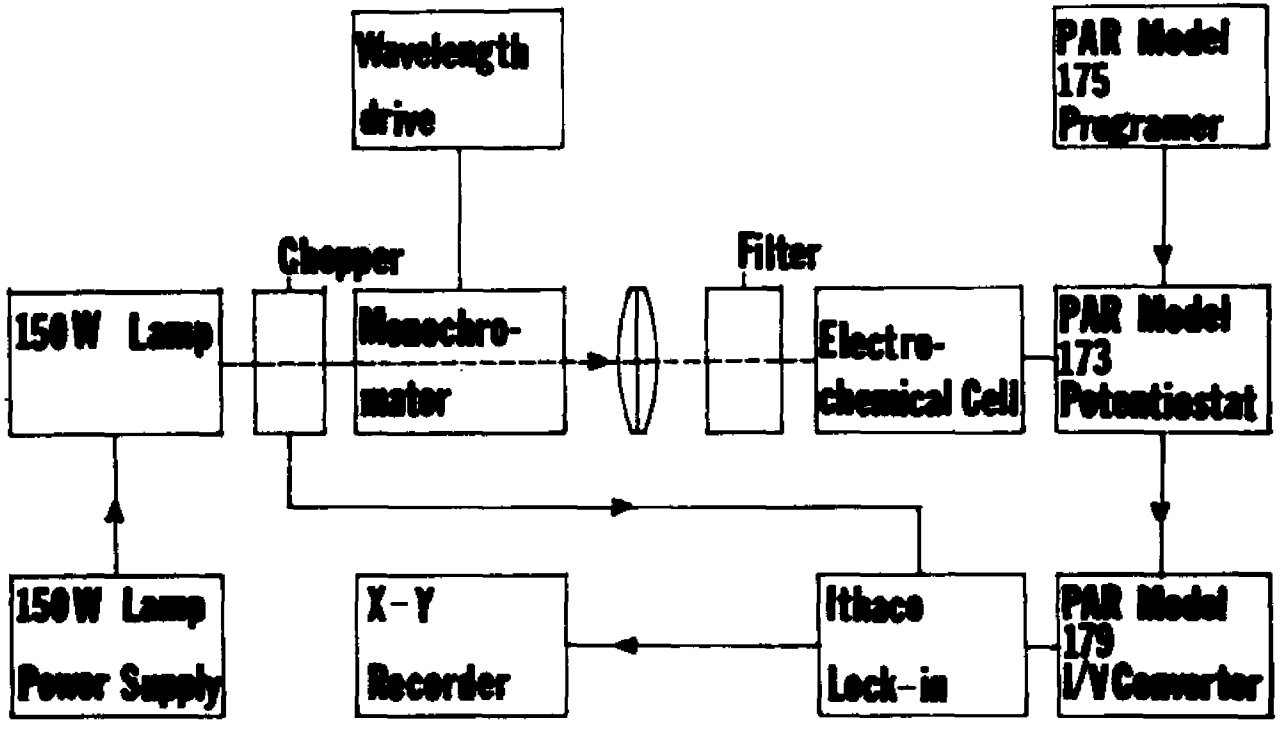

Fig.6 Schematic functional block diagram of the set up for Photocurrent Spectroscopy.

nature of semiconductor/electrolyte interface [95,99].

Fig.6 shows the schematics of the experimental set up [98] employed for the photocurrent measurements. 150 watt xenon arc lamp (Oriel) is the light source. In conjunction with it is a high intensity monochromator (Jerrel Ash). The output from the monochromator is chopped with a variable frequency chopper (Ithaco Bentham 218 F). Electrochemical cell is fitted with a qartz window and three electrode configuration is adopted during measurements. Application of potential and measurement of the current output from the cell is done by a combination of PAR 173 potentiostat, PAR 175 universal programmer, and PAR 179 digital coulometer/current voltage converter. Output from the current voltage converter is fed to a lockin analyser (Ithaco-Dynatrac 391A), which measures the photoresponse with reference to the reference signal taken from the chopper. Output from the lockin amplifier is sent to the X-Y recorder (Hewlet-Packerd 7111A).

2.3 Relaxation Spectral Analysis

This technique is based on the measurement of complex impedance over a range of frquencies starting from 1-HZ, up to as high as 13 MHz. This technique [100,101]. has been widely used to investigate the electrical properties of semiconductor/electrolyte interfaces [97,100-102]. The basic goal is to evaluate the frequency independent passive elements in an equivalent circuit representing the interface. This equivalent circuit is designed, according to dif-

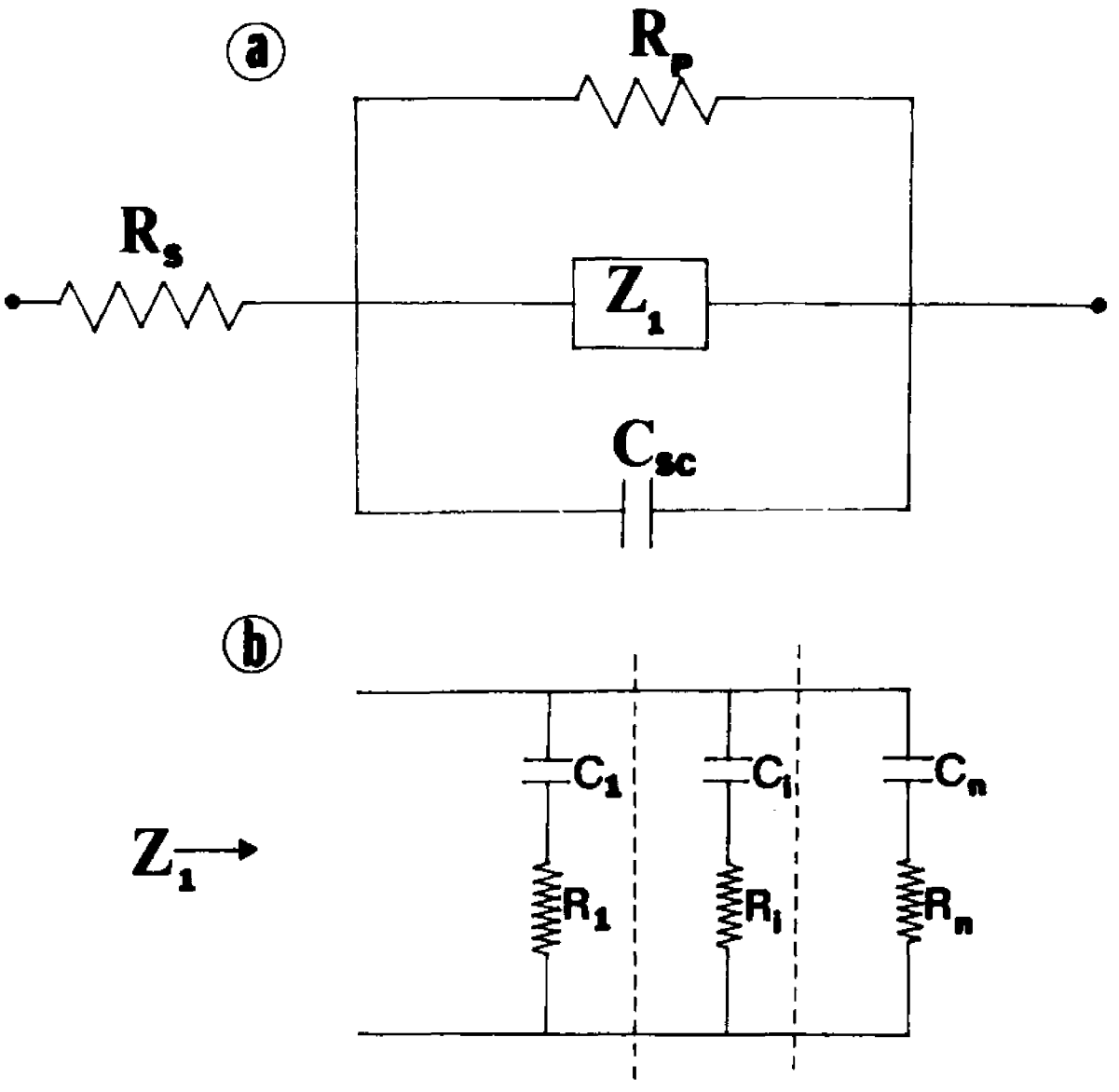

Fig.7 Equivalent Circuit of the Semiconductor/Electrolyte Interface. (see the text for details)

ferent charge accumulation modes at the interface.

Fig.7 represents the semiconductor/electrolyte interface, in which the total charge is shared among all the charge accumulation modes [100]. C_{sc} stands for the space charge layer capacitance, and R_s is the series resistance associated with the resistance of the semiconductor plus that of the electrolyte. R_p is the resistance associated with the faradaic current flow across the interface. Z_1 is the impedance of the other possible charge accumulation modes. The origin of these charge accumulation modes may be surface states or additional space charge layer with a different doping density than the main one [100]. Depending on the relaxation time each accumulation mode, Z_1 may contain more than one RC element. Heimholtz layer capacitance, C_H which should be in series with the entire equivalent circuit is deliberately not shown in fig 8(a). In a general case $C_H >> C_{sc}$ and when C_H is in series with C_{sc} one can approximate the equivalent capacitance to C_{sc} alone. Thus as far as the experiment is concerned the total capacitance in series can be considered equal to that of space charge layer, C_{sc} only. But if the inequality given above is not true, one has to correct the measured capacitance for that of Helmholtz layer, C_H [102,103].

Fig.8 shows the schematics of the experimental set up, employed for the relaxation spectral analysis. What follows is the methodology and analysis given in the original paper by Tomkiewicz [101]. The frequency synthesiser (hp 3320-B) has the capability of producing an ac signal within the frequency range from 1 Hz to 13

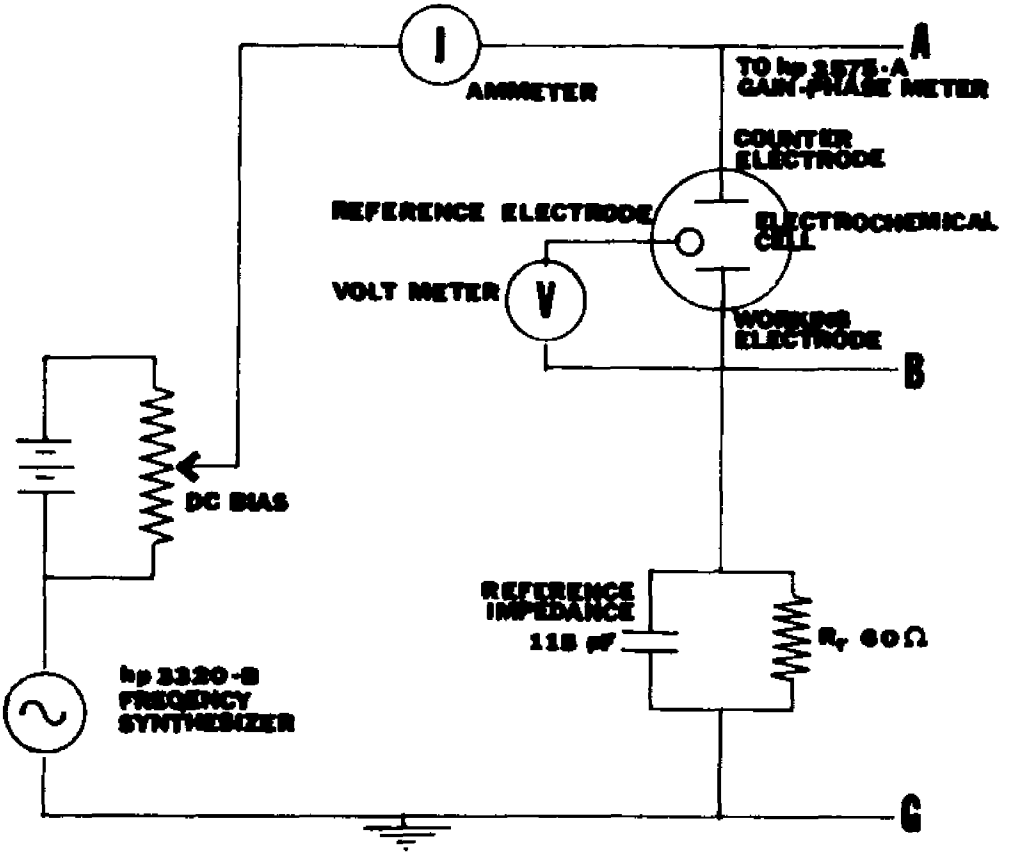

Fig.8 Schematic diagram of the experimental set up for the technique of Relaxation Analysis. (After ref.100)

MHz.

This ac signal superimposed on the dc bias, is applied across the serial combination of the sample cell and reference impedance circuit. The signal originating at A and B respectively are input to the two channels of the Gain Phase meter (hp 3575A), which measures their relative magnitude M and, the phase difference θ, this measurement is equivalent to the complex voltage ratio between the two signals at A, (E_A)and at B, (E_B) which can be expressed

$$\frac{E_B}{E_A} = \frac{Z_r}{Z_{el} + Z_r} \qquad [23]$$

where Z_{el} and Z_r are the impedance of the electrochemical cell and that of the reference circuit respectively.

$$Z_{el} = R + J(X) \qquad [24]$$

and

$$Z_r = R_r - J/C_r\omega \qquad [23]$$

Combining the equations [23], [24], and [25]

$$X = \frac{R_r}{1 + (\omega\tau_r)^2}\left[\omega\tau_r - \frac{\sin\theta}{M} - \frac{\omega\tau_r\cos\theta}{M}\right] \qquad [26]$$

$$R = \frac{R_T}{1+(\omega\tau_r)^2}\left[\frac{\cos\theta}{M} - \frac{\omega\tau_r \sin\theta}{M} - 1\right] \qquad [27]$$

Where ω is the angular velocity, θ is the Phase angle, M is the relative magnitude, and $\tau = C_r R_r$ is the relaxation time of the reference circuit. In the actual experiment one measures the R and X as a function of frequency f. Application of ac signal and measurement of the electrical response of the cell is done under computer control. Results are presented graphically as log(2Πx) and log(R) against log(f). In general for sufficiently concentrated electrolytes, the space charge layer has the smallest time constant $R_s C_{sc}$. Thus at high frequency, the network that represented in Fig.7(a), reduces to a serial combination of a single capacitor, C_{sc} and a single resister R_s. In this frequency range the impedance of the cell can be given as,

$$Z_{HF} = R_{HF} - J/\omega C_{sc} \qquad [28]$$

Thus the real part of the impedance is a frequency independent value which is equal to R_s and imaginary part of the impedance is inversely related to ω. In other words in this frequency region log(2Πx) is linearly related to log(f) with a slope equal to -1

and an intercept, from which C_{sc} can be derived. In the low frequency range, the real and imaginary part of the impedance has contributions from the other elements of the equivalent circuit. Analysis of the measured Impedance data can be extended to elucidate these RC components [100], which represent various charge accumulation modes. In the case of polymeric semiconductors Impedance technique was basically used as a means to measure the value of space charge layer capacitance and the analysis for various RC elements was not attempted.

2.4 Other Experimental Aspects.

2.4.1 Preparation of samples.

Synthesis of Polyacetylene and P3MT was carried out at Sandia National Laboratories, New Mexico, and following is the methodology which was used by them. Polyacetylene samples were prepared by the Shirikawa technique [15], using the catalytic system $(Et_3)Al$ - $Ti(Buo)_4$ in dry distilled toluene at -78°,in order to grow the Cis isomer. The acetylene was purified by bubbling through two successive concentrated sulphuric acid columns, then through a KOH column and a P_2O_5 drying column. Films were deposited on the inner surface of the glass reaction vessel, previously wetted by the catalyst solution. At the end of the polymerisation, the samples were peeled off the container wall and washed with dry methylene chloride, thoroughly to remove the excess catalyst. Finally films were treated at 160 C° for 15 to 20 minutes to effect the thermal isomerisation to

trans isomer.

Doping of trans Polyacetylene was carried out in 0.3 M propylene carbonate solution of $LiClO_4$, following the procedure published by Nigrey et. al. [70] with Li counter and reference electrodes. The doping was done under galvanostatic conditions usually at a current density of $0.1\mu A/cm^2$ to ensure doping uniformity until the desired amount of charge was passed.

Poly 3-methylthiophene (P3MT) was grown electrochemically from acetonitrile or propylene carbonate electrolyte onto clean metallic substrates (Au or Pt) by passing 100 to 300 mA anodic current pulse. The total charge passed for the growth run was typically 5 Coulombs, for a film of 6 cm^2 area. The electrolyte consisted of, distilled, dried, 0.5 M methyl thiophene with 1.0 M Bu_4N^+ $^-CF_3SO_3$ as the supporting electrolyte. 'as grown' material obtained this way could be reduced by the application of -1.0 V vs. Ag^+/Ag reference electrode in acetonitrile or propylene carbonate containing supporting electrolyte only, until the current flow becomes sufficiently small to assure quantitative reduction. In propylene carbonate where Li reference is used, one could bring the potential down slowly, starting from the open circuit potential to 2.5 Volts vs Li^+/Li and allow to stand at that potential until the current flow reduced to sufficiently low values. Most of the time, reduction was carried out in Propylene carbonate. In order to obtain intermediate doping levels, a fraction of the total recoverable charge was removed either by potentiostatic control as given above or alternatively galvanostatically at sufficiently

low current densities until the desired amount of charge is removed.

2.4.2 Electrode Configuration

special topology of Polyacetylene and its porosity demand a new electrode design. Preservation of electrode surface from any mechanical damage is of paramount importance in Photoelectrochemical experiments. Details of the working electrode configuration are shown in the Fig.9.

The gold contact plate, rubber pad and the circularly shaped sample are pressed together between two teflon plates and are tightened with two nylon screws. All the edges including the perimeter of the sample are carefully sealed with wax using a "hot" wire. This arrangement prevents the transverse flow of electrolyte into the back contact. In the case of P3MT, electrode preparation is done in a rather conventional way. Film on one side of the metal substrate is scraped and a copper wire is attached to that side with silver epoxy. Then all the exposed edges including the perimeter of the sample is covered with ordinary epoxy leaving an approximately 0.2 Cm^2 of the film exposed.

2.4.3 Chemicals

Propylene carbonate (Fisher) is distilled at 80°C under reduced pressure using a 3 ft fractionating column. Only the middle fraction is collected. This fraction is stirred with Linde 4A molecular sieves (Alfa), activated at 450° under Ar atmosphere for two days,

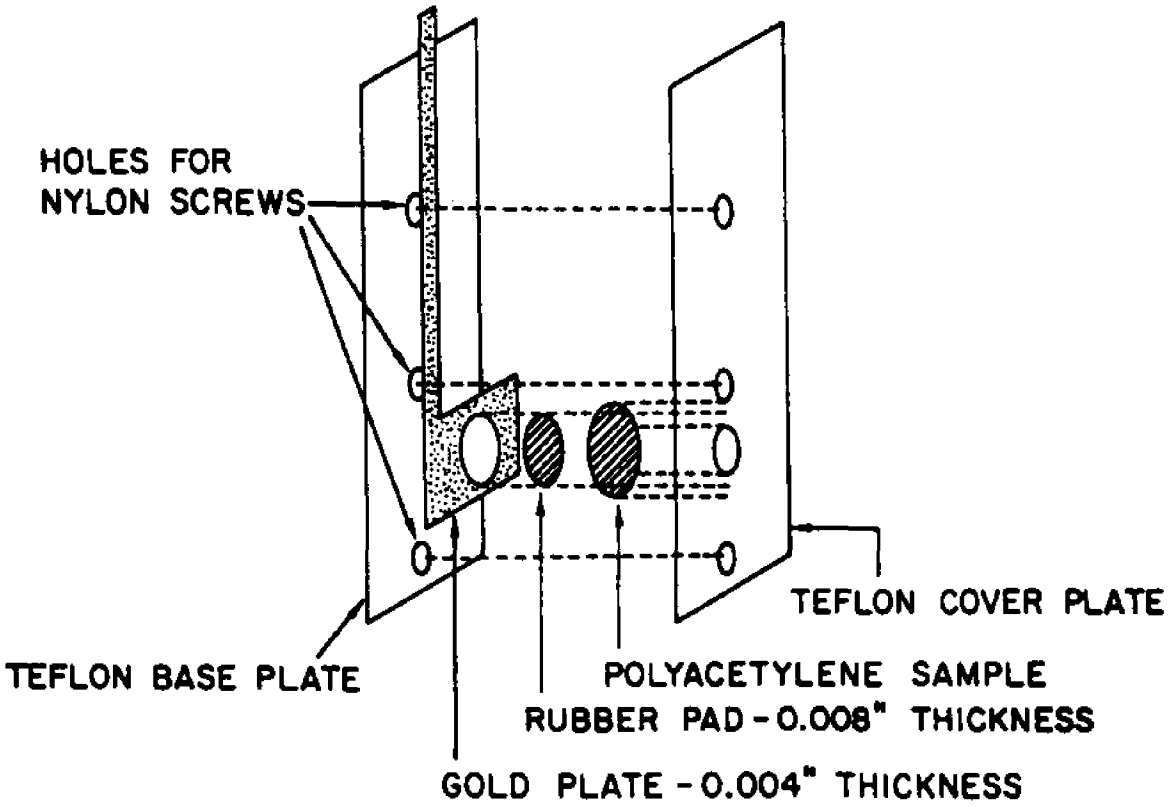

Fig.9 Schematic representation of the electrode used for Polyacetylene.

followed by filtration and vacuum distillation. Again only the middle fraction is collected. $LiClO_4$ supporting electrolyte is melted in vacuum before use. Methyl viologen (Aldrich) and Na_2SO_4 were used as received. Analytical grade Li (Fisher) is scraped in dry propylene carbonate before use and contacts are made with nickel mesh pressed onto Li. In propylene carbonate Li was used as both reference and counter electrodes. Water deionized at a millipore deionizing plant (18 MΩ) was used througout. All solutions were purged with Ar before use. Ar is purified by sending first through a column of Cu-turnings at 550°C to remove oxygen, followed by drying successively with drierite (Fisher) and P_2O_5. Organic electrolytes are handled in a dry box filled with Ar or high purity N_2. Activated neutral alumina (Fisher) is added to electrochemical cell to ensure purity of the electrolyte in it and to remove traces of moisture that are absorbed during the experiment.

Chapter 3

TRANS POLYACETYLENE/ELECTROLYTE INTERFACE.

3 : EXPERIMENTAL RESULTS.

3.1 IR and Photoelectrochemical measurements.

Fig.10 shows the IR spectra of trans Polyacetylene along with that of lightly doped material. During the actual experiment, sample was exposed to air, but repeated scans show no visible change due to absorbed oxygen. Curve 1 is for the undoped pristine material. Curve 2 represents a sample of undoped Polyacetylene exposed to air for 15 hours at room temperature. Curve 3 is for a sample doped electrochemically to an estimated density of the order of $3x10^{17}$dopants/Cm^3. Curve 4 is for a sample with higher doping concentration. Befor taking IR spectra, doped samples were washed with propylene carbonate and water followed by drying thoroughly in vacuum. The prominent features of curves 2 and 3 are the doping induced bands at 1400 cm^{-1} and 887 cm^{-1}.

Fig.11 shows the variation of photoeffect with potential as a function of dopant concentration. The doping was carried out galvanostatically at 100 nA/cm^2, until a desired amount of charge was passed through. The resulting doping density was calculated in terms of the charge passed, by assuming 100% current efficiency. Each data point was taken few minutes after the application of the potential step, to ensure minimum error due to capacitive transients. The Pristine polymer and the doped material corresponding to Curve 6 in

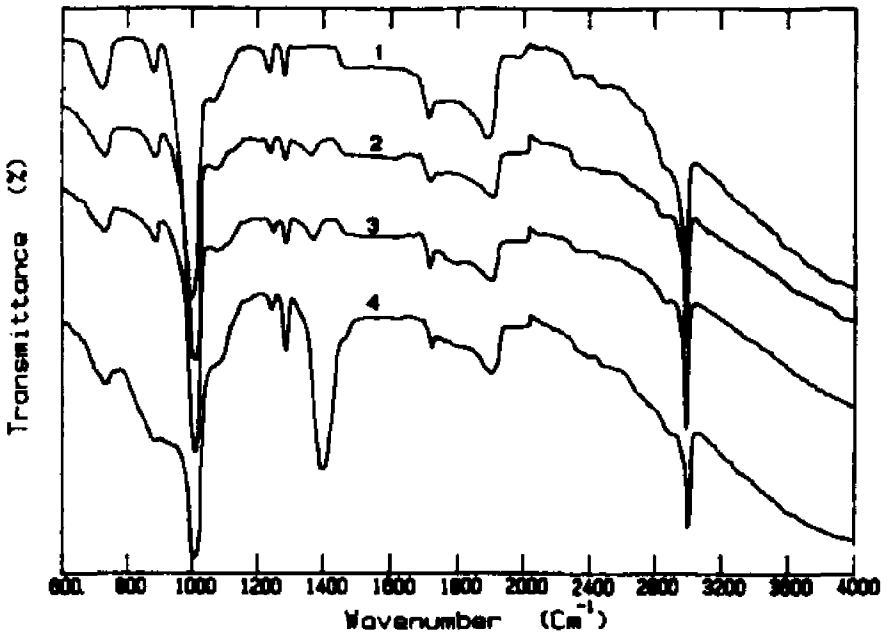

Fig.10. IR Spectra of Trans Polyacetylene.

1) pristine trans Polyacetylene.

2) Pristine Polymer after 16 Hrs.of exposure to Air.

3) Lightly doped polymer (N_d* $10^{17}/cm^{-3}$)

4) Polymer with a higher doping density. (N_d* $6x10^{18}/cm^{-3}$

TABLE - 1

TIME	Q-mC/Cm^2 CATHODIC	I-PHOTO -1.0V nA	I-PHOTO -0.7V nA	I-PHOTO -0.2V nA	I-PHOTO +0.4V nA	Q-mC/Cm^2 ANODIC	I-PHOTO +0.4V nA
10 min	17.03	3.75	4.05	2.55	1.5	18.0	1.8
25 min	31.0	6.3	6.45	3.75	2.86	34.0	1.5
50 min	62.0	7.8	10.9	5.5	4.0	64.0	1.3
100 min	97.5	14.0	13.5	10.05	10.35	97.0	1.3
11 Hrs*	-	57.75	49.5	23.0	12.5	-	-
16 Hrs*	-	61.50	54.0	28.0	15.5	-	-
24 Hrs*	-	69.0	61.0	34.5	19.0	-	-
36 Hrs*	-	69.5	63.0	35.5	19.5	-	-

* STANDS FOR "OPEN CIRCUIT"

Fig.11, generally occupied the same position in the figure while the maximum doping density falls in between.

Table.1 tabulates the photocurrent/voltage data for polyacetylene in viologen electrolyte. A fresh, lightly doped material with optimum photoeffect was used here. Originally the potential was stepped down to -1.0V vs. SCE and allowed to stay for some time before measuring the photocurrent. The cathodic charge passed at -1.0V vs. SCE was recorded. Then the potential was shifted to -0.7 v,-0.2 v, and +0.4 v, in successive steps, and the photocurrent at each step was measured. Finally the electrode was allowed to stay at +0.4V until the passage of an anodic charge which was equal to the cathodic charge passed at -1.0V vs. SCE. At the end the photocurrent at +0.4V was recorded.

Fig.12a illustrates the evolution of photocurrents in viologen electrolyte as a function of soaking-time. The electrode was allowed to soak in the electrolyte for some time and the potential was stepped up starting from -1.0V vs. SCE to -0.7,-0.2,+0.4V vs. SCE successively. After a brief pause at each step photocurrent was measured and the observations are tabulated in Table.2 as a function of cumulative soaking-time.

Fig.12b illustrates the measurements taken in an experiment similar to the one described above, but using Na_2S,S,NaOH (1:1:1) as the electrolyte.

Table.3 tabulates the results of an experiment, parallel to the one used to obtain the results shown in Fig.12a. But in this

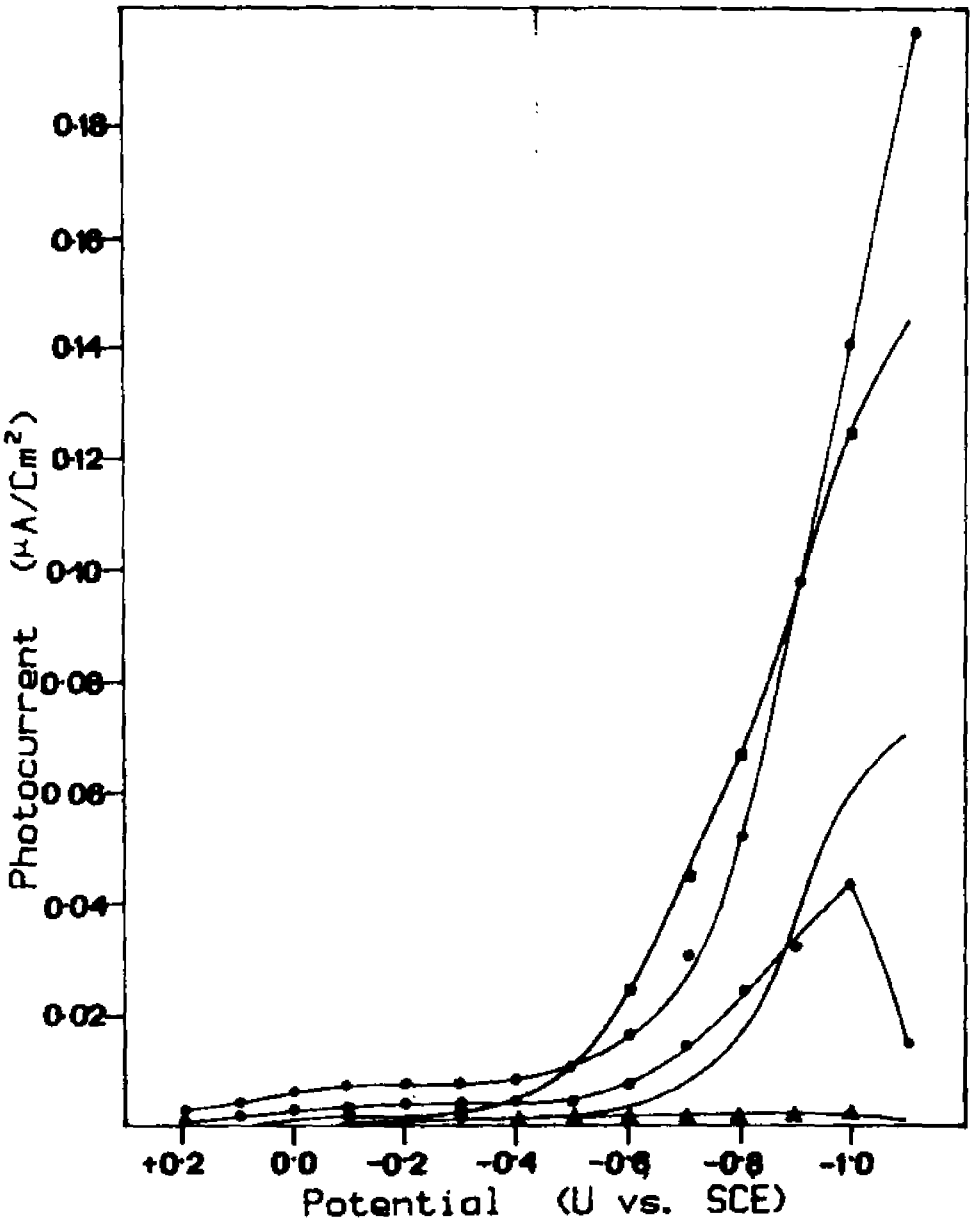

Fig.11. Photocurrent vs.potential plots for lightly doped trans Polyacetylene with different doping densities. aq.0.2M Na_2SO_4 and 20mM Viologen Illumination 410nm, Intensity 0.35 mW/cm^2

(-●-●-●-) $N_d=4x10^{17}$ (-●-●-●-) $N_d=8x10^{17}$

(-⊡-⊡-⊡-) $N_d=1.6x10^{18}$ (———) $N_d=3.2x10^{18}$

(-▼-▼-▼-) $N_d=6.4x10^{18}$

Table.2 : Evolution of photocurrents of lightly doped trans -$(CH)_x$ in viologen electrolyte as a function of Soaking time.

Time Hours	Photocurrent nA/Cm^2 at -1.0 v	-0.7 v	-0.2 v	+0.4 v
0.0	22.0	12.9	7.2	3.1
0.5	34.5	22.8	9.2	3.4
1.0	41.5	30.0	10.3	2.7
1.5	47.5	31.0	10.1	3.0
2.5	63.0	37.0	13.4	1.8
4.5	84.0	48.0	12.0	1.0
6.0	100.5	46.0	10.8	1.0
8.5	105.0	45.0	11.7	1.5
10.5	99.0	51.0	12.3	1.2
24.5	87.0	41.0	8.7	1.7
26.5	82.5	34.0	9.0	1.5

* all potentials vs. SCE

case lightly doped Polyacetylene already soaked for nearly 11 Hours in aqueous Na_2SO_4 was used. Testing for the photoeffect was done in viologen electrolyte. The photocurrent at several potential steps were measured as described above. Even though soaking in the electrolyte has a favourable effect on the overall Photoeffect, the later always deteriorated at anodic potentials. For example, photoactivity of an electrode improved through soaking deteriorated gradully, to undetectable levels, when it is kept at +0.4V vs. SCE for a pro-

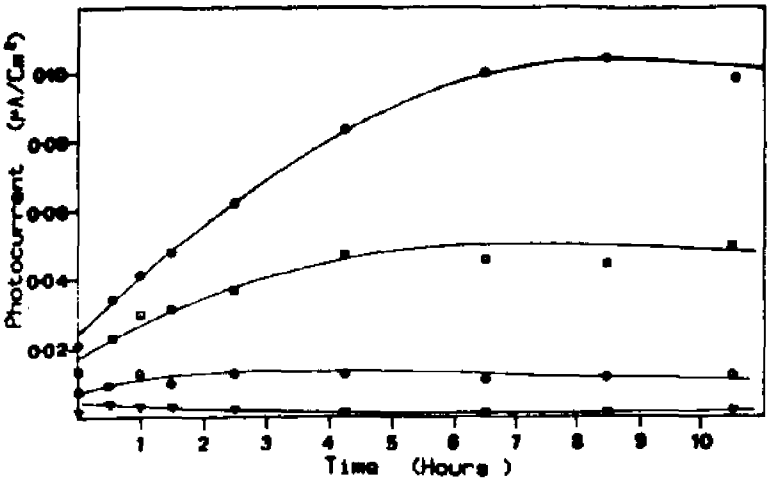

Fig.12a. Evolution of the Photocurrent with soaking-time, for Lightly doped Trans-Polyacetylene in aq Viologen Electrolyte.
(-●-●-●-) -1.0 v (-●-●-●-) -0.2 v
(-●-●-●-) -0.7 v (-▼-▼-▼-) +0.4 v

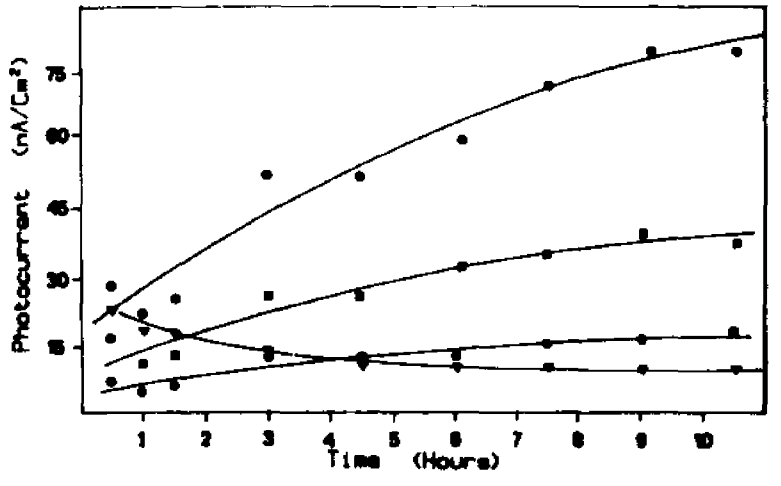

Fig.12b. Evolution of Photocurrent with soaking-time, for Lightly doped Trans-Polyacetylene in aq. Sulfide electrolyte, NaOH:S:Na_2S (1:1:1:), Same conditions as in Fig.11.
(-●-●-●-) -1.0 v (-●-●-●-) -0.2 v
(-●-●-●-) -0.7 v (-▼-▼-▼-) +0.2 v

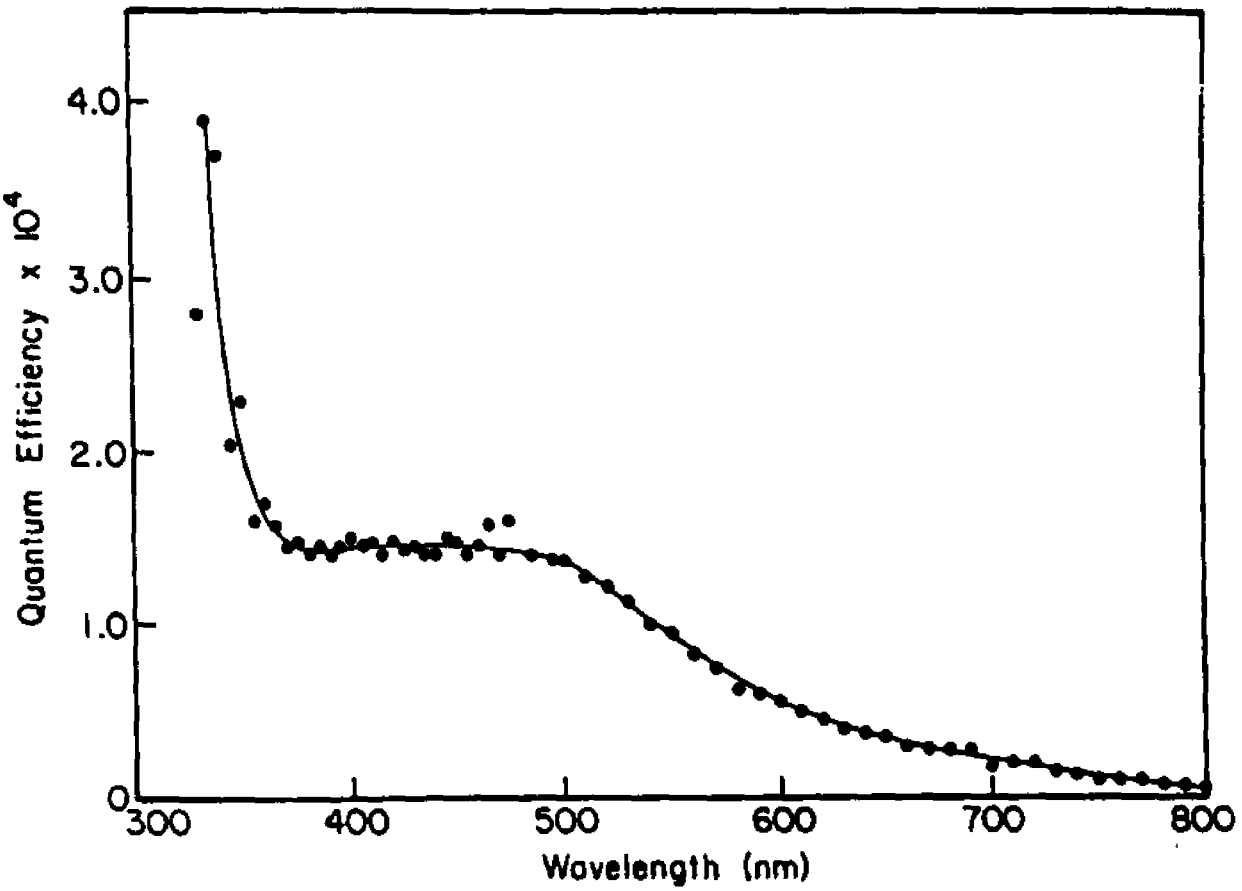

Fig.13. Spectral response of the Quantum efficiency of the Photocurrent of lightly doped trans Polyacetylene. Same conditions as in Fig.11., Potential 0.0 v vs. SCE.

Table.3 : Variation of photocurrent of a trans $-(CH)_x$ electrode already soaked for 11 hours in aq.Na_2SO_4 as a function of time at different potentials.

Time	Photocurrents nA/Cm^2 at			
Hours	-1.0 v	-0.7 v	-0.2 v	+0.4 v
0.0	55.3	33.0	14.2	2.1
1.5	62.0	33.0	13.8	2.3
3.0	57.0	31.0	13.8	2.2
4.5	62.3	29.0	12.9	2.1
8.0	59.0	30.0	13.0	2.2

longed period. But again the photoeffect could be partially rejuvenated just by allowing the electrode to stand in the electrolyte under open circuit conditions. Measurements taken in this experiment are tabulated in Table.4. The spectral response of an electrode with optimum doping density is shown in Fig.13. Absolute quantum efficiencies are low. The photoresponse, turns on in the vicinity of 800 nm, and then begins to rise gradually till 500 nm and then increases dramatically towards shorter wavelengths.

3.2 Electrolyte Electro Reflectance (EER) measurements.

EER spectra of lightly doped Polyacetylene taken at different electrode potentials are shown in Fig.14a. The spectrum 1 is shown again in Fig.14b for the sake of clarity. Dopant concentration of this sample is of the order of 3.2×10^{18} Dopants/Cm^3. Two peaks

Table.4 : Rejuvenation of the photocurrent of an $-(CH)_x$ electrode after a prolonged stay at +0.4 V vs.SCE, through soaking.

Time	Photocurrents nA/Cm^2 at			
Hours	-1.0 v	-0.7 v	-0.2 v	+0.4 v
0.0	1.3	0.6	0.3	
0.5	1.5	0.8	0.4	
1.5	2.5	1.2	0.8	0.3
3.5	5.0	2.1	1.4	0.5
5.5	12.0	5.1	2.5	1.1
7.5	15.8	7.5	3.1	1.6
9.5	19.2	9.0	3.5	1.8
11.5	18.7	8.9	3.2	2.3
21.5	17.6	8.2	3.1	2.5

were observed at negative potentials, one at 1.45 ev and the other at 1.6 ev. But in the region of positive potentials, this simple spectrum gave way to a fairly complex spectra with a very broad structure centered around 2.1 ev with a width well over 1.5 ev. The peak height of both EER signals present in spectrum.1 varied linearly with the modulating amplitudes as high as 0.6 volts. Thus the modulation amplitude of 0.5 Volts used in taking this spectra satisfied the low field requirement. Variation of EER peak height with potential is shown in Fig.15. EER signals at 1.45 ev and 1.6 ev started low at -1.0V vs. SCE and then attained a maximum around 0.0V vs. SCE.

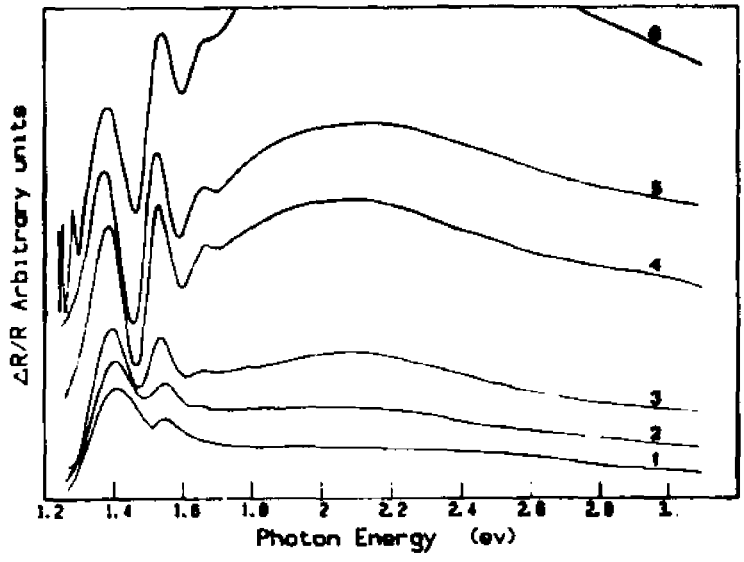

Fig.14a. EER of Lightly doped Polyacetylene (N_d = 3.2×10^{18} cm^{-3}

1) -0.5 v 3) 0.0 v 5) +0.45 v
2) -0.25 v 4) +0.25 v 6) +0.75 v
all potentials vs. SCE.

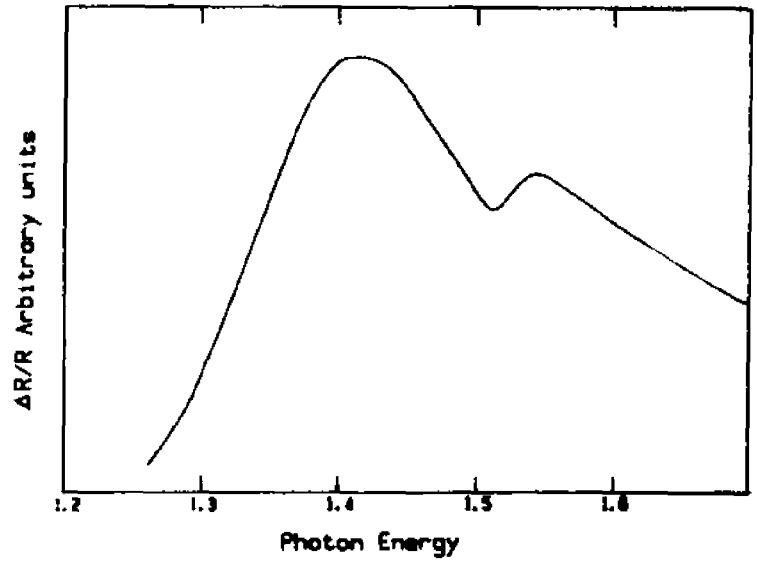

Fig.14b. Spectrum marked 1) shown in the Fig.19a.

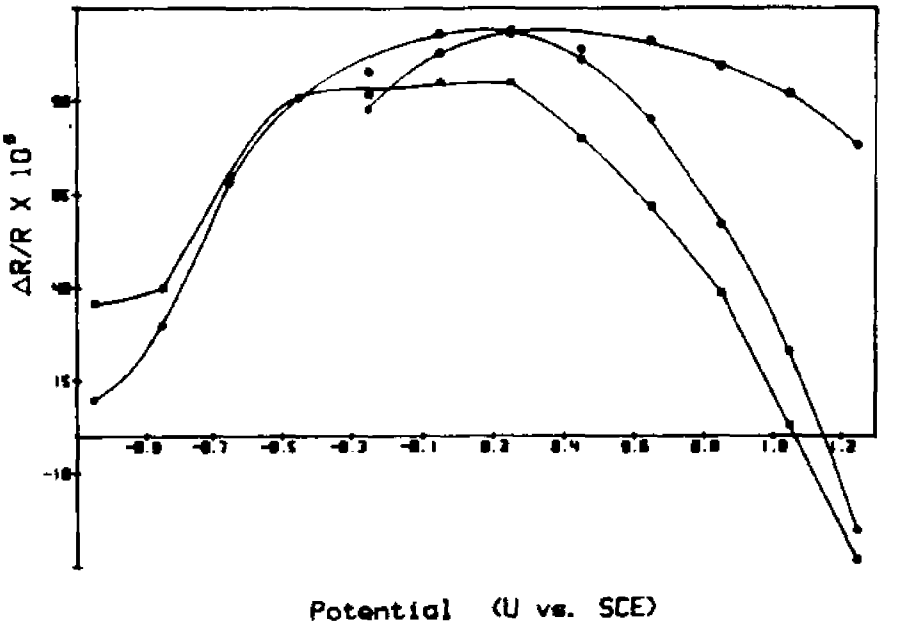

Fig.15. EER peak amplitude of lightly doped trans Polyacetylene as a function of the electrode potential, in aqueous Viologen electrolyte.
(—●—●—●—) Peak at 2.1 ev (—●—●—●—) Peak at 1.55 ev
(—●—●—●—) Peak at 1.4 ev.

In the region of potentials positive to maximum, both signals assumed a steep decline and finally crossed the x axis in the vicinity of +1.0V vs. SCE. The peak at 2.1 ev which began to appear at potentials positive to -0.2V vs. SCE, passed through a maximum around +1.0V vs. SCE and then decline slowly towards more positive potentials. Experimental conditions used in the EER measurements were the same as in photocurrent measurements.

3.3 Measurements related to achieving homogeniety of doping.

One of the factors that determine the electrochemical behaviour of semiconductor electrodes is their homogeniety. Non linear Mott- Schottky plots or EER spectra with excessively broad peaks and distorted line shapes are often connected with the lack of homogeniety. Low conductive materials, especially Organic polymers, are extremely prone to produce inhomogeneously doped materials. This problem is even worse for Polyacetylene, because dopants are initially introduced into a polymer matrix which is almost an insulator. There is experimental evidence supporting the fact that gas phase doping often produces an inhomogeneously doped material unless special experimental procedures are adopted [72]. The rate of introduction of dopants into the polymer is an important factor which determine the homogeniety of the final product. In the case of electrochemical doping, the rate of introduction of dopants can be controlled by regulating the current density. During the experimental procedure described below, doping is done galvanostatically and evolution of the Cell volt-

age of Polyacetylene/0.5M $LiClO_4$ in Propylene Carbonate/Li Cell is monitored as a function of different current densities.

The electrochemical Cell was constructed by using a sample of Polyacetylene as a working electrode and Li as the counter and reference electrode. Initial potential was found to be in the vicinity of 3.1 V vs. Li. Then the doping was carried out by passing a constant anodic current through the cell. After a certain time interval the process was interrupted and the cell was allowed to stabilize for some time (about 1 min) before measuring the cell voltage. Doping is resumed until the next voltage measurement. At higher current densities, the cell voltage showed a steep rise at the onset of doping, and immediately returns to a slowly ascending plateau. Steep rise of the cell voltage at the onset is indicative of the inhomogeneous nature of the doping process. As the current density was brought down the initial sharp rise in the Cell potential which was observed at higher densities, became more gradual and the plateau was reached at higher doping charge. The gradual evolution of the cell voltage is indicative of a homogeneous doping process.

Fig.16 indicates the results obtained in these measurements. At each current density the cell was doped until the passage of 21.4 mC/Cm^2, corresponding to a calculated doping density of 6.44 x 10^{18} dopants/Cm^2. At the end of the doping process, resistance of a film of 0.5 Cm x 0.2 Cm was measured parallel (R_{AC}) and perpendicular (R_{AB}) to the film surface by using pressed platinum contacts. Table.5 shows the results obtained in these resistivity meas-

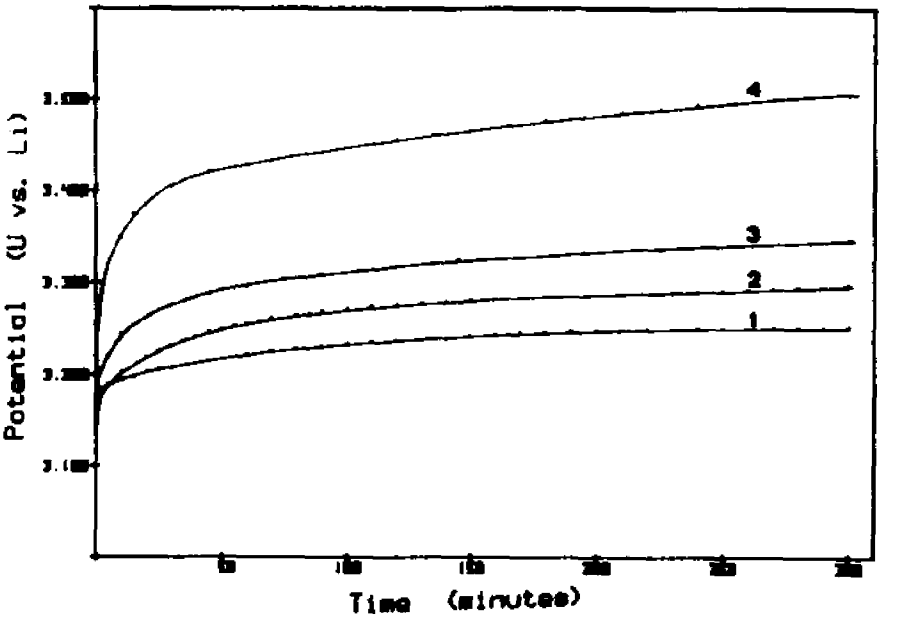

Fig. 16. Development of opencircuit voltage of trans Polyacetylene/ 0.5M $LiClO_4$ in Propylene Carbonate/Li cell, with time in response to the charging under Galvanostatic conditions.

1) 0.2 $\mu A/cm^2$ 3) 1.25 $\mu A/cm^2$

2) 0.5 $\mu A/cm^2$ 4) 5.0 $\mu A/cm^2$

urements. The third column of the table shows the open circuit voltage of the cell after the passage of 21.4 mc/cm^2, at the specified current densities given in the first column of the same table.

Table.5 : Conductivity measurements of $-(CH)_x$ doped at different current densities.

$\mu A/cm^2$	R_{AB}	R_{AC}	V_{OC}
5	$2.3x10^5$	$1.6x10^6$	3.43
1.25	$2.5x10^5$	$3.1x10^7$	3.34
0.5	$1.7x10^5$	$6.0x10^7$	3.327
0.2	$2.3x10^5$	$5.0x10^7$	3.28
0.05	$2.0x10^5$	$8.7x10^7$	3.19

Diagram.1 : Diagram showing the press contacts made to a Trans Polyacetylene film.

3 : DISCUSSION AND CONCLUSIONS.

3.4 IR behaviour of Electrochemically doped Polyacetylene.

IR spectra shown in Fig.10 are in agreement with the published data on Trans Polyacetylene [17]. IR bands at 1000 cm^{-1} and 740 cm^{-1} are attributed to out of plane C-H deformations of Trans and cis Polyacetylene respectively. Bands at 1290 cm^{-1} and 1240 cm^{-1} are assigned to Trans and Cis , C-H in plane deformations. Presence of both sets of these bands in the IR spectra of trans-Polyacetylene used in this study, indicates the presence of cis material, which was estimated to be around 7%. Cis and Trans contents of a Polyacetylene specimen can be estimated by the use of the following formula [18].

$$\text{Cis content } (\%) = 100[1.3\ A_{cis}/(1.3\ A_{cis} + A_{trans})] \qquad [29]$$

Where A_{cis} and A_{trans} stand for the absorbances of the 740 and 1015 cm^{-1} bands in the spectrum of a sample respectively. The most important feature shown in the spectra 3 and 4 in the Fig.10 is the appearance of additional bands in the spectra upon doping. Bands at 1400 cm^{-1} and 887 cm^{-1} (0.17ev, 0.11ev) have been attributed to local IR modes of the charged Solitons. The intensity of solitonic bands increases with the increasing amounts of charge used during the electrochemical doping. This indicates the effectiveness of the doping procedure adopted in our laboratory. Spectrum 4 in the Fig.10 corresponds to a sample with a Cis content of nearly 11%. This observation is in keeping with the reported observation

that Cis/Trans isomer ratio of a Polyacetylene specimen is altered as a result of doping. Another aspect that requires mentioning is the change in the IR spectrum upon exposure to Air. Again a weak band appearing at 1400 cm^{-1} suggests the possibility of air (oxygen) acting as a dopant also. But no additional bands due to oxygenated material are observed.

Assuming a 100% charge efficiency one can calculate the Doping density in terms of the quantity of charge used during the doping process. Assuming the bulk density and the Floating density of trans Polyacetylene as 0.4 and 1.2 g/cm^3 respectively, an anodic charge of 3×10^{-4} C used to oxidize a sample of 1 cm^2 area and 0.25 mm thickness would results in a doping density of 2×10^{17} dopants/cm^2. This doping density would correspond to an oxidation level of 0.0004%, which is extremely small and well below the semiconductor-metal transition region.

3.5 Photoeffect at the Lightly doped Polyacetylene /Electrolyte interface.

3.5.1 Photoeffect as a function of doping density.

As in the case of Inorganic semiconductors, conductivity of the polymer increases with, increasing doping density. This would enhance the photoeffect of the material. But at the same time additional effects, such as increasing degeneracy of impurity levels, recombination through defects, and decrease in space charge layer thickness, would accompany the higher doping densities. Higher

doping densities would alter the potential distribution at the semiconductor/electrolyte interface in such a way, a significant portion of the potential drop between the semiconductor and the electrolyte appear in the Helmholtz part of the interface. This would lower the electric field within the space charge region, thereby lowering the effectiveness of the photoinduced charge separation. Because of the higher resistivity of the pristine (undoped) material organic semiconductors have additional problems related to inhomogeniety of the distribution of dopants. As a result of these effects of opposing nature, photoactivity of a semiconductor generally passes through a maximum, with increasing doping density. Data shown in Fig.11 are related to optimising the doping density for the highest photocurrent. Starting from positive potentials the photoeffect rises towards the negative potentials. This agrees with the p-type conductivity of the lightly doped trans Polyacetylene. The turn on potential seems to be positive to +0.25 V vs. SCE. Cathodic peak for the one electron reduction of MV^{++}, is in the vicinity of -1.0 V vs. SCE. Unlike inorganic semiconductors, the photoeffect follows the increase in dark current towards negative potentials and it goes through a maximum positive to the dark current peak. This behaviour again is expected for a p- type semiconductor. Electrode with optimum doping density showed a photovoltage of 80 to 150 mv.

Overall shape of the photocurrent voltage curves shown in Fig.11 are indicative of an electrode with a large series resistance. Because of the low doping levels used, the electrodes

used are indeed very resistive. The magnitude of the photocurrent was found to be insensitive to the distance between the counter and working electrode. This indicates, that the resistance of the electrolyte does not contribute significantly to the over all series resistance. Fig.11 indicates that there is an optimum doping density for the photoresponse of the material. In this region of doping densities electrical conductivity of the material shows a very steep rise [67,69] This effect when combined with the variation of properties of individual samples (morphology etc.) would lower the precision of these photocurrent measurements. Another feature worth mentioning is the photoeffect in the region of positive potentials. Curve 2 and 3 of Fig.11 show higher Photoresponse while samples with higher doping levels show little or no photoactivity. This indicates the influence of recombination effects in the direction of forward bias, which is more severe when the doping density is high.

3.5.2 Influence of Soaking on thp Photoeffect of lightly doped Polyacetylene.

As shown in the Table.1, the time spent by the electrode at -1.0 V vs. SCE appears to have a marked influence over the magnitude of the photoeffect. The cathodic charge passed at -1.0 V vs.SCE seems to have a favourable effect on the photocurrent. As shown in Table.1 over all photoeffect within the span of -1.0 V vs. SCE to +0.4 V vs. SCE is increased. At the same time anodic currents seem to reverse this gain in photoeffect, regardless of the

amount of charge involved (column 8, Table.1). This observation is in agreement with the situation in which, the dopants are mobile and the doping can be changed by manipulating the electrode potential. But there is a fundamental problem with this speculation. As mentioned before, Polyacetylene acquires it's doping through a process in which the polymer matrix undergoes oxidation, thereby creating charge soliton carriers. Fundamentally this kind of a process is favored only at anodic potentials, which is quite opposite to our observations. Besides, the amount of charge involved is so high, if used in 100%, efficiency of the resulting material would possibly show no photoeffect, because of the high doping density. The reason for this increase in photoeffect at cathodic potentials is not clear, but it is speculated that, adsorption of a reduced solution species facilitates the heterogeneous electron transfer across the interface. But the most interesting aspect shown in table.1 is the significant gain in photocurrent when the cell is allowed to stand open circuit. This indicates that another factor, which is not taken into consideration yet, contributes to the photoeffect. Surprisingly, the electrode receives this gain by just sitting idle in the electrolyte. Results given in the table.2 are aimed at providing an understanding of this phenomenon. As illustrated in the Fig.12a and Table.2, soaking seems to have a favourable influence on the photoeffect. Photocurrent reaches a maximum value in about 10 hrs of soaking. Since a parallel effect is observed in sulfide electrolyte, as shown in Fig.12b it is obvious, that the increase of photocurrent with soaking-time does not

depend on the identity of the redox material. Effect of soaking is further established by the time invarient photoeffect observed for an electrode already soaked in aqueous electrolyte for 10 hrs as shown in Table.3 The effect of foreign materials adsorbed on organic solids has been widely studied [104]. Soaking of a crystalline polymer surface by a polar solvent is known to increase its amorphous character, thereby increasing the mobility of ionic carriers in the region soaked by the solvent. This increase in ionic mobility has a favourable effect on the heterogeneous charge transport in that region thereby augmenting the photoeffect. But still the reason for the deterioration of the photoeffect at anodic potentials and it's rejuvenation at cathodic potentials, as shown in the table.4 is not clear.

3.5.3 Spectral response of Lightly doped Polyacetylene.

The spectral response of the film is shown in Fig.13. Absolute quantum efficiences are low. The gross features of the spectral response agrees well with the work of Yamase et al [11]. Since the photoeffect is produced by the generation of nonequilibrium carriers upon absorption of light by the semiconductor, the relationship of the photoeffect to the wavelength of the incident radiation normally follows the characteristics of the spectral distribution of the absorption coefficient. In particular the photoeffect reaches the maximum value close to the main absorption edge of the semiconductor [78]. But Polyacetylene seems to be an exception. The only correlation between absorption spectrum and the action spectra is evident in

the region of the commencement of the photoresponse .

The simplest approximation to a charge separation across an abrupt interface is based on the Gartner model [105]. The model assumes, that there is no recombination of minority carriers at the surface or in the space charge region. Recombination takes place only in the bulk of the semiconductor and is being represented by the minority carrier diffusion length. The model predicts that if $\alpha d << 1$ and $\alpha L_p << 1$ where α is the absorption coefficient and d is the space charge layer thickness and L_p is the minority carrier diffusion length, the photocurrent should be linear with α. Often most systems obey the linearity even when the underline assumptions of the model prove to be invalid. Fig.17 shows the fit of the spectral response to the equation [17] for a direct bandgap semiconductor where linearity between α and the photocurrent is already used. There is an agreement between observed data and the predicted behaviour in terms of the Gartner model. Linearity is observed with n=1 in a range from 3.5 ev to 2 ev. The intercept of nearly 1.7 ev give the band gap which is close to the published value of 1.65 ev.

3.6 Analysis of Electroreflectance data on Polyacetylene/Electrolyte interface.

EER spectra of Polyacetylene shown in Fig.14b has two peaks, one at 1.4 ev and the other at 1.55 ev. The line shape of both peaks do not fit the third derivative line shape expected from low field electroreflectance, although the position of these two peaks

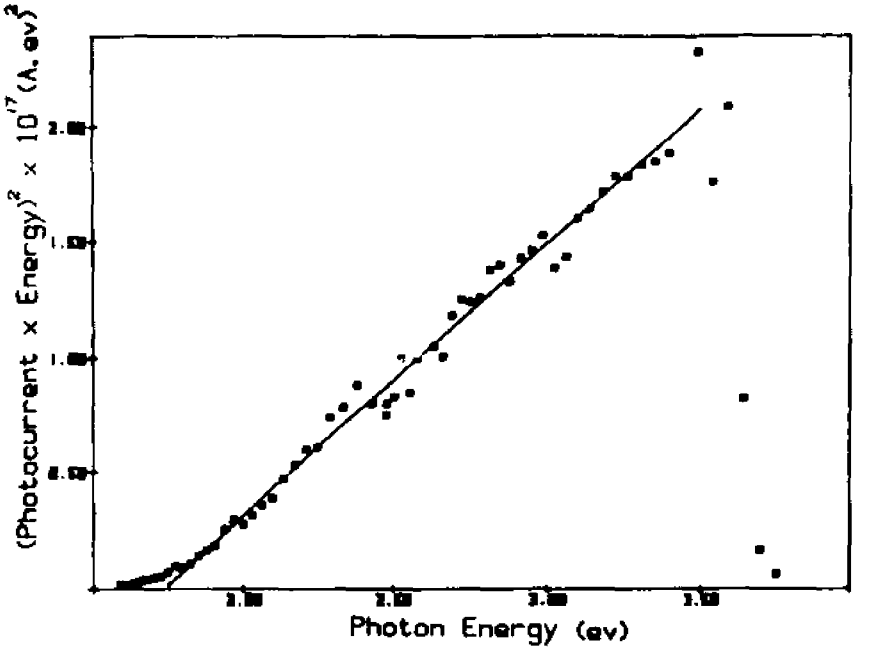

Fig.17. Fit of the spectral response of trans-Polyacetylene, with a doping density of 8 x 10^{17} cm^{-3}. at 0.0 v vs.SCE to the theoretical model for a direct band gap semiconductor, based on the equation.[17]

remain the same in the range from 0.00 v to -0.5 v vs.SCE. Organic Polymer/ Electrolyte interface is not sharply defined. Because of the porocity of the polymer, the electrolyte may actually penetrate the polymer surface, forming a region, which is usually a composite between the polymer and the electrolyte. On it's way in and out of the surface, the reflected light travel this composite region which might have a highly inhomogeneous distribution of the electric field. The modulation of reflected light therefore represents a complicated superposition from a wide spectrum of values of the electric field strength. This would present a problem for the line shape discussions. This aspect together with the possibility that the modulated electric field gives rise to periodic chemical changes in the polymer may seriously distort the line shape. Polymeric semiconductors often show electrochromic behaviour. The modulated change of color, caused by the modulating voltage, creates a modulated change of reflectance. This contribution, when considered as a function of wavelengh, is very similar to the absorption spectrum of the material itself. This noncritical background might deform the line shape associated with the transitions at critical points. There is a possibility that, the huge peak centered around 2.1 ev, shown in Fig.14a represents a noncritical background, resulted from the electrochromic behaviour of Polyacetylene. This particular peak extending over an energy span of about 1.5 ev is too broad to account for a transition at a critical point. Polyacetylene has it's main absorption peak around 2.1 ev and it's magnitude changes with the doping level. When the

film is polarized to anodic potentials there is a possibility that, at least the oxidation level of the surface layers fluctuate, in responding to the modulating voltage, thereby creating a noncritical EER background. Spectra at negative potentials do not have problems due to electrochromic effects. But still the experimental line shapes do not fit to the expected line shape. Under these circumstances only a tentative assignment of the two peaks in the EER spectra shown in Fig.14b, can be presented. The peak at 1.55 ev and 1.4 ev can be assigned to direct band transition and an excitonic transition respectively. This will put an excitonic level 0.15 ev below the band edge.

The amplitude of EER signal changes it's sign at the flat band. In viologen electrolyte, the flat band potential of trans Polyacetylene/Electrolyte interface lies around 1.1 v vs. SCE, as indicated in Fig.15. As the space charge region is varied from the flat band into the fully depleted regime the EER signal does not become independent of bias as required by equation [21], but decreases dramatically towards the reverse bias. This behaviour is interpreted to be due to Fermi level pinning, due to surface state levels that are fast enough to equilibrate at the modulating frequency. This causes a part of the potential drop to fall across the Helmholtz layer, thus modulating the position of band edges relative to the reference electrode. This results in a decrease in modulation amplitude in the space charge layer and hence a decrease in elctroreflectance signal. When the fermi level is completely pinned the signal intensity goes down to zero.

3.7 charging characteristics of Polyacetylene electrode

As mentioned earlier, crystalline fibriller morphology of Polyacetylene makes this polymer prone to non uniform doping. Uniform distribution of dopants can be expected, only if the rate of introduction of dopants is slow enough in comparison to the rate of charge transfer and the rate of diffusion of dopants into the polymer bulk. The open circuit potential of a Polyacetylene/Li cell is dependent on the activity or concentration of dopants at the Polyacetylene/ Electrolyte interface. The initial steep rise in the open circuit potential with the current density of $5\mu A/cm^2$ (Fig.16) clearly indicates a surge of dopants at the interface in a short period of time. After this initial rise the potential increases very slowly, and it is possible that during the initial rise of potential, dopants form tiny metallic islands that maintain the potential at the interface at a nearly steady value. But at lower current densities the rate of introduction of dopants becomes more and more compatible with the diffusion process. As a result of this the cell voltage develops more and more gradually. According to a recent report, the equilibrium time required to achieve doping uniformity in a film of 70μm thickness would be of the order of 300 hours due to the slow rate of diffusion of dopants inside the film. Considering the fact that the film we used was about 250μm in thickness, it is uncertain whether we can achieve true homogeniety within the time scale of an experiment. Lowering the current density would help the situation as shown in Fig.16. But reducing the current density less than $0.1\mu A/cm^2$, which we normally used in our

experiment is rather impractical.

Even though there are problems with measuring resistance of highly resistive films by using two probe method, the data shown in Table.5 on parallel and perpendicular resistance of the film, following the introduction of equal amount of charge (but at different rates), are consistent with the discussion above. Since the accumulation of charge at the interface (probably forming tiny metallic islands) is possible at high charging current densities; parallel resistance should be more sensitive to the rate of charging. From the data presented in Table .5 on parallel resistance, one can see a trend to increase the parallel resistance with decreasing current density. The open circuit potential observed at the end of a passage of equal amount of charge, complements these findings. The lower voltage resulted at low current densities indicates that the activity of dopants (concentration) at the polymer electrolyte interface is low, because at low current densities more of them have enough time to diffuse into the polymer.

3.8 Summary and conclusions.

Photoelectrochemical and Electroreflectance characteristics of trans Polyacetylene were studied in this part of the work. The porous nature and reactivity of the film called for special handling and a new design for electrodes used in Photoelectrochemical experiments. Doping of the polymer can be done electrochemically and can be verified by taking the IR spectra of doped samples. Lightly

doped trans Polyacetylene forms a photovoltaic junction with aqueous electrolyte containing methyl viologen as the redox material. Even though the exact photovoltage is sample dependent, it's magnitude generally falls somewhere around 80-150 mv for an electrode with optimum photo effect. photocurrent behaviour of trans Polyacetylene consistent with a semiconductor with p-type semiconductivity. The turn on potential seems to be positive to +0.45 v vs.SCE. The overall shape of photocurrent voltage curve resembles an electrode with a large series resistance. Photocurrent is observed in a narrow region of doping densities with a maximum corresponding to about $10^{18}/cm^3$. Soaking of the electrode appears to have a favourable effect on the Photoresponse of $-(CH)_x$ and it levels off in about 10 hours of soaking in an aqueous eletrolyte. Similar effect was observed regardless the identity of the redox material. The photoelectrochemical behaviour of $-(CH)_x$ is unlike any known inorganic semiconductor and is strongly correlated with the anodic current which causes deterioration of the photoeffect and cathodic dark current which causes rejuvenation of the photoeffect. The exact reason for this phenomenon is unclear, but it may well be connected with the possible chemical interactions between the electrode and the electrolyte which might affect the effectiveness of charge separation at the interface. The quantum efficiency of the photocurrent is low and the fact that quantum efficiencies at various wave length did not correspond to the absorption spectrum make this material very different from Inorganic Semiconductors. Only correlation between the absorption spectrum

and quantum efficiency for charge separation is found in the region of photocurrent onset. The photoresponse of trans Polyacetylene can be analysed in terms of the Gartner model, and the findings are consistent with a direct band gap semiconductor with a band gap of about 1.7 ev. EER of trans polyacetylene at negative potentials consist of two peaks located at 1.4 ev and 1.55 ev. Although both of these signals satisfy the low field requirement, they did not fit to the third derivative line shape expected for low field EER. In this case only a tentative assignment could be made. The peak at 1.55 ev was assigned to direct band transition and the one at 1.4 ev was assigned to a excitonic level 0.15 ev below the conduction band edge. At positive potentials, the EER spectra of trans $-(CH)_x$ became more complex and a broad peak around 2.1 ev with a width over 1.5 ev is speculated to be a non critical back ground originating from the electrochromic nature of polyacetylene. The amplitude of both EER peaks change the sign around 1.2 v vs. SCE. This position is identified as the flat band position for this interface. Variation of EER peak height with potential indicates that Fermi level pinning occurs as the film enters into depletion. Considering the question of homogeniety in the doping process low charging current densities seems to promote a homogeneous doping process. High current densities resulted in a sample with low resistance parallel to the film surface, which is interpreted in terms of the inhomogeniety of doping at high current densities

Conclusions of this part of the study can be wrapped

up as follows. Techniques such as Photocurrent Spectroscopy and EER, which are traditionally used to characterize Inorganic Semiconductor/Electrolyte interface can be used to study the Organic Semiconductor/Electrolyte interface too, despite the complexity of the interface. The photocurrent spectra can be analysed in terms of the Gartner model and the band gap value obtained from this analysis agrees with the EER data. Amorphous character induced by the absorption of a solvent by a crystalline polymer seems to favor the charge transfer kinetics between the polymer and the redox electrolyte. Specfic interactions between the polymer surface and the redox material seems to dominate the processes at the illuminated interface, because no inorganic redox couple gives photocurrents comparable to the viologen electrolyte used in this study. High modulation amplitude required to observe the EER and possibly the inhomogeniety of the electric field at the interface due to the porous nature of the polymer, may be responsible for the distortion of the EER line shape to the extent that no line shape analysis is possible. Electrochromic behaviour of the polymer seems to introduce broad structures into the EER spectrum that interfere with EER observations. Even though $-(CH)_x$ cannot be considered as a potential candidate for applications such as solar energy conversion, photoelectrochemical and EER investigations on these material are fundamentally important to characterise these semiconductive polymers.

Chapter 4

POLY 3-METHYLTHIOPHENE/ELECTROLYTE INTERFACE.

4 : EXPERIMENTAL RESULTS

4.1 Photoeffects at the P3MT/Electrolyte interface.

Fig.18 shows the Photoelectrochemical response as a function of doping. Doping content was varied by removing a fraction of the total recoverable charge electrochemically until the desired oxidation level is achieved. Reduction could be carried out either potentiometrically by lowering the electrode potential down in small steps, or Galvanostatically at Current densities of 0.27 $\mu A/Cm^2$. Essentially the same Electrical and Optical properties were observed for films that were reduced by using either method, provided the cathodic charge involved was the same. Total recoverable charge was measured potentiometrically by bringing the potential down with the starting potential of 'as grown' film at 3.8 V vs. Li, which was brought down to 2.5 V vs. Li at the rate of 1.7 mv/min and finally carrying out the reduction exhaustively at 2.5 Volts for another 30 hrs until the current flow becomes small enough to assure complete reduction. Table.6 represents the data related to the preparation of six samples with varying doping densities. [Q(6)-Q] indicates the amount of charge removed. The data tabulated in the last column: N_R/cm^3, which is the density of dopants remaining in the film, was obtained by dividing the remaining charge by the volume of the film. Oxidation level y, corresponding to the formula

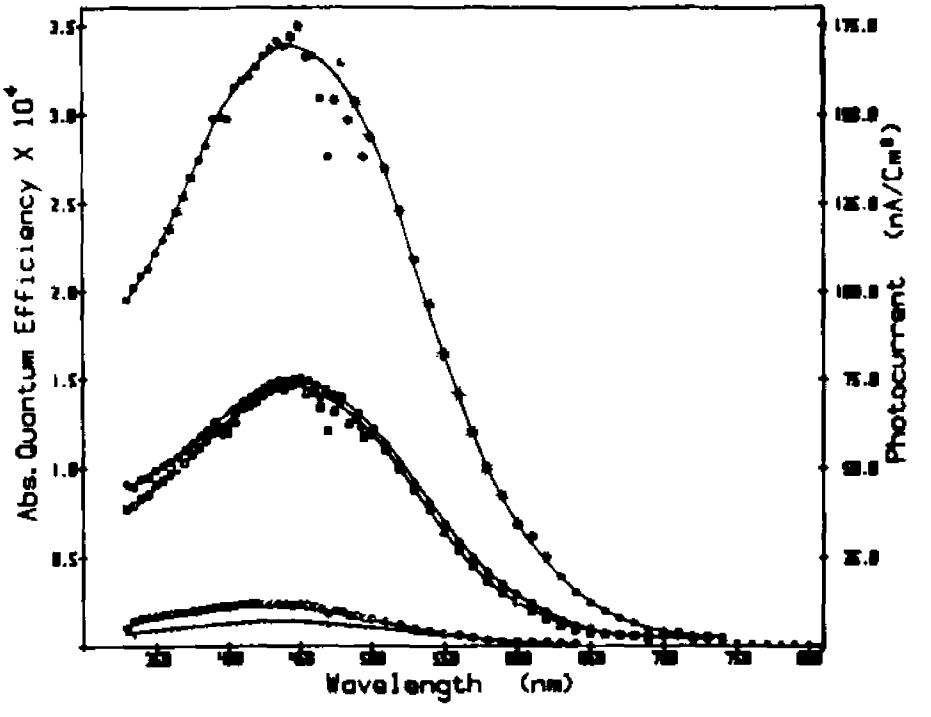

Fig.18. Spectral response of the Quantum Efficiency of the Photocurrent, of Poly 3-methylthiophene with different doping densities. Same conditions as in Fig.11., Potential 0.15 v vs.SCE.

(—•—•—) 1.3×10^{21} (—•—•—) 6.5×10^{20}

(—•—•—) 1.5×10^{21} (—•—•—) 0.0

(—•—•—) 1.1×10^{21} (Estimated doping densities)

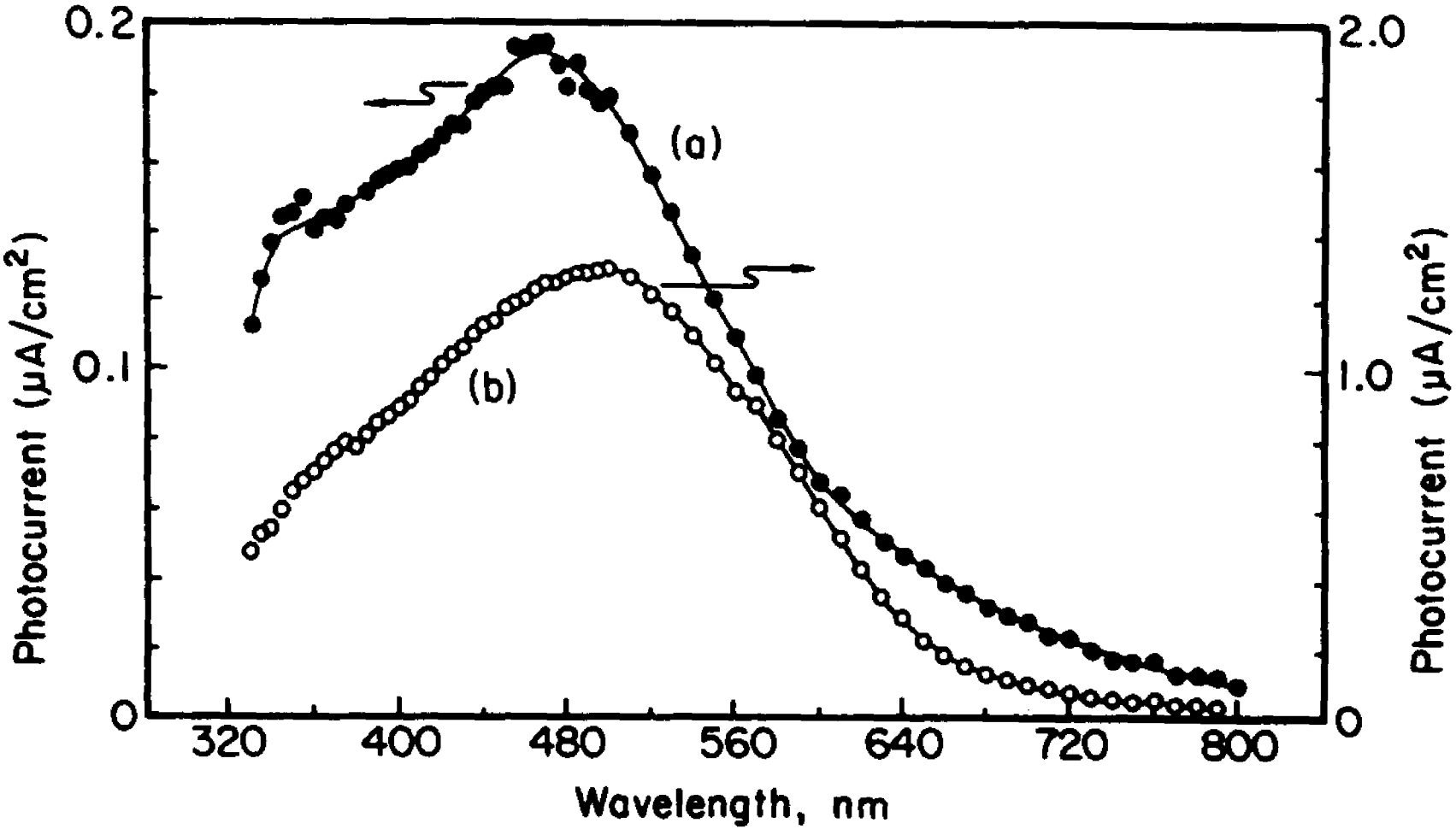

Fig.19. Spectral Response of "as grown" P3MT. Same conditions as in Fig.11.

a) at 0.0 v vs. SCE b) at -0.5 v vs. SCE

Table.6 : Partial reduction of P3MT to achieve different doping concentrations

Sample #	Q (removed), C/cm^3	Q(6)-Q	mole % /ring (anion)	N_d/cm^3
1	as grown	280.0	41.6	$1.7x10^{21}$
2	34.0	246.0	36.5	$1.5x10^{21}$
3	65.0	215.0	31.9	$1.3x10^{21}$
4	95.2	184.8	27.5	$1.1x10^{21}$
5	175.3	104.7	15.6	$6.5x10^{20}$
6	280.0	0.0	0.0	0.0

$[(P3MT)^{+y}(CF_3SO_3)^-_y]_x$ can be calculated by dividing the number of charge carriers that remain, by the number of thiophene rings in the film that was calculated from the weight of the film. Fig.19 shows the spectral response of 'as grown' P3MT measured at 0.0V vs. SCE and 0.5V vs. SCE. Fig.20 illustrates the spectral response of fully reduced or neutral sample taken at two different potentials 0.15V vs. SCE and -0.5V vs. SCE. Measurements were taken in viologen electrolyte under monochromatic radiation of 410 nm. Fig.21 illustrates the photocurrent potential and dark current potential characteristics of 'as grown' P3MT measured under quasi steady state conditions. In this case after the application of a potential, the electrode was allowed to stand for some time, long enough to assure quasi steady

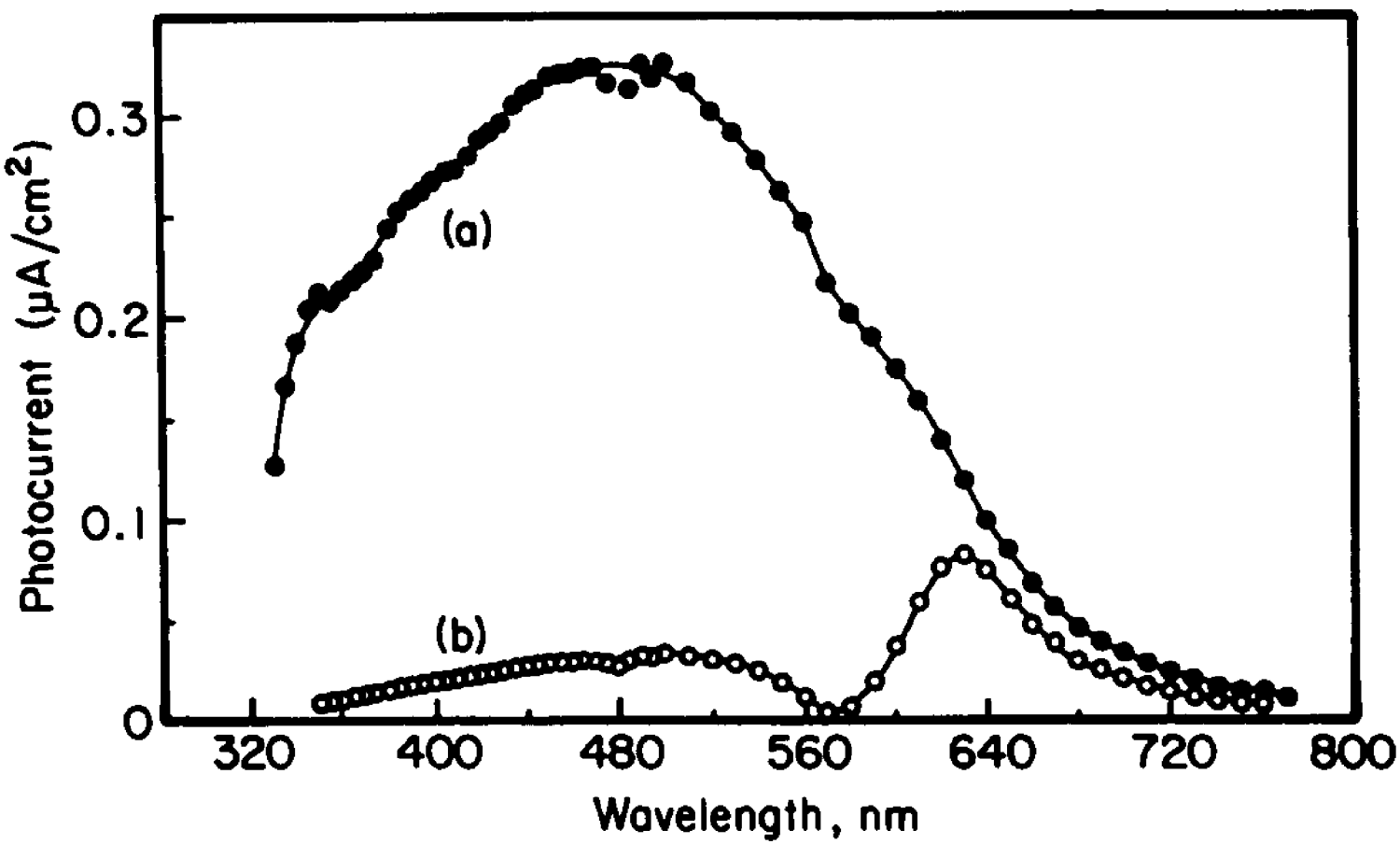

Fig.20. Spectral Response of the Neutral Poly 3-methylthiophene. Same conditions as in Fig.11.

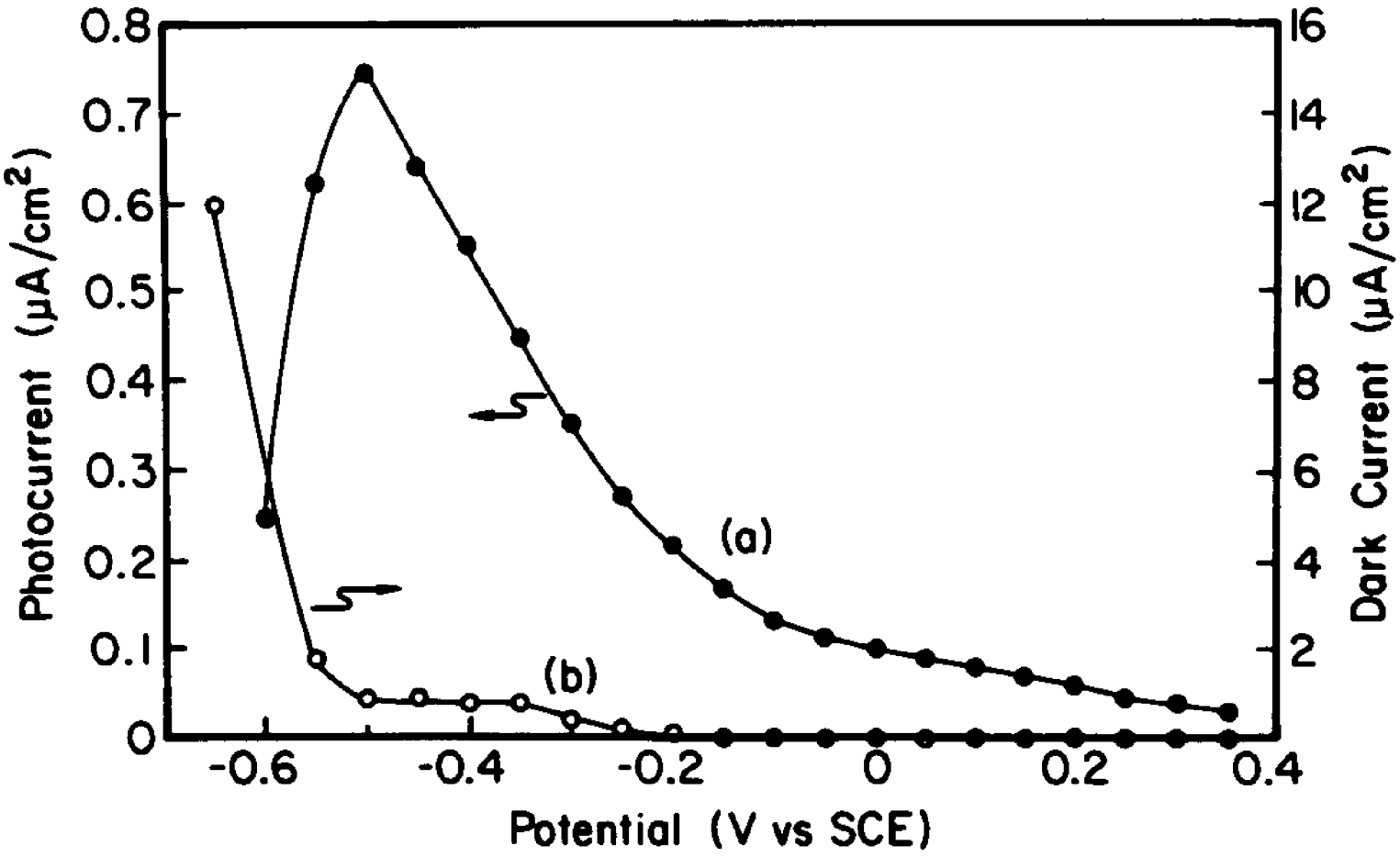

Fig.21. Photocurrent - Potential (a) and Dark current - Potential (b) characteristics of "as grown" P3MT. Same conditions as in Fig.11.

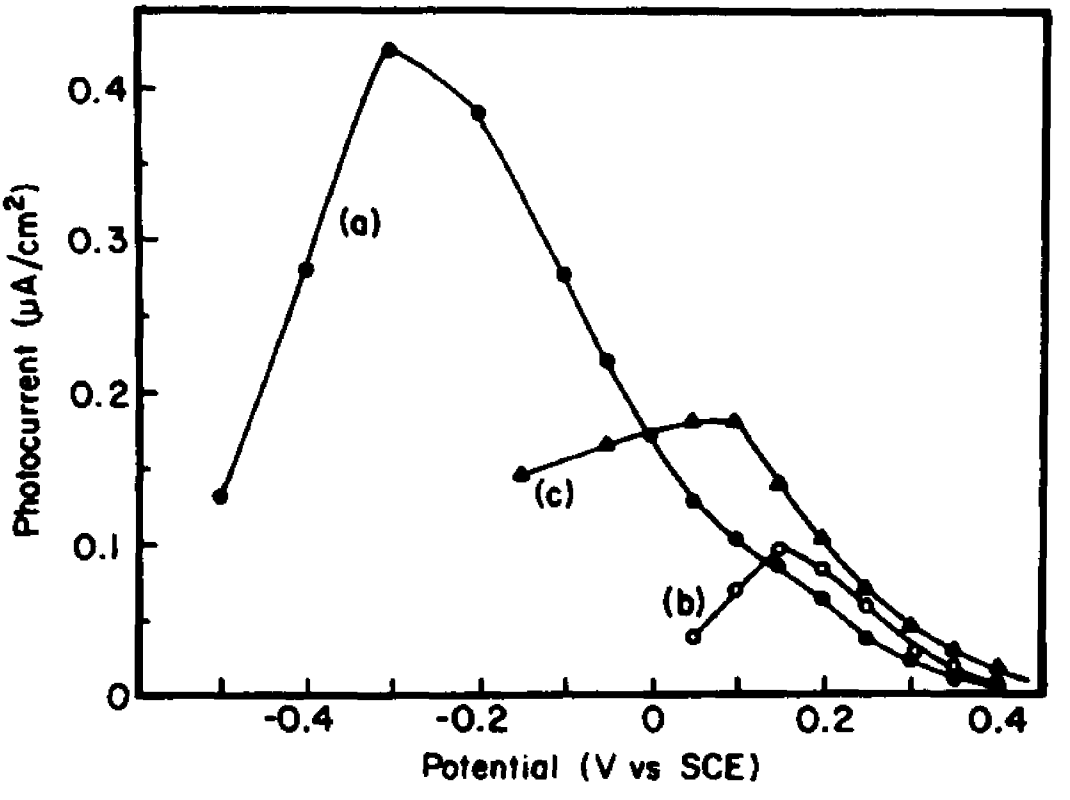

Fig.22. a) Photocurrent - Potential response for reduced P3MT
b) Same as a., after holding the electrode at -0.35 v vs. SCE for 4 hours.
c) The same as a., after holding the electrode at 0.75 v vs. SCE for one hour following b.
Same conditions as in Fig.11.

state photocurrent. Fig.22 illustrates the photocurrent potential characteristics of the reduced (neutral) P3MT measured under similar conditions.

4.1.1 'as grown' and neutral Poly 3-Methylthiophene.

Fig.23a shows the EER spectra of neutral P3MT at various electrode potentials. Again the experimental conditions were the same as in photocurrent measurements. Unlike Polyacetylene, EER of neutral P3MT showed only one peak within the region of potentials studied. But the position of the peak maximum shifted towards high energy, as the potential moved towards the flat band condition. Fig.24a shows the variation of the EER signal with the amplitude of modulation voltage. The observed linear dependence is maintained up to, about 0.5 Volts. Therefore, operating amplitude of about 0.2V vs. SCE satisfied the low field requirement and the lineshape analysis can be performed according to the theory of low field electroreflectance. Fig.24b shows the variation of EER signal amplitude as a function of applied potential. Signal starts to rise steeply as the potential moves away from the region of flatband towards the reverse bias. The signal passes through a maximum at about+0.4V vs. SCE. But instead of maintaining a signal amplitude at constant value, as required by equation 21, the signal begins to lose its height around +0.4V vs. SCE and finally drops nearly to zero as it approach 0.0V vs. SCE. This phenomenon has been attributed to the pinning of the fermi level to a mid gap surface energy state.

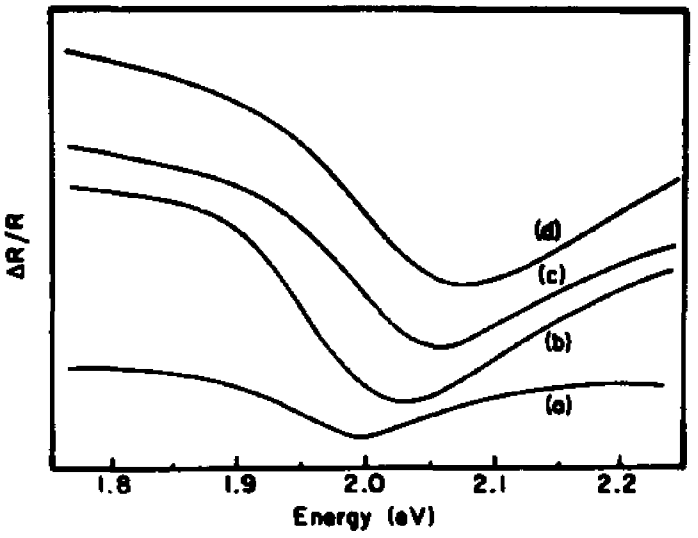

Fig.23a. EER spectra of Neutral P3MT in Viologen electrolyte.
(a) 0.0 v (c) 0.4 v
(b) 0.2 v (d) 0.6 v
all potentials are vs. SCE, modulation amplitude = 0.25 v modulation frquency = 31 Hz.

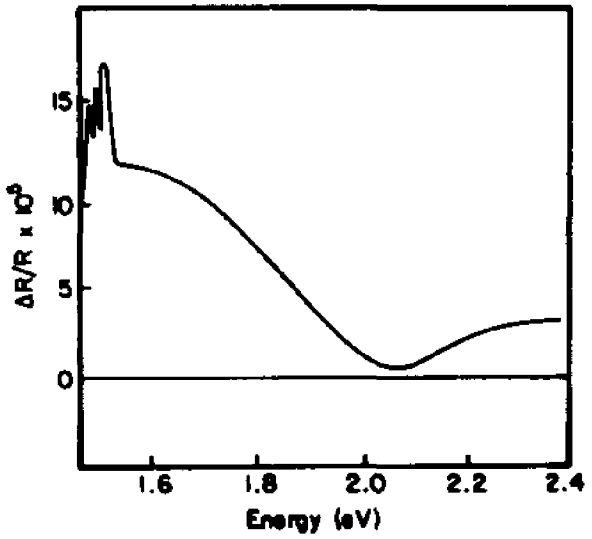

Fig.23b. EER spectrum of "as grown" P3MT at U = 0.4 v vs.SCE. Modulation amplitude = 0.2 v, Modulation frequency = 31 Hz.

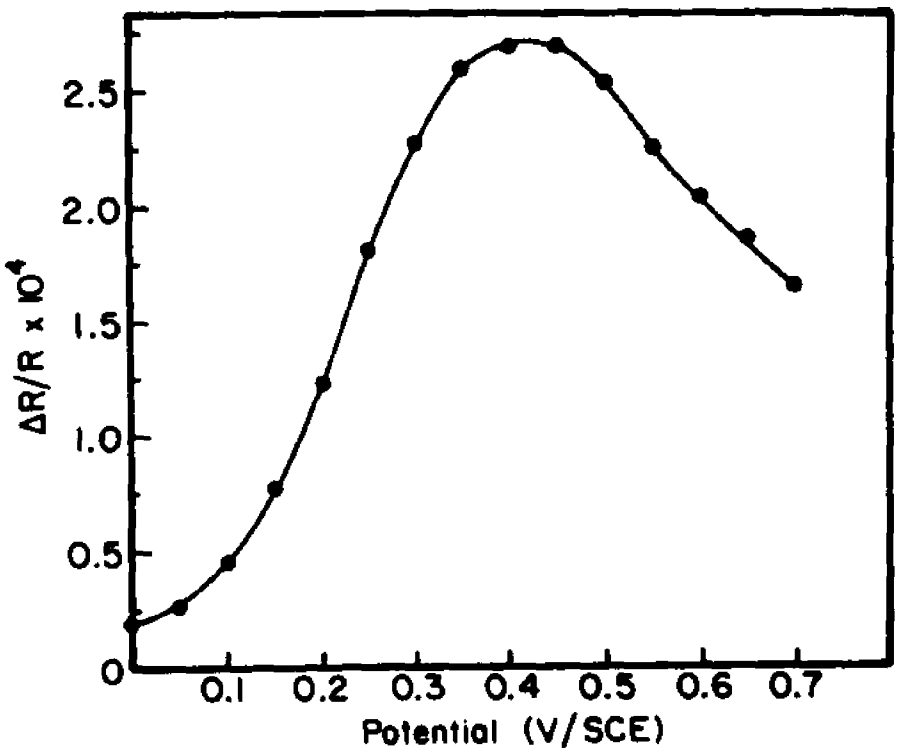

Fig.24a. Variation of the EER peak amplitude of reduced P3MT as a function of the electrode potential.

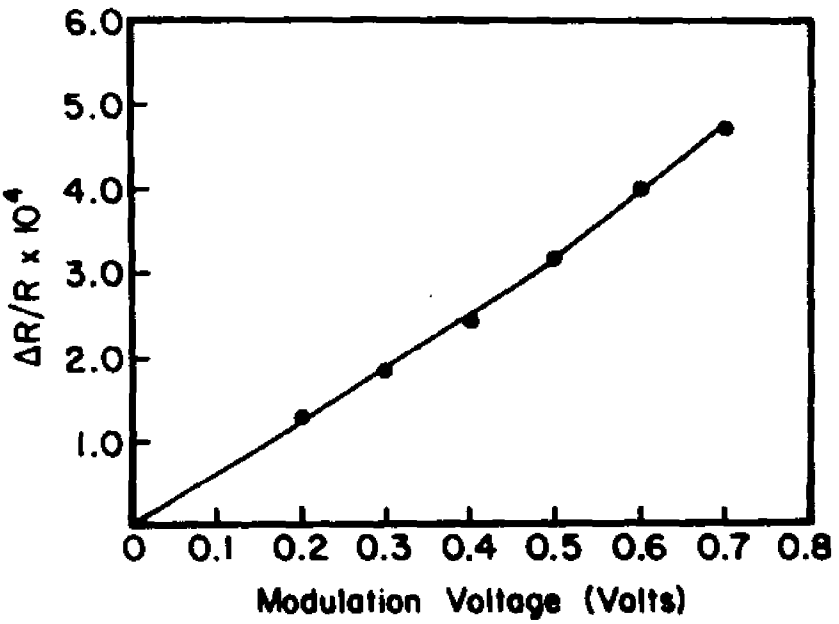

Fig.24b. Variation of the EER peak amplitude of reduced P3MT as a function of the electrode potential.

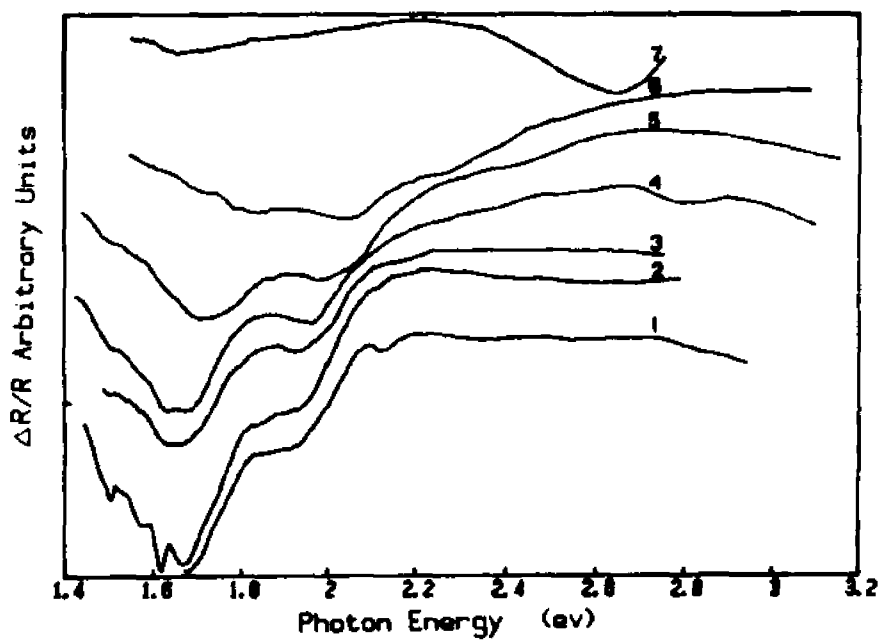

Fig.25. EER spectra of P3MT with a doping density of 1.6×10^{20} cm^{-3} in Viologen electrolyte.

1) 0.0 v 4) 0.6 v 6) 1.0 v

2) 0.2 v 5) 0.8 v 7) 1.2 v

3) 0.4 v

all potentials vs.SCE, modulation amplitude 0.15 v, modulation frequency 31 Hs.

Fig.23b shows the EER spectrum of the "as grown" polymer taken at +0.4V vs. SCE. the EER signal appears at the same energy as that is observed for the neutral polymer. But the signal strength does not show a linearity with the modulation amplitude. Thus, the spectrum cannot be analysed in terms of the theory for low field Electroreflectance. The spectrum shows a strong response down to energies lower than 1.5 ev.

Fig.25 shows the EER response of a P3MT sample with moderately high doping density. Sample was prepared as described in section 3.2 and it corresponds to the sample 3 shown in Table.6. Two structures are clearly visible. In addition to the peak around 2 ev there is another structure near 1.6 ev, which is not present in the neutral sample and, is different from the low energy broad response of the 'as grown' sample. Both peaks satisfy the low field requirement, by showing a linear dependence with modulation amplitude. Therefore these two structures can be analysed in terms of low field EER as an overlap of two EER signals.

4.2 Impedance measurements.

Fig.26a and 26b, show typical impedance spectra of 'as grown' and reduced P3MT respectively. These two samples correspond to sample 1 and sample 6 shown in Table.6. The high frequency part of the spectra of highly doped sample (as grown) behave as a passive RC element for which the impedance is given by the equation.28. In this region, log plot of the imaginary part of the impedance spec-

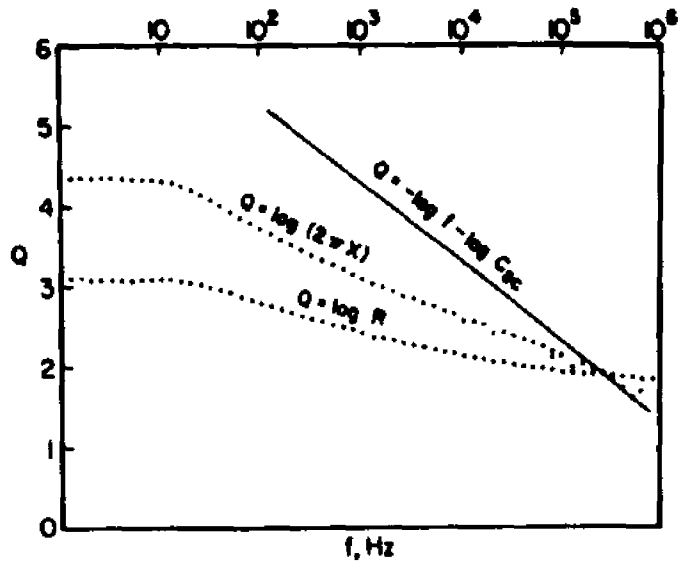

Fig.26a. Impedance Spectrum of Neutral P3MT in Viologen electrolyte. Potential +0.4 v vs. SCE, modulation amplitude 20 mv

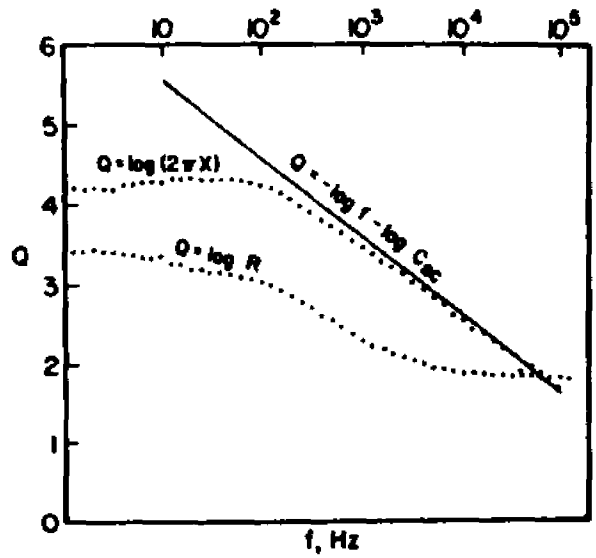

Fig.26b. Impedance spectra of "as grown" P3MT. conditions as in Fig.24a.

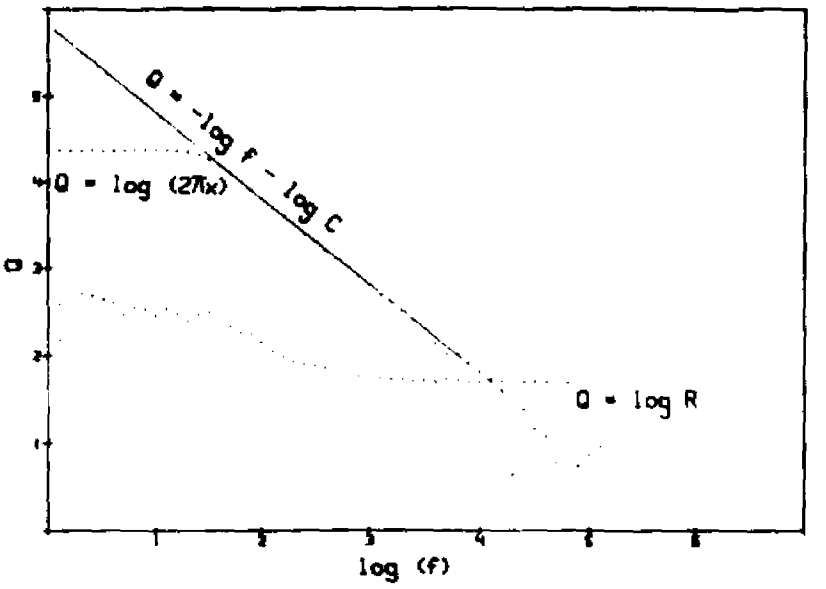

Fig.27a. Impedance spectra of partially reduced P3MT with a doping density of 1.6×10^{20} cm^{-3} (sample # 3 in Table.5), in Viologen electrolyte. conditions same as Fig.24a.

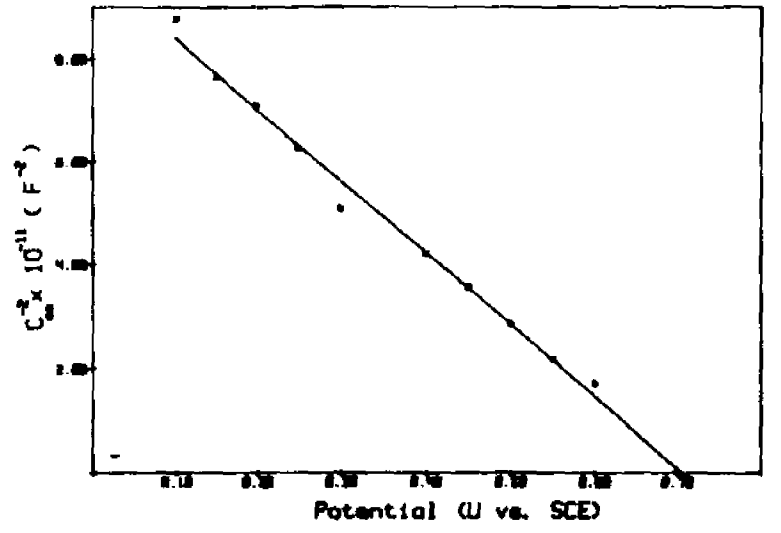

Fig.27b. Mott-Schottky plot for the sample # 3 (Table.5)

tra (log 2ΠX) relates to log (f) with a slope of -1 whereas the real part becomes independent of frequency. But the capacitance values do not vary with potential as required by the Mott-Schottky relationship given by the equation.14, indicating that the passive capacitive element does not represent a space charge layer. Fully reduced or neutral sample does not show a region where there is a linearity between log (2ΠX) and log(f) with a -1 slope. Sample 2 and 3 (Table.6), both showed a region with a -1 slope in the imaginary part of their respective impedance spectra and in both cases, the capacitive elements varied with the electrode potential according to the Mott Schottky relation (equation.14) and the straight line graph can be extraploted to cross the potential axis at +0.71V vs. SCE. Fig.27 a and b show the impedance spectra for sample 3 at 0.4V vs. SCE and Mott-Schottky plot for the sample 3 respectively.

4.3 Quantum efficiency measurements with Pt(0) coated P3MT electrode.

Fig.28 indicates the variation of Quantum efficiency of neutral P3MT with the area concentration of Pt(0), in viologen electrolyte. Coating of electrode with Pt(0) was done electrochemically, by potentiostating the electrode, illuminated with intense white light at 0.1 v vs.SCE in a solution of 1 mM K_2PtCl_6 and 0.1M $NaClO_4$, until a desired amount of charge is passed. Testing of the electrode was done in viologen electrolyte. The basic photocurrent/voltage characteristics of modified electrode is the same as the unmodified

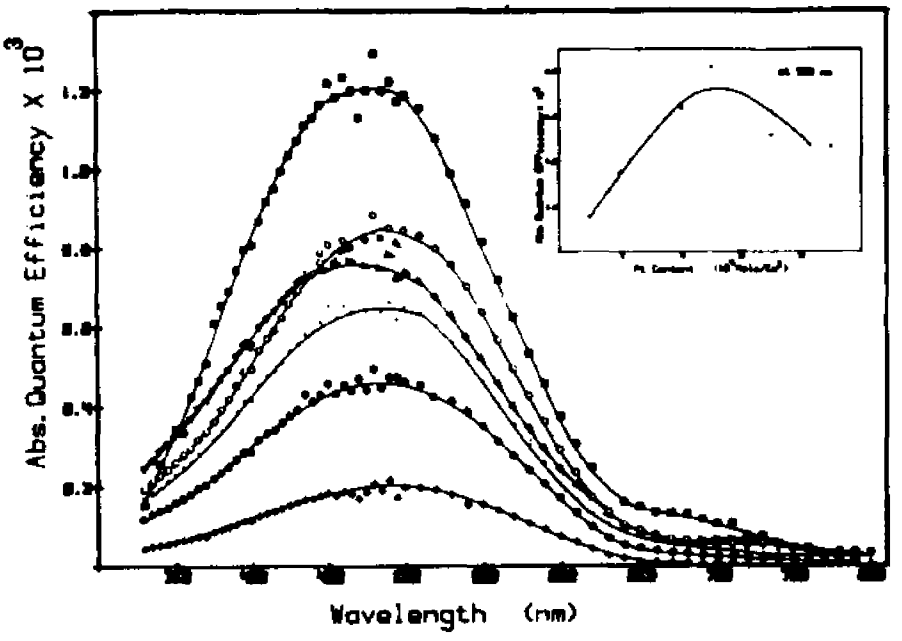

Fig.28. Spectral response of the Quantum efficiency Of the Photocurrent of Poly 3-methylthiophene coated with different amounts of pt, in Viologen electrolyte, Illumination 410 nm Intensity 0.35 mW/cm^2, Potential 0.15 v vs. SCE. Inset: Variation of Abs.Quantum efficiency at 550 nm, with different Pt content.

(-+-+-+-) Naked (-●-●-●-) 20X10^{-8}

(-●-●-●-) 5X10^{-8} (-▶-▶-▶-) 30X10^{-8}

(-●-●-●-) 10x10^{-8} (——) 40X10^{8}

Pt content,in Mol/cm^{-2}

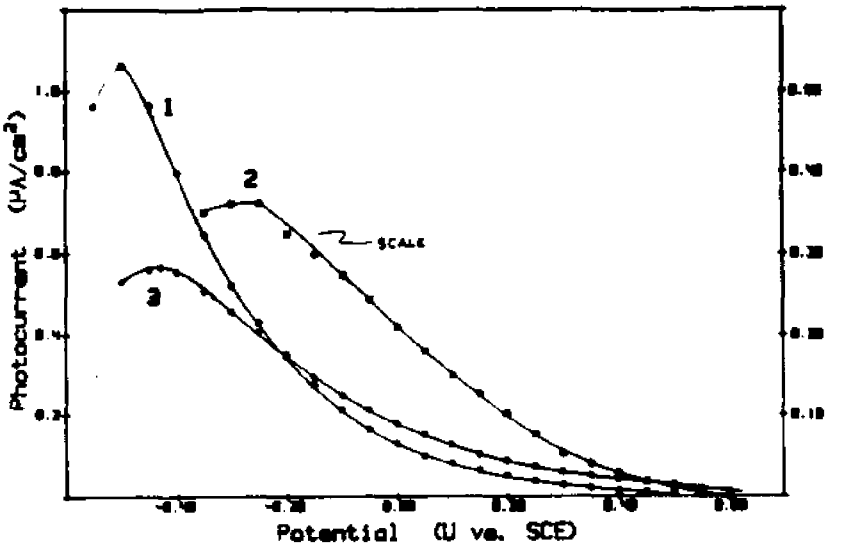

Fig.29a. Photocurrent/Voltage behaviour of
(1) Fresh P3MT in Viologen Electrolyte, Illumination 410 nm
(2) Same electrode, after holding at -0.5 v vs.SCE for 2 hours.
(3) Same electrode, after holding at +0.75 v vs.SCE for 3 hours

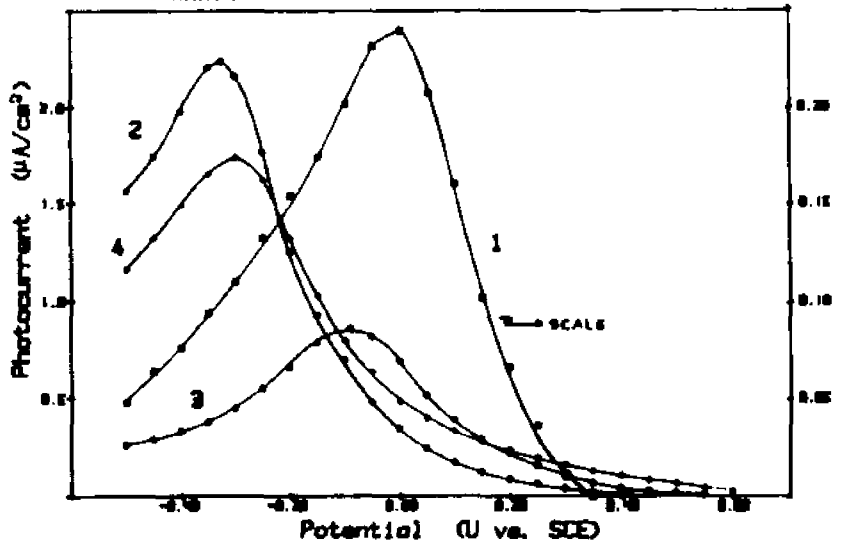

Fig.29b. Photocurrent/Voltage behaviour of
(1) P3MT electrode treated with $NaBH_4$ for 30 minutes.
(2) Same electrode treated with $Na_2S_2O_8$ for 30 mins
(3) Same electrode after holding at -0.5 v vs.SCE for 5 hours.
(4) Same electrode after holding at +0.75 v vs.SCE for 5 hours.

one, except high photoresponse. Coating with Pt(0) always improved the performance of the electrode compared to the naked one with a maximum amount of Pt(0) in the vicinity of $2x10^{-7}$ mol/cm^2

4.4 Observations relating to the stability of P3MT in aqueous electrolyte.

Fig [29a] shows the photocurrent/voltage characteristics of P3MT in viologen electrolyte. The scanning was done at 1 mv/sce and illumination was 410 nm. The fresh sample showed a I/V curve with a cathodic photocurrent peak in the vicinity of -0.5 v vs.SCE, consistent with previous results. Then the electrode was held at -0.5 v vs.SCE for 2 hours which resulted in an I/V behaviour shown in curve 2. In this case not only the magnitude of the photocurrent is low, but also the photocurrent peak has shifted towards positive potentials. This shift became larger with more time the electrode spent at -0.5 v vs.SCE. If the same electrode is held at +0.75 v vs.SCE for 3 hours, the resulting I/V character is similar to curve 3. After three hours at the anodic potential the photoeffect has rejuvenated and the photocurrent peak appears close to where it was for the fresh electrode.

In Fig [29b], curve 1 shows the photoeffect of an electrode, which was in contact with $NaBH_4$ for 30 minutes. This treatment resulted in very low photoeffect and a photocurrent peak shifted to positive potentials. Curve 2 shows the I/V behaviour of the same electrode after the oxidative treatment with 10% solution of

$Na_2S_2O_8$. This, increased the photoresponse, an order of magnitude higher than the electrode treated with $NaBH_4$, and shifted the photocurrent peak towards the negative potentials. Now the same electrode can be held at -0.5 v vs.SCE and then at +0.75, to observe essentially the same behaviour already described. Curve 3 represents the situation when the electrode is held at -0.5 v for 5 hours and Curve 4 shows the I/V behaviour of the same electrode after holding it at 0.75 v for five hours.

4 : DISCUSSION AND CONCLUSIONS.

4.5 Photoeffect at the Poly 3-methylthiophene/Electrolyte interface

4.5.1 Variation of photoeffect with the doping density.

It is evident from Fig.18 that for Electrochemically reduced samples the photoeffect increases with decreasing doping density. This observation is in accord with that of inorganic semiconductors, which show a similar reduction of photoeffect when the solid becomes semimetallic. Variation of the photoeffect can be compared qualitatively with a similar variation of absorption coefficient with doping density. Absorption coefficient for the band gap transition decreases with the doping density [62,106]. Thus observations shown in Fig.18 are very much expected. But there is a major disagreement worth mentioning too. When the doping density of P3MT is increased starting from the neutral sample, in addition to the decrease in band to band transition, additional structures begin to appear in the absorption spectrum. The absorption peak appearing around 650 nm becomes the most visible structure when the doping density is increased to metallic region. This additional absorption peak has been attributed to the presence of mid gap bipoloron energy levels [62]. But surprisingly, the photocurrent spectrum does not have a structure corresponding to this bipoloron absorption at any doping level investigated. According to Fig.18 the spectral response of the photocurrent is apparently insensitive to the doping level, except for its magnitude. This was rechecked by normalising the

spectra shown in the Fig.18 to the same peak height. They virtually coincide with one another and no additional structure in the region of 600 nm was observed. This observation is in contradiction to a report published [107] in which a sub-band gap response in the vicinity of 600 nm was observed for the 'as grown' samples. There is no immediate explanation for this discrepancy. Being defect sensitive systems, electronic properties of organic polymers may well be influenced by the differences in the processes and solvent/electrolyte systems used for the film deposition. Thus the differences in the observed photoelectrochemical properties are not unexpected.

4.5.2 Photoelectrochemical response of P3MT.

As shown in Fig.19 variation of steady state photocurrent of 'as grown' P3MT with wave length, follows closely the absorption spectrum of the material. Efficiency of the photocurrent is much higher at -0.5 V vs. SCE compared to that at 0.0 V vs. SCE. this is expected for a p-type material, since the higher reverse bias would cause more effective separation of photogenerated carriers. Actual magnitude of the photoresponse is somewhat sample dependent, but the spectral response is always a replica of the one shown in Fig.19. Fig.30a shows the fit of the spectral response at 0.0 V vs. SCE to the equation [17]. From 2.7ev down to 2.1ev there is a linear relation with n=1 and intercept at 2.09 ev.

In the case of reduced P3MT (Fig.20) the action spectrum at positive potential eg.+0.15 V vs.SCE, closely resembles the one which is shown in Fig.19 for the 'as grown' polymer. The fit of

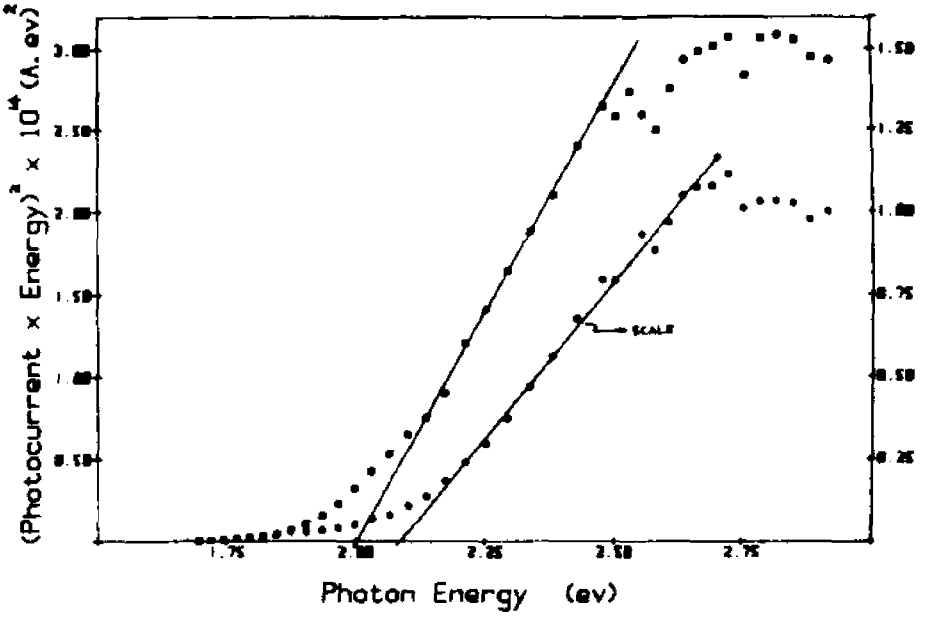

Fig.30. Fit of the spectral response of Poly 3methylthiophene to the theoretical model for a semiconductor based on equation [17].
(••••••) "As Grown" polymer at 0.0 v vs.SCE.
(▪▪▪▪▪▪) Neutral P3MT at 0.15v vs. SCE.

the spectral response for the reduced (neutral) film at this potential using equation [17] is shown in Fig.30b. Similar to the 'as grown' case, a linear relation is observed for the neutral film from 2.5 ev down to about 2.1 ev with an intercept of 2.00 ev for n=1, also indicating a direct transition. After potentiostating the neutral electrode for about 3 hrs at -0.35 V vs.SCE, dramatic change in the spectral response is observed. As will be discussed later the photoresponse in this region of potentials deteriorates rapidly. In addition to the expected reduction in quantum efficiency, a new peak around 630 nm is observed (Fig.20b). The position of this peak agrees with the reported position of the low energy absorption peak of $MV^{+\bullet}$ [108]. These results strongly suggest that when the neutral film is kept at a potential negative enough to cause the reduction of MV^{++}, some of the reduced $MV^{+\bullet}$ absorbs on the polymer. This absorbed layer is capable of producing photoelectrochemical response and that the $MV^{+\bullet}$ is stabilized on the surface.

It is speculated that coulombic effects play a key role in the stabilisation of $MV^{+\bullet}$ on the surface. In this case one would expect only a sluggish absorption of $MV^{+\bullet}$ on to the 'as grown' polymer. Because, as grown material is already oxidized, and contains a substantial positive charge in the polymer matrix, it opposes the absorption of likely charged $MV^{+\bullet}$. The action spectra shown in Fig.19 and 20 are consistent with this speculation. The neutral material shows a weak shoulder even at +0.15 V vs. SCE (Fig.20a), whereas the action spectra of 'as grown' material shown in Fig.19b,

taken at more reducing potential -0.5 V vs. SCE, shows a more pronounced shoulder.

There is yet another important aspect connected with Fig.30. As stated in Chapter.1, polymers such as Polythiophene with nondegenerate ground state, support localized charge defects called bipolorons, which are the most erergetically favourable charge configuration for those polymer systems. When electrons are removed from the polymer chain during the doping process, bipoloron levels are created as symmetrically located mid gap levels [109]. Since bipoloron states coming in the gap are taken from the VB and CB edges band gap of the material is widened with increasing doping density. In the case of Polypyrrole the band gap is known to increase from 3.2 ev in the neutral state to 3.6 ev in the 33% doped state [110]. In the case of Polythiophene, the band gap transition in the absorption spectrum shifts blue, as the doping progresses from neutral to semimetallic state [106,62]. The observations presented in Fig.30 are consistent with the observations given above. The fit of the spectral response of neutral and 'as grown' P3MT to equation [17] yields, a band gap value 2.00 ev for the neutral material and 2.09 for the 'as grown' material. Eventhough these values indirectly support the existence of bipoloron states, surprisingly none of the action spectra of P3MT observed so far in this study show any direct evidence confirming their presence.

As shown in Fig.21 reductive peak in the photocurrent shifts by, more than +0.15 V positive to that in the dark current.

This 'up hill' reduction of viologen is in agreement with the p-character of P3MT. But the actual shift in the potential may be influenced by several factors including possible chemical changes in the material itself. However at this point it is important to establish, that the origin of the observed photoeffect is photovoltaic and is not due to photoconductivity, or photostimulated undoping of the polymer. The fact that we observed a positive shift of about 0.19 V in the rest potential due to intense white light illumination, demonstrates that the junction indeed acts as a photovoltic device.

4.6 Analysis of EER data on P3MT/Electrolyte Interface.

Set of EER spectra shown in Fig.23a for reduced P3MT consists of a single peak with the position of maximum shifting to higher energies as the potential shifts towards the flat band potential. Changes of the position or shape of EER with dc bias have been observed before, for inorganic semiconductors [111]. They were interpreted to originate from interference effects between the front surface and either the edge of the space charge layer or the back of the film. In the case of neutral P3MT no interference fringes were observed. The four parameters in equation [22] that determine the lineshape could be fitted to all four spectra. Result of the fit for the spectra (a) and (d) (Fig.23) are as follows.

spectrum (a)	E_g= 1.97 ev	Γ= 0.19 ev	θ= 28°	n= 3.5
spectrum (d)	E_g= 2.01 ev	Γ= 0.28 ev	θ= 72°	n= 3.5

The value of n is indicative of a one dimensional direct transition. The value of the band gap agrees well with the spectral response measurements and it is also in a very good agreement with optical absorption measurements [112]. The broadning parameter Γ and the Phase factor θ are sensitive to the doping level. From the data given above one can see an increase in both of these factors from spectrum (a) to spectrum (d). This increase may be associated with a removal of surface defects when the electrode is polarized to anodic potentials. With reference to the observations given in Fig.22 one can see an increase in photoeffect in the region of positive potentials as a result of a prolonged anodic polarization of the neutral P3MT photocathode. This observation is consistent with the removal of surface defects. In this case the increase in E_g in going from spectrum (a) to (d) may be significant too, as discussed under photocurrent measurements. But in view of the complexities of this system further consideration of this effect is unwarrented. Fig.31a shows the fit of the spectral lineshape of the spectrum (c) (Fig.23) to the equation [22] with the following parameters.

spectrum (c) E_g= 1.99 ev Γ= 0.23 ev θ= 242° n= 3.5

Observations given in Fig.24b are consistent with the Fermi level pinning. As discussed before Fermi level pinning is observed as a result of the drop of modulation voltage across the Helmholtz layer when the film enters into depletion. This drop is associated with a change in the number of ionized surface states N_{ss}.

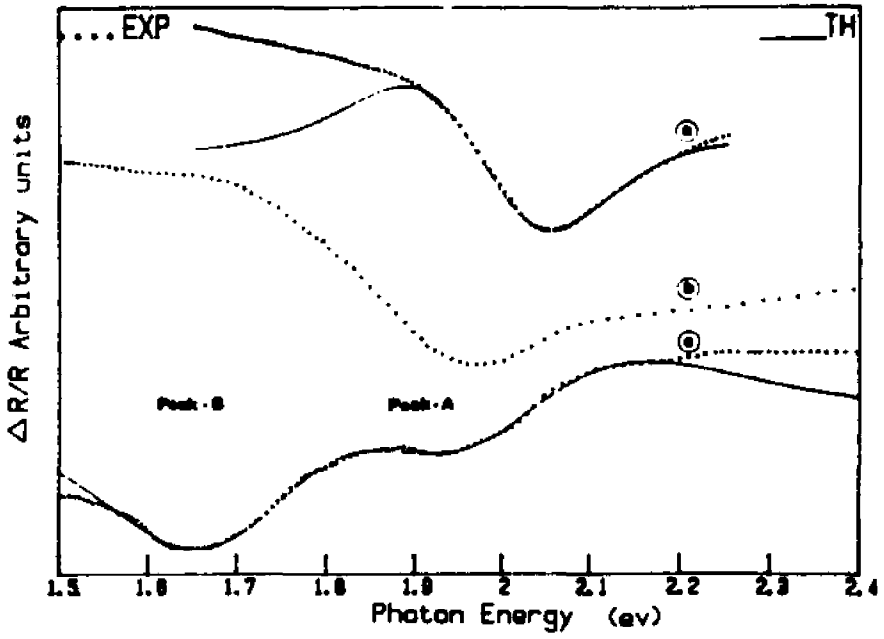

Fig.31. EER response of reduced P3MT, at U = 0.4 v vs. SCE
(.....)- Experiment, (————)- Best fit to equation .[17] with the parameter given in the text.
(a) Neutral (Reduced) Poly 3methylthiophene.
(b) "As Grown" (fully doped) polymer.
(c) Partially reduced polymer, with a doping density of 1.3×10^{21}.Details of Peak.A and Peak.B are given in the text.

If the Fermi level of the semiconductor is pinned, then equation [22] can be modified to yield [113]

$$\frac{\Delta R}{R} = K\left(1 - \frac{e}{C_H}\frac{dN_{ss}}{dU}\right)dU \qquad [30]$$

where C_H is the capacitance of the Helmholtz layer, N_{ss} is the area concentration of ionized surface states and U is the electrode potential. The Fermi level will be pinned or partially pinned whenever $dN_{ss}>0$, in this case part of the modulated potential drop will result in charging of the surface and will not be available for the modulation of the space charge field. As a result of this EER amplitude will be decreased. In the limiting case in which dN_{ss}/du is equal to C_H/e the EER amplitude will be reduced to zero. This situation is shown in Fig.24b. At 0.0 v vs. SCE the Fermi level appears to be completely pinned. Assuming that $\Delta R/R$ attains its maximum value when $dN_{ss}/du=0$ the equation can be modified to characterize the surface

$$\frac{\Gamma}{1-\Gamma} \quad \frac{eN_t}{C_H\sigma(2\pi)^{1/2}}\left[\exp\frac{-1}{2\sigma^2}\left(U_{t_0} - U + \int_{U_{max}}^{U}\Gamma dU\right)^2\right] \qquad [31]$$

states responsible for the pinning [113]. Where Γ stands for $1 - \frac{\Delta R/R}{(\Delta R/R)_{max}}$, N_t is the total concentration of surface states. U_t potential at the maximum surface state density. σ is the standard deviation of surface levels relative to the maximum. The data shown in Fig.24b

gives an excellent fit to the equation [30] to yield following parameters.

N_t/C_H = $7.6X10^{18}$, σ = 0.21, U_t = -0.31 v vs. SCE. Assuming the Helmholtz layer capacitance C_H to be 11 $\mu F/Cm^2$, which is the value obtained for polyacetylene, if only the exterior surface is wetted by the electrolyte [114], N_t can be estimated to be $8x10^{13}$, which is close to a one tenth of a monolayer over a geometric area.

EER spectra for fully doped P3MT shown in Fig.23b cannot be analysed in terms of the theory of low field electroreflectance. But in the case of moderately doped sample: sample 3 (Table.6) both EER peaks could be fitted to the equation [22] with the following parameters.

Peak (a)	n=3.5	E_g=1.98 ev	θ =169.8°	Γ=0.320 ev
Peak (b)	n=2.0	E_g=1.70 ev	θ=32.1°	Γ=0.238 ev

The spectrum 3 (Fig.25) for the sample 3 (Table.6) is reproduced with the theoretical fit to the equation [22] in Fig.31c. The parameters: n and E_g evaluated for the peak (a) are identical to those, obtained for neutral P3MT. No comparision can be made for θ and Γ values because of their sensitivity to variety of surface conditions, and differences in these parameters are expected for samples with different doping densities. But E_g value is very much in agreement with the optical data presented earlier and, since n = 3.5 corresponds to a one dimensional critical point, the peak(a) can be identified to be associated with the direct band to band transition. The

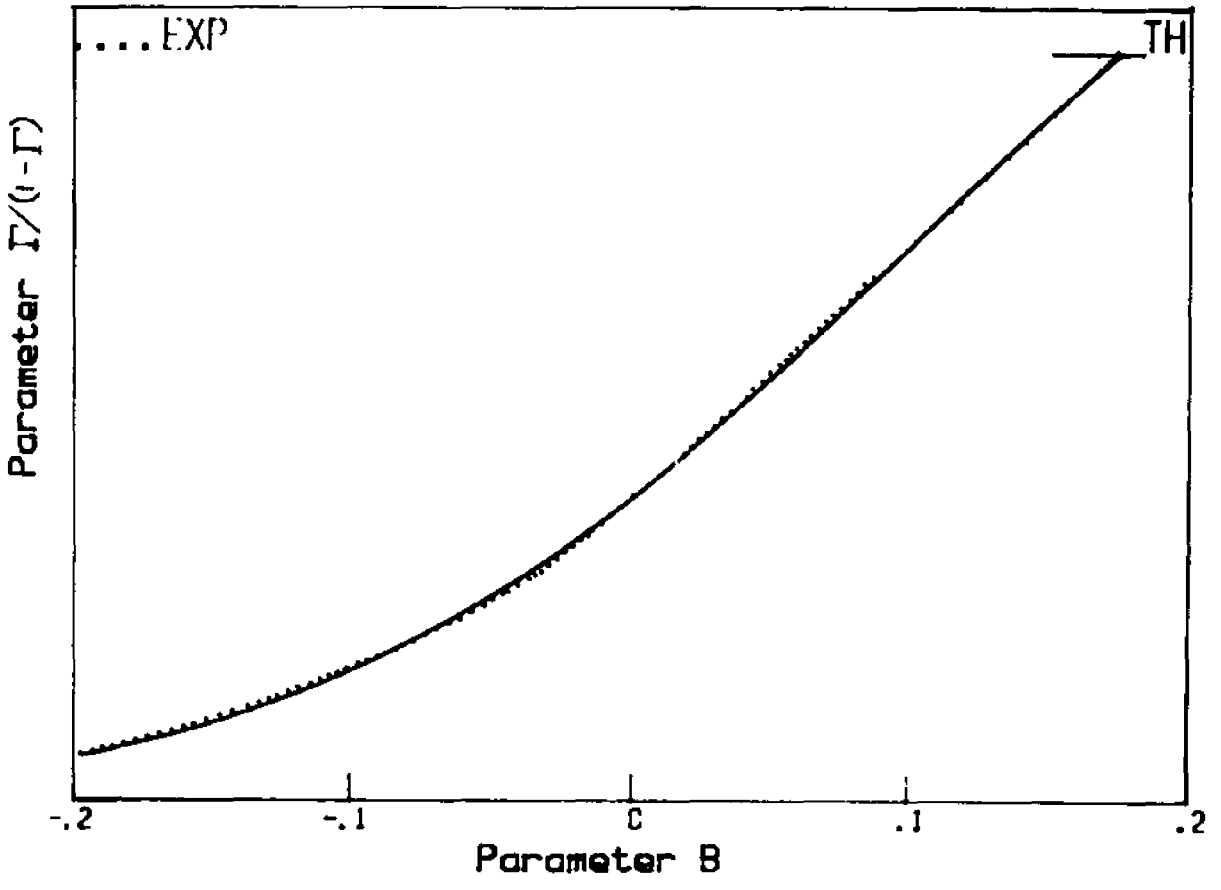

Fig.32. Fit of the EER data for Neutral P3MT to the equation.[31]

The parameter shown in x axis is, $B = \left(-u + \int_{U_{max}}^{U} \Gamma du\right)$

Where u is the potential vs. SCE and $\Gamma = 1 - \frac{\Delta R/R}{(\Delta R/R)_{max}}$

question, whether this sub band energy level which give rise to peak(b) represents a localized impurity state, is yet to be resolved. The EER behaviour of localised sub band gap impurities has been reported [115]. In this case EER follows the potential dependence of the dark current (high near the flat band and low in depletion) and has been interpreted in terms of the modulated changes in the absorption coefficient, caused by the current induced periodic changes in the population of impurity levels. But as shown in the Fig.25 magnitude of both peaks is very small around +1.0, which is the region of flat band and increases towards the negative potentials as the film enters into depletion mode. Both peaks essentially follow the shift of the fermi level relative to the band edges. In other words, the EER intensity of peak (B) does not follow, what is expected for localized, sub band impurity states. This situation is entirely different from that for neutral P3MT, for which, the intensity of the band gap transition reduces, as the film enters into depletion mode, due to unpinning of the band edges as discussed before. Since we already know that P3MT supports bipoloron energy levels, an alternative approach is to consider the possibility of a poloron level located within the gap giving rise to this new sub band EER response. Depending on the level of population (spin) these midgap energy levels can be either polorons (spin =1/2) or bipolorons (spin =0). The polorons are associated with localized mid gap levels, located symmetrically with respect to to the gap center as shown in the Diagram.2 [63]

Diagram.2 Representation of the direct gap and Poloron energy levels in Poly 3-methylthiophene.

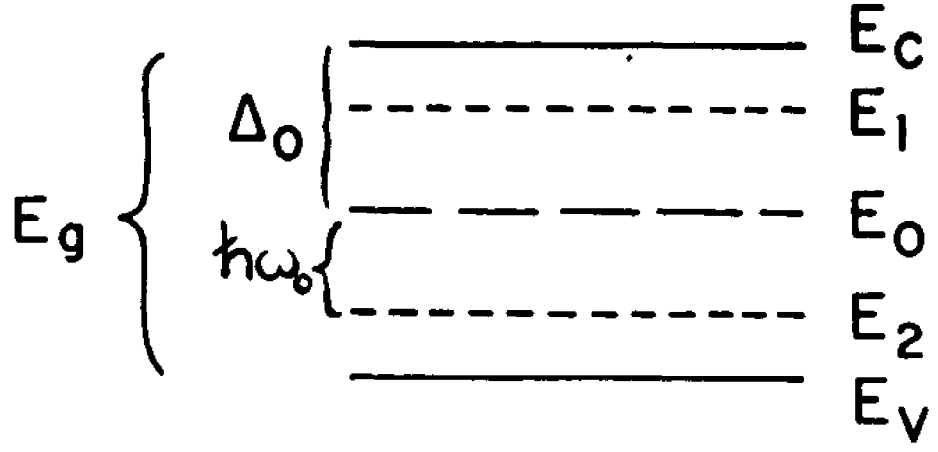

In the case of Poloron three sub band optical absorptions: E_v-E_2, E_v-E_1, E_2-E_1 are expected . This situation has been experimentally observed for ClO_4^- doped PPY [109]. In the case of bipoloron only two optical absorption peaks: E_v-E_2 and E_v-E_1 are possible. This has been experimentally verified for Polythiophene [62], which shows two sub band absorption peaks in the vicinity of 0.6 ev and 1.4 ev. The sum of these two is equal to the band gap as required by the symmetry of the poloron levels. Most important fact is that both of these peaks are induced by doping.

The origin of the mid gap observed in EER for moderately doped P3MT (Peak.B) can be discussed in relation to the poloron model. The peak is induced by doping and neutral material does not show such transition. It does not represent a mid gap localized impurity state. Since our EER observation does not extend to the energy region corresponding to E_v-E_2, which is in the energy range: 0.15 ev - 0.3 ev, the origin of Peak (B), as to whether E_v-E_1, or

E_2-E_1 is uncertain. If peak (B) is associated with the E_2-E_1 transition, it is seen from the Diagram.2 that $h\omega_o/\Delta = 0.85$. According to Fig.4 of Ref.[63] one can estimate that this $h\omega_o/\Delta$ value corresponds to either a poloron with the confinement parameter of 0.4 or a bipoloron with confinement parameter of 1.5. If the peak (B) is associated with the E_v-E_1 transition $h\omega_o/\Delta = 0.707$ and this value corresponds to either a poloron with confinement parameter of zero or bipoloron with a confinement parameter of 2. With the available data, analysis cannot be carried out further than this point.

4.7 Relaxation spectral analysis of Poly 3-Methylthiophene.

The MS plots of Sample 3 (Table 5) consistent with an abrupt junction of a p-type semiconductor with a flat band potential of 0.71 v vs.SCE. This value is consistent with the electroreflectance data and Photoelectrochemical data reported earlier. From the slope of the Mott Schottky plot doping density of sample 2 and 3 (Table.6) can be estimated by assuming the value of dielectric constant as 6. Table.2 shows comparison of these values with the calculated doping

Table.7 : Comparision of Doping densities calculated from Mott Schottky plots and coulombic data.

sample	N_A/cm^2 (coulombic)	N_A/cm^2 (MS plot)
2	$1.5x10^{21}$	$6.6x10^{20}$
3	$1.3x10^{21}$	$1.6x10^{20}$

densities based on the charge involved in electrochemical reduction.

The doping density calculated from the slope of MS plot deserves some comments. In this case the area of the sample was assumed to be the geometric surface area. Since the degree of penetration of the electrolyte into the polymer is uncertain, there is an uncertainty as to the true area. The roughness factor is unknown. Calculation of doping density based on the charge removed during the electrochemical reduction, assumes a uniform distribution of dopants throughout the polymer, following the reduction. On the other hand, Impedance measurements deals with the interface and the calculated doping density gives an estimation of the dopants concentration, only in the interfacial region. These fundamental differences in the two methods of estimating the doping density make this comparison somewhat questionable.

The value of flat band was not corrected for the contribution from the electrolyte. For the Mott Schottky equation [14] to hold, it is necessory that $C_{sc} << C_h$ and $\phi >> \Delta\phi_H$ where $\Delta\phi_H$ is the potential drop in the Helmholtz layer. But the validity of the second inequality is questionable for a semiconductor, such as sample 2 and 3 with high doping density. But even under these circumstances linearity of Mott Schottky plots is preserved, provided there is no charge present in surface states [103]. Since no Fermi level pinning was observed for sample 3, there is a possibility that the population of surface states remain constant within the region from flat band to about 0.0 v vs.SCE. Thus, instead of having a surface state free

system, one can imagine a system with fixed population in surface levels, and any error due to this population should be included in the flat band value. Following the treatment by De Gryse et al [103] one can estimate a flat band value excluding the contribution from the electrolyte to be 0.94 v vs.SCE. Assuming C_H=11μF and dielectric constant of p3MT as 6 one can estimate that the Helmholtz layer accounts for more than 70% of the potential drop across the interface, when the electrode potential is +0.4 v vs.SCE. For high doped materials eg. sample 1 (Table.6) the thickness of the interface dominated only by the electrolyte. In this case poor Mott Schottky behaviour is observed as expected.

4.8 Attempts to improve Photoelectrochemical performance of P3MT through the deposition of Pt.

It is well documented that the mediated electron transfer across the Photoelectrode/Electrolyte interface can be enhanced by the introduction of electrocatalysts on the photoelectrode surface. deposition of noble metals, eg. Pt,Au,Rh, the covalent attachment of a redox mediator to the photoelectrode surface [116] and polymer films bearing photoelectrochemically deposited Pt [117].

In this study we have already seen that the illuminated P3MT can be used to effect the up hill reduction of Methyl viologen Hydrate.

$$MV^{2+} + e \longrightarrow MV^{+\cdot} \qquad [32]$$

Since the junction showed a photo voltage of around 200 mv, the reduction can be effected at least 200 mv more positive than at a reversible electrode such as Pt. The photoelectrochemical generation of $MV^{+\bullet}$ has a special significance, because of the following reaction [118].

$$2MV^{+\bullet} + 2H_2O \longrightarrow H_2(g) + 2OH^- + 2MV^{++} \qquad [33]$$

This reduction allows the light driven evolution of H_2 from H_2O in an up hill sense. The P3MT/viologen system contributes at least 200 mv towards the 1.23 v needed to split H_2O according to the equation [119].

$$H_2O \longrightarrow H_2(g) + 1/2O_2(g) \qquad [34]$$

Reduction of MV^{++} to $MV^{+\bullet}$ alone is not sufficient to give improvement in photogeneration of H_2, since $MV^{+\bullet}$ does not react with H_2O despite the fact that reduction of H_2O is thermodynamically allowed for a wide range of pH ($E^{o'}(MV^{2+/+\bullet})$ = -0.69 v vs. SCE). The Pt(0) incorporation procedure provides a mechanism to equilibrate ($MV^{2+/+\bullet}$), with (H_2/H_2O). In other words Pt(0) acts as a mediator for the reaction [33]. The effectiveness of Pt(0) as a mediator has been demonstrated [117,120]. In the present study, the current densities involved are certainly not large enough to evolve any observable quantities of Hydrogen. But this factor alone is not sufficient to rule out the proven role of Pt(0) as a mediator for H_2 evolution.

As shown in Fig [28], deposition of Pt caused an improvement of the quantum efficiency for the charge separation by

nearly a decade. In the absence of viologen as the redox material, naked P3MT shows only a negligible photoeffect. The platinized P3MT seems to have an improved performance. But still photocurrent is too small to make any quantitative evaluation. This situation is very different from the case of Pt deposited p-type Si where, platinization improves the efficiency for the photoelectrochemical generation of H_2 compared to naked p-type Si [117a]. Considering the absence of any kinetic limitation for evolution of Hydrogen on Pt and the lack of significant improvement of photoeffect of platinized P3MT (in the absence of viologen) indicate that there is no enhanced electron transfer between the conduction band of P3MT and Pt(0) which is on the surface. This inference is extremely puzzling, because noble metals are generally used as pressure contacts for organic semiconductrors with p-type conductivity. But, this difficulty cannot be resolved with the available data.

The improvement of quantum efficiency shown in Fig [28] may be the result of effective scavenging of $MV^{+\bullet}$ in the vicinity of the electrode by the surface Pt as given in equation [33] combined with the improved heterogeneous electron transfer between the semiconductor and the redox material mediated by Pt(0). Naturally both of these effects would be favoured by increasing amounts of Pt, thereby improving the efficiency steadily. But as the quantity of Pt(0) increases, semiconductor begins to feel the effect of attanuation of light by the Pt(0) islands residing on the surface. This effect would cause the quantum efficiency to go through a maximum.

4.9 Stability of P3MT in aqueous electrolytes

Deterioration of the photoeffect of P3MT is common for both 'as grown' and 'neutral' polymer, when they are subjected to cathodic potentials for an extended period of time. The loss of photoactivity may be related to a reduction process or with equal results, to a compensation of dopants, which is possibly have triggered by reduced viologen species. The neutral P3MT already has a low concentration of dopants and the effect of compensation (reduction) even to a smaller degree would be felt quite substantially. This view is consistent with the fact that, high doped 'as grown' material suffers only a minor, deterioration of its photoeffect at negative potentials. Deterioration of the photoeffect is more pronounced with the neutral P3MT. It is highly probable, that the reduction or compensation, would results in the formation of an insulative over layer, on top of photoactive P3MT. This explains the reduction in photoeffect in the region of cathodic potentials as shown in Fig [22] and Fig [29]. But it does not explain the shift of cathodic photocurrent peak towards the positive potentials. Because, a pure resistance would shift the peak further to the negative side. One possibility is the slow diffusion of viologen species through the insulating layer, thereby creating a premature depletion of redox material close to the active surface.

But the most important point is, whatever the true course of the observed reduction of photoeffect in the region of cathodic potentials and rejuvenation of the photoeffect at anodic

potentials, we could simulate the same effect chemically, by subjecting the electrode to strongly reductive and oxidative environment respectively. This strongly supports the idea, that the P3MT is succeptible to chemical changes in aqueous electrolytes and this chemical change can be related to a reversible reduction and oxidation process of the polymer itself.

4.10 Summary of the discussion and conclusions.

as grown material is already in an oxidized state and the doping density of 41.6 mol%/ring, estimated in this study is actually higher than 25-30 % published in the literature. 'as grown' material could be reduced electrochemically to achieve a desired doping level ranging from 'as grown' to neu ral state. P3MT is observed to form a photovoltaic junction with viologen electrolyte with a photovoltage around 200 mv.

All three techniques; Photocurrent Spectroscopy, EER and Impedance Spectra, were used to study this interface. The photo current behaviour of P3MT is consistent with a p-type semiconductor with a photocurrent onset in the vicinity of +0.5 v vs.SCE. The photo response decreases with increasing doping density as in the case of inorganic semiconductors. Action spectra for P3MT closely follows the absorption spectrum except in the region of 600 nm, where, an absorption peak attributed to the transition to a bipoloron level, begins to appear with doping. The action spectra of 'as grown' material taken at 0.00 v,-0.5 v,and that of neutral material

taken at +0.15 v vs.SCE could be analysed in terms of Gartner model. This analysis confirmed that the photoexcitation in P3MT is due to rect band transition. Further, the band gap value of neutral material is found to be 2.00 ev and 'as grown' material has a band gap of 2.09 ev. The difference between these two cases can be discussed in terms of the poloron model. The action spectra of neutral P3MT at -0.5 v not only has very low current densities, but it also has a peak around 650 nm. It is speculated that, this new peak is to be due to the reduced viologen species; $MV^{+\bullet}$ absorbed onto the electrode at negative potentials. This speculation is based on the fact that the absorption spectra of $MV^{+\bullet}$ has a permanent structure around 640 nm. But no explanation is offered for observing a photoresponse due to the adsorbed species.

EER spectra of neutral P3MT has only one structure located in the vicinity of 2 ev. This signal satisfied the low field requirement and the signal could be analysed in terms of the line shape expected for third derivative EER. This analysis resulted in a band gap value; 2.00 ev, which is in excellent agreement with the photoelectrochemical and published data. The most striking feature of this analysis is the confirmation of the one dimensionality of P3MT structure. The variation of EER peak height, with potential showed a flat band positive to +0.7 v vs.SCE. As the film enters into depletion the EER peak height deminshed and this effect was explained in terms of fermi level pinning due to the charging of the electrode surface by the modulating voltage. This effect was quantitatively

analysed by the use of concepts already available and a surface state located at -0.31 v vs.SCE, with a population of about one tenth of a monolayer is found to be responsible for the unpinning of the band edges (Fermi level pinning).

The EER spectra of partially reduced sample with an intermediate doping concentration shows two signals located around 1.65 ev and 1.95 ev. Both signals satisfy the low field requirement and the line shape analysis can be performed to identify two transitions, one of which is identified to be the direct band gap transition. Again this peak can be associated with a one dimensional critical point. The other signal corresponds to a sub band gap level with an energy gap of 1.7 ev, which was identified to belong to an excitonic type transition. Considering the facts available in the literature, we could exclude the possibility of a localized, surface impurity state being responsible for the sub band gap response and this sub band gap response could be analysed in terms of the poloron model. Because of the limitations of the available data no discrimination could be made as to whether this sub band response, represent a poloron or bipoloron level.

The imaginary part of the relaxation spectra of neutral P3MT did not have a region with a slope of -1, that could have been correlated with the fast relaxing capacitive element of the interface; which is in most cases, the space charge region. The reason for this may be related to the composite nature of the interface with frequency dependent dielectric constant or limitations with regard to the

physical size of the fibre compared to the width of the space charge region at low doping densities. In the case of as grown materials, since the majority of the potential drop appear outside the space charge layer, no good mott schottky behaviour is observed, despite the fact that there was a region with a slope of -1, with the imaginary part of the impedance spetra. Moderately doped materials exhibited good mott schottky behaviour with a flat band value of 0.71 v vs.SCE which is in agreement with EER observations. The intercept gives an average doping density which is different from the doping density calculated from coulombic data, as expected. The photoelectrochemical performance of P3MT can be improved by the deposition of Pt(0) on the P3MT electrode. The maximum amount of Pt(0) is around 0.2 μmois/cm^2 and this improvement in photoeffect can be explained in terms of the improvement of the kinetic of charge transfer beteween the semiconductor and solution phase.

P3MT loses its photoactivity when the electrode is subjected to cathodic polarization and it rejuvenates at anodic potentials. This behaviour is common for all the P3MT electrodes. But for the as grown material it is less pronounced. Exact reason for the correlation of photoeffect with the electrode polarization is not known but the results can ber simulated by treating the P3MT electrode with reducing and oxidizing agents.

Conclusions for this part of study can be summarized as follows.

Poly 3-methylthiophene; P3MT acts as a p-type semiconductor and

this junction has a photovoltage of at least 200 mv. Similar to inorganic semiconductors the photoresponse of P3MT decreases with increasing doping density. The slope of the photo response curve is insensitive to the doping level except for its magnitude. The action spectra can be analysed in terms of the Gartner model. This analysis reveals that P3MT is a direct band gap semiconductor with a band gap around 2.00 ev. which is in excellent agreement with EER and published data. The observed difference in the band gap value for 'as grown' and neutral P3MT can be analysed in terms of the Poloron model, but no direct evidence for a transition to the poloron level can be seen in the photocurrent spectra. The photo response of a neutral P3MT elcctrode, which was kept at a negative potential for a long time showed a substantial loss of its photoeffect and a new structure in the action spectra. The latter could be correlated with the absorption spectra of reduced viologen. The analysis of the EER spectra of reduced (neutral) P3MT revealed that P3MT is a quasi one dimensional material with a band gap of 2.00 ev. The variation of the height of EER signal as a function of potential shows the effect of fermi level pinning and the later could be quantitatively analysed by using the concepts already available. The two signals observed for P3MT with a moderate doping densitiy could be analysed in terms of an overlap of two EER signals corresponding to two transitions. One of them is identified to be due to direct band gap and the other one, could be associated with the transition to a poloron level. But no discrimination could be made as to the true nature of this poloron

level. Good mott schottky behaviour could be observed only for the moderately doped samples. The MS plot corresponds to a flat band value of 0.71 v vs.SCE. The photoresponse can be enhanced for nearly an order of magnitude by the deposition of Pt(0) on the electrode and the maximum amount of Pt(0) is about 0.2μmol/cm^2. There is evidence to the possibility that P3MT chemically interact with the aqueous electrolyte.

4.11 Comparison between the trans-Polyacetylene with Poly 3-Methylthiophene.

* The Polyacetylene has a degenerate ground state, whereas the ground state of the P3MT is non degenerate. Because of these differences, stable charge configuration for Polyacetylene is solitons and the structure of P3MT supports polorons.

* Both of these polymers belong to quasi one dimensional materials. In this study, direct evidence in supporting this fact could be obtained from the analysis of EER data.

* Polyacetylene is synthesised by chemical methods, whereas synthesis of P3MT is done electrochemically. Both polymers are fibrillar, with each fibre 200° in diameter and indifinite length. Polyacetylene is a polymer with low compactness. Only 1/3 to 1/2 of the bulk is acetually filled with the polymer. But P3MT has a fairly compact structure, which has a porosity of the order of 30%

* The Cis and Trans content of Polyacetylene is temperature dependent and at high temperature trans isomer is the most stable form,

which has a higher conductivity. In the case of P3MT, the carbon back bone is locked to a structure similar to Cis Polyacetylene by an intra molecular sulphur bridge.

* Polyacetylene is reactive towards exposoure to air and other chemical vapours, and handling of this polymer requires an inert atmosphere exclusively devoid of oxygen. But the P3MT has an exceptional stability towards the ambient.

* The Polyacetylene is a neutral polymer and it can be oxidized either chemically or electrochemically which results in increasing the conductivity over 12 orders of magnitude, ranging from an insulator to a one with metallic conductivity. In contrast to this, 'as grown' P3MT is already highly conductive and generally, it is doped (oxidizd) to an extent of about 30 mol%. This 'as grown' material can be undoped electrochemically to yield the neutral polymer.

* The absorption spectra of Polyacetylene has peaks which are exclusively attributed to the doping process. In this case dopant-induced bands appear at 0.17ev,0.11ev, and 0.5 - 0.8ev. The first two are due to local IR modes of solitons and the third one represents the transition to the solitonic level. In the case of Polythiophene which is structurely similar to P3MT there are two dopant induced bands at 0.65 and 1.5ev. These bands are attributed to the transition to mid-gap poloron levels.

* Both lightly doped Polyaceylene and P3MT are p-type semiconductors, and they form a blocking junction with viologen electrolyte. The Polyacetylene/electolyte junction has a photo voltage of about 100 mv

and the Junction between P3MT and the electrolyte shows a photovoltage of about 200mv.

* In the case of trans Polyacetylene, photoeffect is observed only within a narrow range of dopant concentrations. Above this range there is no photoactivity at all. The photoresponse of P3MT decreases with increasing doping densities, as in the case of inorganic materials. Unlike the high doped trans Polyacetylene, the 'as grown' P3MT shows a fairly high photoeffect.

* In the case of trans-Polyacetylene, the absorption spectra correlates with the action spectra (Quantum efficiency) only in the region of photocurrent onset. Our study indicates that the action spectra of P3MT exhibits a good correlation with its absorption spectra at all dopant concentrations. This situation contradicts certain reports published in the literature. Generally, P3MT has a higher quantum efficiency for the charge separation compared to that of Polyacetylene. But compared to most inorganic counterparts they both have low efficiencies.

* The action spectra of trans-Polyacetylene and P3MT can be analysed in terms of the Gartner model. Both polymers show direct band to band transitions. The higher band gap associated with the 'as grown' P3MT compared to neutral P3MT can be attributed to the formation of poloron bands within the gap.

* The EER spectra of lightly doped trans Polyacetylene has only two signals at positive potentials. Buth of these signals satisfy the low field requirement. But none of them did fit to the line shape

expected for third derivative EER. In the case of neutral P3MT there is only one EER signal, which can be analysed for its line shape. The results obtained in this analysis, not only agree with our findings in Photoelectrochemical aspects of P3MT, but also confirm the quasi one dimensionality of the P3MT structure. The EER of moderately doped P3MT has a sub band gap signal that could be attributed to the transition to a poloron level.

* The EER data of both trans Polyacetylene and P3MT show evidence for fermilevel pinning at polymer/electrolyte interface. Data acquired for neutral P3MT could be dealt with quantitatively by using the concepts developed to understand similar situations in inorganic semiconductors.

* The photoeffect of both trans Polyacetylene and P3MT depends on the anodic and cathodic dark currents in a picular way. In the case of trans Polyacetylene, the photo effect deteriorates at anodic potentials and rejuvenates at negative potentials. But P3MT was observed to behave exactly opposite way. There is a possibility that, the P3MT film itself undergo chemical changes under the ordinary testing conditions.

* The photoeffect of P3MT is enhanced when Pt is deposited on the electrode. No similar study was conducted for trans-Polyacetylene.

4.12 Future work.

As a continuation of the investigations we have performed, following work can be suggested.

* The present work demonstrates the applicability of EER to investigate the organic semiconductor/electrolyte interface. Since we are interested in a contact between a porous material and a liquid this investigation is plagued with difficulties such as seepage of the electrolyte into the polymer, chemical interactions involving the polymer itself, electrochromic characteristics of the polymer, change of reflectance of the electrolyte due to the formation of coloured solution species. If one can conduct this investigation without an electrolyte contact, these difficulties can be resolved. In this case the technique of Photoreflectance is ideal as a substitute for EER. The success of this technique depends upon the initial bending of the bands, due to the interaction between the semiconductor and the ambient. In Photoreflectance the ambient is generally air, but the possibility of using an optically thin film of a metal, which has a work function smaller than the polymer should be examined. Investigations with different doping densities and different temperatures and atmospheres will diversify the Photoreflectance investigation.

* Photoelectrochemical study of organic polymers is apparently complicated by the chemical processes involving the polymer itself. It is worthwhile to investigate the Photoelectrochemical behaviour of P3MT coated with a thin layer of a conductive polymer such as Nafion. This will avoid the film being in direct contact with the reaction products such as Oxygen and reduced electrolyte species which will chemically attack the polymer. Investigations on light induced photocurrent-voltage behaviour, without added complications from these chemical

attacks, would be helpful to understand the nature of light induced charge separation inside the polymer.

* The improvement of Quantum efficiency through the platinization of P3MT is encouraging. The nature of interaction between Pt(0) and the film has to be investigated. Impedance measurements of naked and platinized P3MT and the resulting Mott-Schottky plots would be beneficial in this respect. Variation of flat band potential with solution pH is to be investigated. Influence of mixed catalysts on the Quantum efficiency is to be included in this study.

* None of the polymers were tested with the intention of using them as devices for energy conversion. Study involving steady-state photocurrent-voltage curves in stirred, high concentration viologen electrolyte is to be conducted. The data can be analysed with regard to the stability of the device.

* At present Organic polymers have acquired immense attention due to their possible uses such as electrochromic materials and charge storage devices. The diffusion of dopants inside the polymer and the composition of the electrolyte are major factors that limit their possible use. Search for suitable candidates involves synthesis of new polymers with systematic changes in their structure and testing them under variety of experimental conditions.,

REFERENCES

[1] Y.Okamoto and W.Brenner, Organic Semiconductors., Reinhold, New-York (1964)

[2] Organic semiconducting Polymers, J.E.Katon,monograph in macromolecular chemistry.,Marcel Dekker Inc, NY, 1968.

[3] Organic Solids: Is Band theory enough? Charles B.Duke and L.B.Schein, Physics Today Feb 1980.,p-43

[4] W.P.Su,J.F.Schrieffer, and A.J.Heeger, Phys.Rev.Lett. 421,698(1979)

[5] W.P.Su,J.F.Schrieffer, and A.J.Heeger, Phys.Rev. B22,2099(1980)

[6] T.Holstein Ann Phys.(N.Y) 8,343(1959);J.Yamashita,T.urosawa, Phys.Chem.Solids 5,34(1958); .Phys.soc.Jap. 15,802(1960)

[7] Dielectrics: A.R.Blythe, Electrical Properties of Polymers, cambridge U.P, Cambridge (1979)

Resists: L.F.Thompson and R.E.kerwin Annu.Rev.Mater.Sci. 6,276(1976)

Transduser : A.L.Robinson, Science 200 ,1371(1978)

Photodielectrics: S.Riech, Angew chem (int.ed.Engl.) 16,411(1977)

Electrophotography: J.W.Weigl, Angew chem (int.ed.Engl.) 16, 374(1977)

[8] J.R.Waldrop and marshall J.Cohen,A.J.Heeger and A.G.MacDiarmid Appl Phys.lett 38,1(1981)

[9] D.Peramunage, Withana Siripala, Micha Tomkiewicz, D.S.Ginley Chem Phys.lett 99,5-6(1983)

[10] S.N.Chien,A.J.Heeger,Z.Kiss,A.G.MacDiarmid,S.C.Gau, and D.L.peebles, Appl.Phys.Lett., 39,2(1982)

[11] T.Yamase, H.Harada, T.Ikawa,S.Ikeda and H.Shirakawa, Bull.Chem.Soc.Japan 54,2817(1981)

[12] H.A.Pohl and R.P.Chartoff, J.Polymer Sci.,A2 2787(1964)

[13] J.Rose and F.Statham, J.Chem.Soc., 69,117(1950)

[14] Franzus, P.J.Cantarino, and R.A.Wickilffe, J.Am.Chem.Sic., 81, 1514(1959)

[15] H.Shirakawa, T.Ito and S.Ikeda, Polym.J. 4,460(1973)

[16] Electronic Properties of Polymers : Edited by J.Mort,G.Pfistor, John wiley and sons , p-272

[17] H.Shirakawa, and S.Ikeda, Polym. J. 2,231(1971)

[18] T.Ito, H.Shirakawa and S.Ikeda, J.Polym.Sci. Polym. Chem. Ed., 12,11(1974)

[19] T.Ito, H.Shirakawa and S.Ikeda, J.Polym.Sci. Polym. Chem. Ed., 13,1943(1975)

[20] H.Shiriakawa and S.Ikeda, Synth.Met.,1 ,175(1980)

[21] G.E.Wnek, J.C.W.Chein, F.E,Karasz, M.A.Druy, Y.W.Park, A.G MacDiarmid, and A.J.Heeger, J.Polym Sci.Polym Lett.ed 17 , 779(1979)

[22] F.E.Karasz, J.C.W.Chein, R Galkiewicz, G.E.Wnek, A.J.Heeger and A.G.MacDiarmid, Nature, 282, 286(1979)

[23] J.C.W.Chien, J.D.Capistran, L.C.Dickinson, F.E.Karasz and M.A.Schen, J.Polym.Sci.Polym.Lett.Ed. 21,93(1983)

[24] H.Shirakawa, T.Ito and S.Ikeda,Macromol.Chem.,179(1978)1565

[25] H.C.Lounget-Higgins and L.Salim,Proc.R.Soc. A25(1959)172

[26] Esther M.Conwell, Physics Today, June 1985

[27] H.Kuzmany, E.A.Imhoff, D.B.Fitchen, and A.Sarhangi Phys.Rev B ,26(1982)7109

[28] D.M.Ivory, G.G.Miller, J.M.Sowa, L.W.Shacklette, R.R.Chance and R.H.Baughman J.Chem.Phys. 71,1506(1979)

[29] K.K.Kanazawa, A.F.Diaz, G.P,Gardeni, W.D.Gill, P.M.Grant, J.F.Kwak and G.B.Street, Synth.Met., 1,329(1980)

[30] G.Tourillon and F.Gaunier,J.Electroanal.Chem., 135,173-178(1982)

[31] T.Yamamoto, K.Sanechika, A.Yammato, J.Polym sci.,Polym Lett. ED 18,9(1980)

[32] G.Tourillon nd F.Garnier, J.Electrochem.Soc., 130,2042(1983)

[33] G.Tourillon and F.Garnier, J.Polym Sci, Polym Phys Ed, 22 33-39(1984)

[34] F.Garnier, J.Tourillon, M.Gazard and J.C.Dubois, J.Electroanal. Chem., 148,229(1983)

[35] J.E.Lennard-Jones, Proc.R.Soc. A158,280(1937)

[36] C.A.Coulson, Proc.R.Soc.A164,383(1938)

[37] L.G.S.Brooker, J.Am.Chem.Soc. 73,1087,5332(1951)

[38] H.Kuhn, Helv. Chem. Acta, 31,1441(1948)

[39] C.B.Duke, A.Paton, W.R.Salaneck, H.R.Thomas, E.W.Plummer, A.J.Heeger, A.G.MacDiarmid, Chem.Phys.Lett. 59,14 (1978)

[40] R.E.Peierls, Quantum theory of Solids" (Oxford University, London),Chap.5

[41] Low simentional Co-operative Phenomena, Edited by H.J. Keller (Plenum, New York, 1975); Chemistry and Physics of One Dimentional Metals, Edited by H.J.Keller (Plenum, New York, 1977)

[42] M.Karplus and R.N.Porter,Atoms and Molecules: An Introduction for Student of Physical Chemistry (Benjamin, New York, 1970), p-391

[43] C.R.Fincher,Jr., D.L.Peebles, A.J.Heeger, M.A.Druy, Y.Matsumura, and A.G.MacDiarmid, Solid State Commun. 27,489(1962)

[44] J.A.Pople and J.H.Walmsley. Mol. Phys. 5,15(1962)

[45] I.B.Goldberg, H.R.Crove, P.R.Newman, A.J Heeger, and A.G.MacDiarmid, J.Chem.Phys. 70,1132(1979)

[46] M.J.Rice, E.J.Mele, Phys. Rev B25,1339(1982)

[47] H.Takayama, Y.R.Lin-Lin, K.Maki, Phys.Rev. B21,2388(1980)

[48] J.H.Kaufmann, J.W.Kaufer, A.J.Heeger, R.Kaner and A.G.MacDiarmid, phys Rev. B26,4(1982)

[49] A.Feldblum, J.H.Kaufman, S.Etamad, A.J.Heeger, T.C.Chung and A.G.MacDiarmid, Phys Rev.B26,815(1982)

[50] J.H.Kaufman, T.C.Chung and A.J.Heeger, Solid State Commun 47, 585(1983) [51] Z.Vardeny, J,Orenstein and G.L.Baker, Phys. Rev. Lett., 50,2032(1983)

[52] G.Blanchet, C.R.Fincher, T.C.Chung and A.J.Heeger, Phys. Rev. Lett., 50,1938(1983)

[53] S.Etamad, T.Martni, M.Ozaki, T.C.Chung, A.J.Heeger and A.G.MacDiarmid,.Solid State Commun, 40,75(1983)

[54] C.R.Fincher, M.Ozaki, S.Etamad, A.J.Heeger and A.G.MacDiarmid, Phys.Rev. B19,4140(1979)

[55] B.R.Winberger, E.Ehrenfreund, A.Pron, A,J,Heeger, and A.G.MacDiarmid, J. Chem. Phys. 72,4749(1980)

[56] J.C.W.Chien, G.E.Wink, F.E.Karasz, J.M.Warakomski, L.C.Dickinson, A. .Heeger, and A.G.MacDiarmid, Macromolecules., 15,614(1982)

[57] J.C.W.Chien, F.E.Karasz, and G.E.Wnek, Nature 285,390(1980)

[58] S.Ikehata, J.Kaufen, T.Woerner, A.Pron, M.A.Druy, A.Sivak, A.J.Heeger and A.G.MacDiarmid, Phys. Rev. Lett 45,1123(1980)

[59] A.J.Epstein, H.Rommelmann, M.A.Druy,A.J.Heeger, and A.G.MacDiarmid, Solid State Commun. 38,683(1981)

[60] N.Suzuki, M.Ozaki, S.Etamad, A.J.Heeger and A.G.MacDiarmid, Phys. Rev. Lett., 45,1209(1980)

[61] B.Horowicz, Solid State Commun., 41(1980)926

[62] T.C.Chung, J.H.Kaufman, A.J.Heeger, and F.Wudl Phys. Rev. B30,702(1984)

[63] K.Fesser, A.R.Bishop and D.K.Campbell, Phys. Rev. B27,4804(1983)

[64] H.Akamatu and M,Kuroda, Organic Crystal Symposium, NRC Ottawa,1922, p.181; R.C.Nelson, J Chem Phys.,39,859(1963); H.Akamatu and H.Inokuchi, in H.Kallmann and M.Silver, eds., Symposium on Electrical Conductivity in Organic Solids, Interscience, New York, 1961, p-297

[65] C.K.Chiang, M.A.Druy, S.C.Gau, A J Heeger, E.J.Louis A.G.MacDiarmid and Y.W.Park, J. am. Chem. Soc., 100,1013(1978)

[66] H.Shirakawa, D.J.Lewis, A.G.MacDiarmid, C.K.Chiang and, A.J.Heeger, Chem Commun.,(1978)578

[67] C.K.Chiang, Y.W.Park, A.J.Heeger, H.Shirakawa, E.J.Lewis A.G.MacDiarmid, J.Chem.Phys., 69,5098(1978)

[68] C.K.Chiang, C.R.Fincher.Jr, Y.W.Park, A.J.Heeger, H.Shirakawa E.J.Lewis, S.C.Gau, A.G.MacDiarmid, Phys. Rev. Lett., 3, 18(1978)

[69] C.K.Chiang, S.C.Gau, C.R.Fincher.Jr, Y.W.Park, A.G.MacDiarmid, A.J.Heeger, App.Phys.lett., 33,18(1978)

[70] P.J.Nigrey, A.G.MacDiarmid, A.J.Heeger, J.C.S. Chem. Commun.,(1979)594

[71] S.C.Gau, J.Milliken, A.Pron, A.G.MacDiarmid and A.J.Heeger., Chem. Commun.,(1979)595

[72] J.C.W.Chien, J.M.Warakomski, F.E.Karasz, W.L.Chia C.P.Lillya, Phys. Rev. B28,6937(1983)

[73] S.Hsu, A.Signorelli, G.Pez, K.Baughman, J. Chem. Phys., 68,5105(1978); 69,106(1978)

[74] H.Gerisher: in Physical Chemistry, an Advanced Treatise, vol, ixA, (Academic Press, New york 1970) Chap.5

[75] M.Tomkiewicz and H.Fay, Applied Physics. 18,1-28(1979)

[76] A.J.Nozik, Phil. Trans. [] Soc. Lond. A295, 453-470(1980)

[77] Allan J. Bard, Larry R.Faulkner: Electrochemical Methods Fundementals and Applications (John Wiley & Sons 1980)p-269

[78] V.A.Mymalin and Y.V.Pleskiv, Electrochemistry of Semiconductors (Plemum press, New York, 1967)

[79] (a) W.Schotty; Z. Phy. 113,367(1939); 118,539(1942)
(b) N.F.Mott; Proc. Roy. Soc. A117, 27(1939)

[80] E.C.Dutoit, F.Cardon, and W.P.Gomes, Ber. Bunsenges. Phys., 80,1285(1976)

[81] J.I.Pankove; Optical Processes in Semiconductors, p.36-38, Prentice Hall, Englewood, N.J(1971); E.J.Johnson; Semiconductors and Semimetals ed, R.K.Willardson and A.C.Beer, Vol 3, Academic press, New York(1967)

[82] M.Cardona, in Modulation Spectroscopy (F.Seitz, D.Turnbull,

and H. Ehrenreich, Eds) Academic Press, New-York (1969)

[83] M.Cardona, K.L.Shaklee, and F.H.Pollak: Phys. Rev. 154,696(1967)

[84] D.E.Aspnes, Sur. Sci., 37,418(1973)

[85] D.E.Aspnes in Hand Book in Semiconductors, Vol 2, North Holland (1980)

[86] D.E.Aspnes, Phy. Rev. Lett., 28,913(1972)

[87] K.L.Shaklee, F.H.Pollak, and M.Cardona, Phys. Rev. Lett., 15,883(1965)

[88] B.Seraphin in Semiconductors an Semimetals, Vol 9, Chap.1 (R.K.Willardson and Albert C. Beer Eds,) Academic press, New Yor (1972)

[89] L.sebastian and G.Wiser, Chem Phys Lett., 64,(1979)396. Phys. Rev. Lett., 17,1156(1981)

[90] C.Kittel; Introcuction to Solid State Physics Fifth Ed, John and Wiely, New- York 1976

[91] L.A.Harris and R.H.Wilson; J.Electrochem. Soc. 123,7(1976)

[92] F.H.Pollak, in Procedings of the Symposia on Photoelectrochemical Processes and Measurments Techniques for Photoelectrochemical Solar Cells, Eds. W.L.Wallace, A.J.Nozik, S.K.Der and R.H Wilson (Electrochemical Society, New York, 1982) P.668

[93] R.P.Silberstein, F.H.Pollak, J.K.Lyden, M.Tomkiewicz; Phys. Rev. B24, 7397(1981)

[94] R.P.Silberstein, J.K.Lyden, M.Tomkiewicz and F.H.Pollak, J. Vac. Sci. Technol, 19,406(1981)

[95] R.H.Wilson; J. Appl. Phys. 48,1914(1977)

[96] M.Tomkiewicz; Surf. Sci. 101,286(1980)

[97] R.H.Wilson; J. Electrochem. Soc. 127,228(1980)

[98] M.Tomkiewicz; J.Electrochem.Soc 127,1518(1980)

[99] Withana Siripala and Micha Tomkiewicz; J. Electrochem. Soc.: Edectrochemical selence and Technology., 130,1062(1983)

[100] M.Tomkiewicz; J.Electrochem.Soc. 126,2220(1979)

[101] M.Tomkiewicz in Semiconductor Liquid Junction Solar Cells, Procedings of the Electrochemical Siciety, 77-3,92(1977)

[102] M.Tomkiewicz; J. Electrochem. Soc. 126,1505(1979)

[103] R.De.Gryse, W.P.Gomas, F.Cardona and J. Veenik; J.Electrochem. Soc 122,718(1975)

[104] S.R.Morrison, advan.catalysis, 7,249(1955); M.Green, in J.o'M.Bockris,ed.,Modern aspects of Electrochemistry, Butterworth, London No.2, 1959, P.378

[105] W.W.Gartner, Phys.Rev., 116,84(1959). See also: M.A.Butler, J.Appl.Phys., 48,1914(1977)

[106] Keiichi Kaneto, Shogo Ura, Katsumi Yoshino, and Yoshio Inuishi, Jap.J.Appl.Phy., 23.189-191(1984)

[107] G.Horowitz, and F,Gariner; Paper presented at the AES meeting, Toronto, Canada, May 1985

[108] E.M.Kosower, and J.L.Cotter, J.Amer.Chem.Soc., 86,582,(1964)

[109] J.L.Bredas, Mol.Cryst.Liq.Cryst 118,79-56(1985)

[110] J.L.Bredas, J.C.Scott, K.Yakushi and G.B.Street, Phys.Rev.B30 ,1023(1984)

[111] J.D.Zook, Phy.Rev.Lett.,20,848(1968)

[112] K.Kaneto,Y.Kohno, and K.Yoshino, Sol. State. Comm., 51,267(1984)

[113] M.Tomkiewicz,W.Siripala,and R.Tenne, J. Electrochem. Soc., 131,4(1984)

[114] F.G.Will, J. Electrochem. Soc., 131,2351(1985)

[115] O.J.Glenbocki, N.J.E.Ferneaux, J. Appl. Phys., 52,432,(1985)

[116] D.C.Bookbinder, J.A.Bruce, R.N.Dominey, N.S.Lewis, and M.D.wrighton, Proc.Natl. Acad. Sci., 77,6280(1980)

[117] a) R.N.Domeney, N.S.Lewis, J.A.Bruce, D.C.Bookbinder, and Mark S.Wrighton, J. Am. Chem. Soc., 104, 467(1982) b) H.D.Abrung and A.J.Bard, J. Am. Chem. Soc. 103,

6898(1981)

[118] A.L.Krasna, Photochem photobiol., 29,267(1979)

[119] W.M.Latimer, "Oxicative Potentials", 2nd ed., Prentice-Hall :Englewood cliffs, N.J., 1952

[120] a) M.S.Wrighton, P.T.Wolozanski, and A.B.Ellis, J. Solid state chem., 22, 7(1977) b) S.Sato and J.M.White, J. Am. Chem. Soc., 102, 7206(1980) c) F.R.Fan, G.A.Hope, and A.J.Bard, J. Electrochem. Soc., 129, 1647(1982) d) M.S.Matheson, P.C.Lee, D.Meiael, and E.Pellzzetti, J. Phys. Chem., 87, 394(1983)